

2006

Quantitative protein detection by pyrosequencing

Roxana Jalili
San Jose State University

Follow this and additional works at: https://scholarworks.sjsu.edu/etd_theses

Recommended Citation

Jalili, Roxana, "Quantitative protein detection by pyrosequencing" (2006). *Master's Theses*. 2955.
DOI: <https://doi.org/10.31979/etd.m3nk-2j33>
https://scholarworks.sjsu.edu/etd_theses/2955

This Thesis is brought to you for free and open access by the Master's Theses and Graduate Research at SJSU ScholarWorks. It has been accepted for inclusion in Master's Theses by an authorized administrator of SJSU ScholarWorks. For more information, please contact scholarworks@sjsu.edu.

QUANTITATIVE PROTEIN DETECTION BY PYROSEQUENCING

A Thesis

Presented to

The Faculty of the Department of Chemical Engineering

San Jose State University

In Partial Fulfillment

Of the Requirements for the Degree

Master of Science

By

Roxana Jalili

August 2006

UMI Number: 1438570

Copyright 2006 by
Jalili, Roxana

All rights reserved.

INFORMATION TO USERS

The quality of this reproduction is dependent upon the quality of the copy submitted. Broken or indistinct print, colored or poor quality illustrations and photographs, print bleed-through, substandard margins, and improper alignment can adversely affect reproduction.

In the unlikely event that the author did not send a complete manuscript and there are missing pages, these will be noted. Also, if unauthorized copyright material had to be removed, a note will indicate the deletion.

UMI[®]

UMI Microform 1438570

Copyright 2007 by ProQuest Information and Learning Company.

All rights reserved. This microform edition is protected against unauthorized copying under Title 17, United States Code.

ProQuest Information and Learning Company
300 North Zeeb Road
P.O. Box 1346
Ann Arbor, MI 48106-1346

© 2006


Roxana Jalili

ALL RIGHTS RESERVED

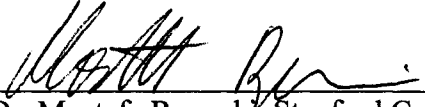
APPROVED FOR THE DEPARTMENT OF CHEMICAL ENGINEERING

 7-12-2006


Dr. Melanie McNeil

 7-12-2006

Dr. Henrik Persson, Stanford Genome Technology Center


 July/12/2006

Dr. Mostafa Ronaghi, Stanford Genome Technology Center

 7.12.06

Dr. Roger Ferrill

APPROVED FOR THE UNIVERSITY

 07/20/06

ABSTRACT

QUANTITATIVE PROTEIN DETECTION BY PYROSEQUENCING

By Roxana Jalili

Quantitative detection of proteins is vital in diagnosing diseases. Most current methods are limited to single protein detection, requiring large sample volumes for rapid diagnosis. The technique employed in this thesis used sandwich immunoassays combined with pyrosequencing to quantitatively detect proteins. Capturing complexes were formed on magnetic beads and detection complexes were made of antibodies that carried self primed oligonucleotides (pyro-tags). This method has the potential for multiplexing, which can simultaneously detect and quantify multiple proteins.

In this thesis, the IL-8 antigen was quantitatively detected using a High Sensitivity (HS) pyrosequencing machine. Results indicated a 78 pg/ml limit of detection. The dynamic range covered two orders of magnitude with a coefficient of variation below 19%. Moreover, three combinations of antigen pairs (IL-4+IL-8, IL-4+IL-10, and IL-8+IL-10) were simultaneously detected in a single sample volume.

ACKNOWLEDGMENTS

I am very grateful to Dr. Henrik Persson for providing me the means to perform this notable research project, and for his constant support, guidance, encouragement, scientific teaching, and professional advice. He always welcomed my questions with a gracious attitude, and was a great role model.

I would like to express my sincere appreciation to Dr. Mostafa Ronaghi for letting me perform my thesis at Stanford Genome Technology Center. His exceptionally brilliant ideas as well as constant support always progressed my thesis forward, and I learned a great deal working in his laboratory.

I wish to thank Dr. Melanie McNeil for her advice and support on this thesis and throughout the whole master's program. Her caring and thoughtful personality was always very encouraging and inspiring. She motivated me to succeed and helped me in every step to completing my master's program.

I like to thank Dr. Terrill for his excellent advice on this thesis, despite the short notice.

I like to thank all the people at the Stanford Genome Technology Center laboratory for their timely recommendations. They made it possible to perform my experiments in the best working environment with great camaraderie.

Finally, I wish to thank and dedicate this thesis to my family for their unconditional love and support. No one supported me more than my husband, not just for his daily assistance with my thesis, but for his help in every aspect of my life.

Table of Contents

List of Figures.....	x
List of Tables.....	xiii
CHAPTER ONE INTRODUCTION.....	1
1.1 Protein, DNA.....	1
1.2 Antibody (Ab), Antigen (Ag).....	3
1.3 Immunoassay.....	4
1.4 Pyrosequencing, Pyro-tag.....	5
1.5 Significance of Research.....	7
CHAPTER TWO LITERATURE REVIEW.....	9
2.1 Immunoassay.....	9
2.2 Immunoassays Employing Magnetic Beads.....	11
2.3 Pyrosequencing Method.....	20
2.4 Summary.....	23
CHAPTER THREE RESEARCH HYPOTHESIS AND OBJECTIVES.....	24
3.1 Research Hypothesis.....	24
3.2 Research Objectives.....	24
CHAPTER FOUR EXPERIMENTAL METHODS AND MATERIALS.....	26
4.1 Materials and Methods.....	26
4.1.1 Single Human IL-8 Detection Using MA Pyrosequencing Machine.....	26
4.1.1.1 Experimental Design for Detecting IL-8 Using MA Machine.....	27
4.1.1.2 Materials for Detecting IL-8 Using MA Machine.....	28

4.1.1.3 Experimental Procedures for Detecting IL-8 Using MA Machine.....	29
4.1.2 Single Human IL-4 Detection Using MA Pyrosequencing Machine.....	34
4.1.2.1 Experimental Design for Detecting IL-4 Using MA Machine.....	35
4.1.2.2 Materials for Detecting IL-4 Using MA Machine.....	36
4.1.2.3 Experimental Procedures for Detecting IL-4 Using MA Machine.....	37
4.1.3 Single Human IL-10 Detection Using MA Pyrosequencing Machine.....	38
4.1.3.1 Experimental Design for Detecting IL-10 Using MA Machine.....	39
4.1.3.2 Materials for Detecting IL-10 Using MA Machine.....	40
4.1.3.3 Experimental Procedures for Detecting IL-10 Using MA Machine.....	41
4.1.4 Multi Protein Detection of IL-8 and IL-4 Using MA Pyrosequencing Machine.....	42
4.1.4.1 Experimental Design for Multi-plexing IL-8 and IL-4 Using MA Machine.....	43
4.1.4.2 Experimental Procedures for Multi-plexing IL-8 and IL-4 Using MA Machine.....	45
4.1.5 Multi Protein Detection of IL-4 and IL-10 Using MA Pyrosequencing Machine.....	46
4.1.5.1 Experimental Design for Multi-plexing IL-4 and IL-10 Using MA Machine.....	46
4.1.5.2 Experimental Procedures for Multi-plexing IL-4 and IL-10 Using MA Machine.....	47
4.1.6 Multi Protein Detection of IL-8 and IL-10 Using MA Pyrosequencing Machine.....	48
4.1.6.1 Experimental Design for Multi-plexing IL-8 and IL-10 Using MA Machine.....	48
4.1.6.2 Experimental Procedures for Multi-plexing IL-8 and IL-10 Using MA Machine.....	49

4.1.7	Multi DNA Detection Using b-CTGC and b-CTCA Pyro-tags as Templates Employing MA Pyrosequencing Machine.....	50
4.1.7.1	Experimental Design for Multi-plexing b-CTGC and b-CTCA Pyro-tags ...	50
4.1.7.2	Experimental Procedures for Multi-plexing b-CTGC and b-CTCA Pyro-tags.....	50
4.1.8	Switching from MA to HS Pyrosequencing Machine.....	51
4.1.8.1	Experimental Design for Switching from MA to HS Machine.....	51
4.1.8.2	Experimental Procedures for Switching from MA to HS Machine.....	52
4.1.9	Single Human IL-8 Detection Using HS Pyrosequencing Machine.....	53
4.1.9.1	Experimental Design for Detecting IL-8 Using HS Machine.....	54
4.1.9.2	Experimental Procedures for Detecting IL-8 Using HS Machine.....	56
4.2	Equipment.....	57
4.2.1	Dynal Magnetic Particle Concentrator (MPC).....	57
4.2.2	Tube rotator.....	58
4.2.3	Pyrosequencing Instrument.....	59
4.3	Data Analysis.....	62
CHAPTER FIVE RESULTS AND DISCUSSION.....		64
5.1	IL-8 Single-plexing Using MA Pyrosequencing Machine.....	64
5.2	IL-4 Single-plexing Using MA Pyrosequencing Machine.....	66
5.3	IL-10 Single-plexing Using MA Pyrosequencing Machine.....	68
5.4	IL-8 and IL-4 Multi-plexing Using MA Pyrosequencing Machine.....	70
5.5	IL-4 and IL-10 Multi-plexing Using MA Pyrosequencing Machine.....	74
5.6	IL-8 and IL-10 Multi-plexing Using MA Pyrosequencing Machine.....	76

5.7	b-CTGC and b-CTCA Multi-plexing Using MA Pyrosequencing Machine	78
5.8	MA Pyrosequencing Machine Versus HS Pyrosequencing Machine	80
5.9	IL-8 Single-plexing Using HS Pyrosequencing Machine	81
CHAPTER SIX CONCLUSIONS		94
CHAPTER SEVEN FUTURE STUDY		96
REFERENCES		97
APPENDIX A EXPERIMENTAL STEPS PRIOR TO THE MAIN APPROACH		100
APPENDIX B CALCULATIONS		149

List of Figures

Figure 1. Protein structures.....	2
Figure 2. Double helical structure of DNA.....	3
Figure 3. Basic structure of antibody with its constant and variable regions, as well as heavy and light chains.....	4
Figure 4. Sandwich Ab-Ag-Ab complex bounded on a surface.....	5
Figure 5. Schematic representation of the pyrosequencing reaction system.....	6
Figure 6. Structure of a specific pyro-tag. CCCCTTTTTGGGGGCCCC is the region that is the template for DNA synthesis. The TAGCGGAACGCTA is the self primed loop.....	7
Figure 7. Sandwich ELISA technique for antigen quantification.....	10
Figure 8. Diagram of SEB detection using a magnetic bead based immunoassay.....	12
Figure 9. Schematic illustration of the determination of Vg based on the sandwich chemiluminescent immunoassay on magnetic beads.....	14
Figure 10. Schematic representation of the enzyme-linked immuno-magnetic chemiluminescent assay.....	15
Figure 11. Experimental protocol for LIFMIA.....	16
Figure 12. The bio-barcode amplification assay (BCA).....	17
Figure 13. Scanometric detection.....	18
Figure 14. Scatter plot from the scanometric detection of barcode DNA released from the bio-barcode assay for 30 subjects.....	19
Figure 15. Schematic representation of the progress of four-enzyme system.....	22
Figure 16. Pyrogram of the raw data obtained from four-enzyme pyrosequencing.....	22
Figure 17. Capturing complex.....	31
Figure 18. Detection complex.....	32

Figure 19. Immunocomplex captured on magnetic beads.....	34
Figure 20. Front view of the dynal magnetic particle concentrator.....	58
Figure 21. Tube rotator.....	59
Figure 22. PSQ™96MA pyrosequencing instrument.....	60
Figure 23. PSQ™HS 96A pyrosequencing instrument.....	60
Figure 24. Microtiter plate and inkjet cartridge used in MA pyrosequencing.....	61
Figure 25. HS plate and inkjet cartridge used in HS pyrosequencing.....	61
Figure 26. IL-8 Ag concentration versus light intensity generated by b-CTGC pyro-tag during pyrosequencing.....	65
Figure 27. IL-4 Ag concentration versus light intensity generated by b-CTCA pyro-tag during pyrosequencing.....	67
Figure 28. IL-10 Ag concentration versus light intensity generated by b-CTCA pyro-tag during pyrosequencing. The error bars represent one SD.....	68
Figure 29. (a) Single detection of IL-8 Ag. (b) Control experiment of IL-8 Ag. (c) Control experiment of IL-4 Ag. (d) Single detection of IL-4 Ag. (e) Multi-plexing of IL-8 and IL-4 Ags.....	70
Figure 30. (a) Single detection of IL-8 Ag. (b), (c), (d) Control experiments of IL-8 Ag. (e), (f), (g) Control experiments of IL-4 Ag. (h) Single detection of IL-4 Ag. (i) Multi-plexing of IL-8 and IL-4 Ags.....	72
Figure 31. (a) Single detection of IL-4 Ag. (b), (c), (d) Control experiments of IL-4 Ag. (e), (f), (g) Control experiments of IL-10 Ag. (h) Single detection of IL-10 Ag. (i) Multi-plexing of IL-8 and IL-4 Ags.....	74
Figure 32. (a) Single detection of IL-8 Ag. (b), (c), (d) Control experiments of IL-8 Ag. (e), (f), (g) Control experiments of IL-10 Ag. (h) Single detection of IL-10 Ag. (i) Multi-plexing of IL-8 and IL-10 Ags.....	76
Figure 33. (a) 1 pmol b-CTGC pyro-tag. (b) 1 pmol b-CTCA pyro-tag. (c) 1 pmol b-CTGC plus 1 pmol b-CTCA pyro-tags.....	79
Figure 34. Reproducibility of IL-8 result: same batch, same run.....	82

Figure 35. Reproducibility of IL-8 result: same batch, different runs.....	84
Figure 36. IL-8 result: different capturing complex batches, different runs.....	86
Figure 37. IL-8 result: different capturing complex batches, same run.....	88
Figure 38. IL-8 result: different capturing complex batches, different runs.....	91
Figure 39. Comprehensive results of IL-8 antigen.....	92

List of Tables

Table 1. Experimental design to determine signal intensities for quantitatively detecting IL-8 antigen.....	28
Table 2. Experimental design to determine signal intensities for quantitatively detecting IL-4 antigen.....	36
Table 3. Experimental design to determine signal intensities for quantitatively detecting IL-10 antigen.....	40
Table 4. Experimental design to determine signal intensities and cross reactivities for multi-plex detection of IL-8 and IL-4 antigens.....	44
Table 5. Experimental design to determine signal intensities and all combinations of cross reactivity for multi-plex detection of IL-8 and IL-4 antigens.....	45
Table 6. Experimental design to determine signal intensities and cross reactivities for multi-plex detection of IL-4 and IL-10 antigens.....	47
Table 7. Experimental design to determine signal intensities and cross reactivities for multi-plex detection of IL-8 and IL-10 antigens.....	49
Table 8. Experimental design for comparison of light intensity between MA and HS machines.....	51
Table 9. Experimental design for comparison of light intensity for different sample concentrations and different moles.....	52
Table 10. Experimental design to quantitatively detect IL-8 antigen.....	55
Table 11. Percent difference between signal intensity of single antigen detection versus multi antigen detection.....	78
Table 12. Comparison of light intensity for different sample concentrations and different moles.....	81
Table 13. Reproducibility of IL-8 result: same batch, same run.....	82
Table 14. Reproducibility of IL-8 result: same batch, different runs.....	83
Table 15. IL-8 result: different capturing complex batches, different runs.....	85
Table 16. IL-8 result: different capturing complex batches, same run.....	87

Table 17. IL-8 result: Limit of detection and noise level.....	89
Table 18. IL-8 result: different capturing complex batches, different runs.....	91

CHAPTER ONE INTRODUCTION

Detection and quantification of known and unknown proteins is a key factor for seeking proper treatments against microorganisms, toxins, cancer cells, or foreign blood and tissue. Any such unknown proteins that can be recognized by the human body's immune system are called antigens. Most antigens are immunogenic, in which the immune system is able to form a response against them. However, harmful antigens that are not immunogenic can also pose a great threat to human health such as cancer cells [1]. The need for rapid detection and quantification of such antigens is vital. Moreover, effective testing of new drug developments requires extensive detection and quantification of antigens.

For the detection and quantification of antigens, many sophisticated methods have been applied to this date. In the research project described in this thesis, a novel method based on sandwich immunoassays captured on magnetic beads that incorporate pyrosequencing detection technique with DNA-based biological barcodes were considered.

1.1 Protein, DNA

Proteins are polymers made of amino acids coupled with peptide bonds. Amino acids are the building blocks of proteins and are composed of carboxylic acid groups

(COOH), amino groups (NH₂), and various side groups. The sequence of amino acids determines the structure of proteins [2]. Proteins are the most abundant organic molecules and fundamental components of living cells. Typical molecular weight of proteins ranges from a few thousand to several hundred thousand Daltons. Major categories of proteins include hormones, antibodies and enzymes [2]. Figure 1 illustrates different structures of proteins.



Figure 1. Protein structures.

Deoxyribonucleic acid (DNA) is a large polymer made of nucleotides with a double-helix structure. Nucleotides are made of three covalently linked parts: at least one phosphate group (H₂PO₅), a pentose (deoxyribose), and a base (purine or pyrimidine). There are two purines present in nucleotides, adenine (A) and guanine (G), and two pyrimidines, thymine (T) and cytosine (C). In the DNA molecule, A binds to T, and G binds to C. The major function of DNA is to store the genetic information of living cells. The order in which A, G, T, and C are positioned determines the genetic code in DNA [2]. Figure 2 shows the basic structure of a DNA molecule.

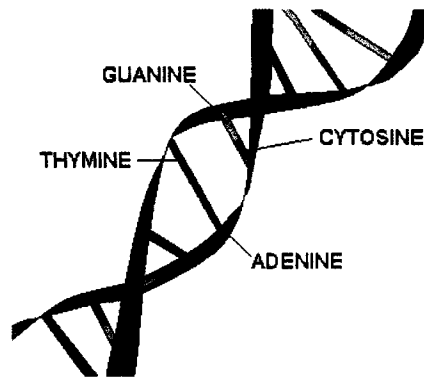


Figure 2. Double helical structure of DNA.

1.2 Antibody (Ab), Antigen (Ag)

Antibodies (Ab), or immunoglobulins, are proteins that bind to specific molecules with a high degree of specificity. Antibody molecules are released into the blood serum in response to antigens (Ag) by the body's immune system. There are five different antibodies present in human blood serum. They are abbreviated: IgG, IgM, IgA, IgD, and IgE. The basic building block of the five classes of antibodies is composed of four polypeptide chains, and has a molecular weight around 150 kilo Daltons. IgG is the most abundant immunoglobulin, and has a Y-shape structure. There are two heavy chains that have about 430 amino acids, and two light chains that consist of about 214 amino acids. Each chain has a constant as well as a variable amino acid sequence region, which are linked together by disulfide bonds. Antibody molecules have two binding sites at variable amino acid sequence regions for binding to antigens [2]. Figure 3 illustrates the basic structure of an antibody.

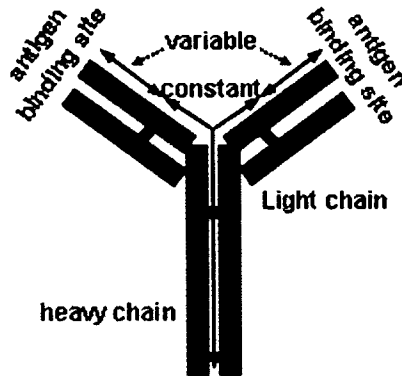


Figure 3. Basic structure of antibody with its constant and variable regions, as well as heavy and light chains.

Antibodies are divided into two categories: Polyclonal and Monoclonal.

Polyclonal antibodies are derived from several clones of cells and recognize multiple epitopes of an antigen. Monoclonal antibodies are derived from only a single clone of cells and recognize a specific epitope of an antigen [3].

Antigens are target macromolecules for antibodies, which bind to their own specific matching antibodies. The complex that is formed due to the binding between antigen and antibody is called the immune response complex [3].

1.3 Immunoassay

An immunoassay is a laboratory test to identify and quantify a specific biological agent such as an antigen. Various immunoassay techniques used in human clinical laboratories were first established in the 1970s and 1980s [4]. One such technique is

known as a sandwich immunoassay. This technique utilizes a primary antibody to capture an antigen and a secondary antibody to identify the captured antigen. The antibody-antigen-antibody (Ab-Ag-Ab) complex is thus called a sandwich immunoassay. The Ab-Ag-Ab complex must be captured onto a surface material while the secondary antibody must be labeled for detection and quantification [4]. The simple structure of a sandwich immunoassay is shown in Figure 4.

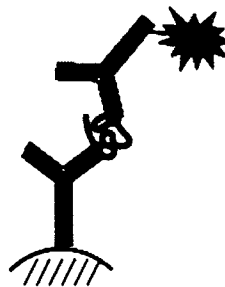


Figure 4. Sandwich Ab-Ag-Ab complex bounded on a surface.

Magnetic immunoassay is a technique in which the Ab-Ag-Ab complex is bound onto a material with magnetic properties. The application of magnetic beads in immunoassays was first introduced around three decades ago [5].

Some existing methods of labeling the secondary antibody include fluorescent, luminescent, radioactive, and electrochemical labels [4].

1.4 Pyrosequencing, Pyro-tag

Pyrosequencing is a DNA sequencing method in which released pyrophosphates (PPi) are detected during DNA synthesis. For each incorporated nucleotide, a single PPi

is released. After a series of enzymatic reactions, visible light energy is produced, which is directly proportional to the amount of incorporated nucleotides [6]. All the reactions involved in pyrosequencing are shown in Figure 5. Pyrosequencing has the advantages of parallel processing, flexibility, accuracy, sensitivity, and favors miniaturizing. In this thesis, the pyrosequencing method was employed.

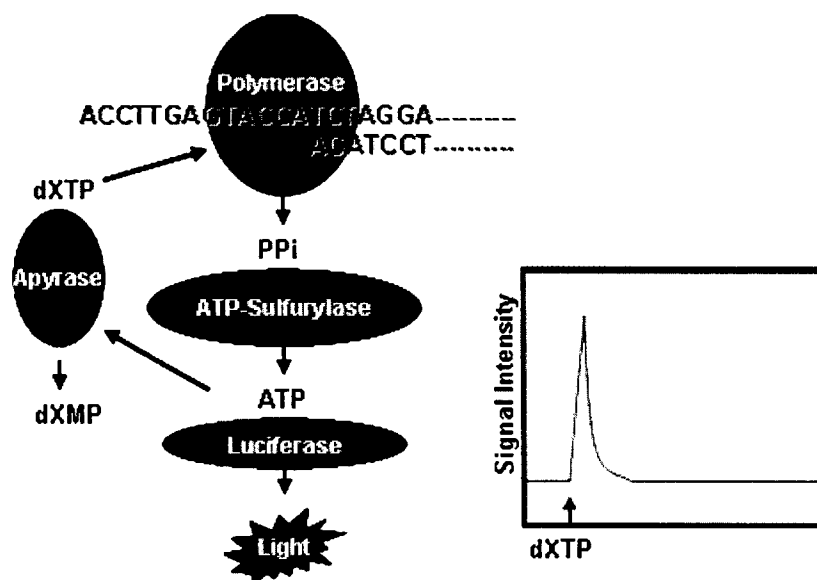


Figure 5. Schematic representation of the pyrosequencing reaction system. Modified from original [7].

A pyro-tag is a self primed oligonucleotide loop, which was used as a template for DNA synthesis during the pyrosequencing in this research. Each pyro-tag can be synthetically made and consists of 10-20 nucleotides prior to a loop region. These nucleotides act as a bio-barcode and are designed for a specific analysis. The loop region serves as a primer. Figure 6 shows a particular pyro-tag with its 20 nucleotides prior to its self primed loop.

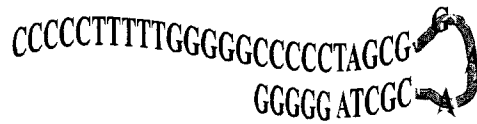


Figure 6. Structure of a specific pyro-tag. CCCCCTTTTGGGGCCCCC is the region that is the template for DNA synthesis. The TAGCGGACGCTA is the self primed loop.

1.5 Significance of Research

Most current antigen detection techniques are limited to single-plex assays. In single-plex assays only one type of antigen can be detected per each sample volume (sample to be analyzed). Therefore, in order to detect different types of antigens, a large number of sample volumes are needed. The technique employed in this thesis offers the prospect to simultaneously detect and quantify multiple types of antigens in a single sample volume. Various types of immunocomplexes (Ab-Ag-Ab) are immobilized onto magnetic beads. DNA barcodes called pyro-tags are used to label each immunocomplex, so that the captured antigen could be detected and quantified. With this technique, different immunocomplexes immobilized on magnetic beads can be mixed together. Thus, many different immunocomplex types, each with its own unique pyro-tag, can be tested in a single sample volume at the same time. This method greatly reduces the need for sample volumes, and is referred to as multi-plexing. By simultaneously detecting and quantifying different types of antigens in one sample volume, the duration of each assay will also decrease significantly.

The rapid detection and quantification of antigens will become more feasible by multi-plexing. There are two major costs associated with this research: magnetic beads with capture antibodies and detection costs. Magnetic beads are commercially available with a relatively low cost. Detection cost is dominated by using the pyrosequencing equipment, as well as its reagents for each assay, which will be amortized by the multi-plexing involved.

CHAPTER TWO LITERATURE REVIEW

The concept of this research is based on the principles of sandwich immunoassays utilizing magnetic beads, combined with the pyrosequencing method. This section reviews previous work done on different sandwich immunoassays with different detection techniques. The pyrosequencing method is also explained in detail.

2.1 Immunoassay

Enzyme Linked Immuno-Sorbent Assay (ELISA) is one of the safest and simplest techniques, which has been used for many decades for quantitative detection of biological content in a solution. In sandwich ELISA, primary antibodies are immobilized on the surface of a microtiter plate well, and the solution to be tested is added to the well. After several washing steps, the enzyme linked secondary antibodies are added to the well, and if the corresponding antigen is present in the solution, these secondary antibodies will bind to them, making a sandwich immunocomplex. When a substrate system for the enzyme is added to the solution, the colored reaction product can be measured by a spectrophotometer. The antigen can then be quantified by the detected signal from the spectrophotometer against a known standard curve [8]. Applying different enzymes for different detection systems yields different detection limits for the antigens to be quantified. The schematic steps of sandwich ELISA technique are shown in Figure 7.

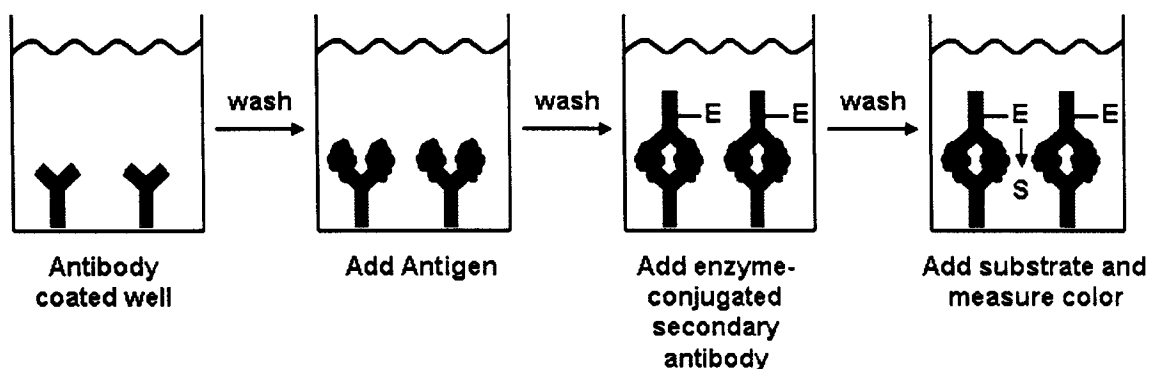


Figure 7. Sandwich ELISA technique for antigen quantification.

Rongen *et al.* [9] have studied a sandwich immunoassay for quantifying the interleukin-5 mouse antigen using two different enzymes: xanthine oxidase and horseradish peroxidase. A luminal chemiluminescent substrate reagent was used for both systems. The immunocomplex was adsorbed onto the surface of microtiter plate wells. The results indicated that the detection limit of xanthine oxidase was about 0.6 picogram per milliliter (pg/ml) of antigen solution, whereas the detection limit of horseradish peroxidase was about 2.9 pg/ml. The lower detection limit corresponds to a more sensitive assay, which this study demonstrated to be almost five times better when using xanthine oxidase enzyme [9].

Alkaline phosphatase (AP) is a commonly used enzyme for labeling the detection antibody in ELISA, because of its high turnover number and its stability. Ciana *et al.* [10] studied a sandwich amperometric enzyme immunoassay to quantify α -fetoprotein in human serum. The immunocomplex was adsorbed onto the surface of microtiter plate wells. AP was used as the enzyme label in the assay and p-hydroxyphenyl phosphate was used as the substrate for the enzyme. The product was detected by an amperometric

detection system. In comparison, the same assay was set up using a different substrate, p-nitrophenyl phosphate, in which the product was detected by a photometric detection system. They reported that the detection limit for α -fetoprotein was about 0.07 nanogram per milliliter (ng/ml) of antigen solution when amperometric detection was applied, which was about 14 times lower and more sensitive when compared with photometric detection [10].

2.2 Immunoassays Employing Magnetic Beads

The application of magnetic beads in immunoassays was established around three decades ago. The advantage of using magnetic beads includes both decreasing the assay time and increasing antigen extraction efficiency. In this technique the immunocomplex is bounded onto magnetic beads' surface.

Gundersen *et al.* [11] developed a magnetic bead enzyme linked immunoassay (MBEIA) for capturing schistosomal circulating anodic antigen (CAA). They compared their results that were obtained from MBEIA method with the ELISA method, in which the immunocomplex was adsorbed onto microtiter plate wells. They stated that the MBEIA method was less laborious and more rapid, and involved less advanced equipment. The assay time for the MBEIA method was about four hours less than the ELISA test time, which offers a more rapid diagnosis in urgent situations. They were able to detect 0.07 ng CAA per each milliliter of antigen solution utilizing the MBEIA

method, which indicated that this method offers slightly more sensitive results than the standard ELISA method [11].

Alefantis *et al.* [12] studied a method to detect Staphylococcal enterotoxin B (SEB), which is a toxin produced by gram positive Staphylococcal aureus. Their assay consisted of a sandwich immunoassay that was captured on magnetic beads. Primary antibodies were bound to the magnetic beads' surface. The solution that contained SEB was added, followed by the addition of secondary antibodies labeled with Alexa flour [12]. Figure 8 illustrates the diagram of this assay.

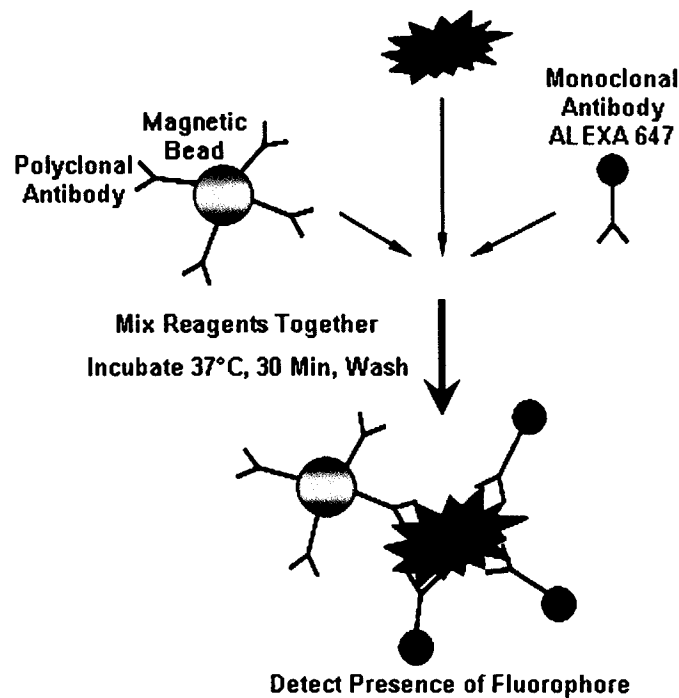


Figure 8. Diagram of SEB detection using a magnetic bead based immunoassay. Modified from original [12].

The experimental results of Alefantis *et al.* indicated that they were able to quantify SEB as low as 100 picograms. They stated that quantitative detection of SEB

utilizing this method had several advantages over conventional existing assays. The assay time was less than 45 minutes, while the sensitivity was increased, which allowed for a very rapid detection. Since the assay utilized magnetic beads, the total sample volume of each assay decreased significantly, making it ideal for high throughput [12].

An enzyme linked electrochemical immunoassay, utilizing immuno-magnetic separation for rapid detection of *Campylobacter jejuni*, was considered by Che *et al.* [13]. They studied eight different types of beads to investigate the optimal capture efficacy of primary anti-C *jejuni*. These included: tosylactivated beads with 4.5 μm and 2.8 μm diameters (T45, T28), sheep anti-rabbit IgG modified beads with 2.8 μm and 1.0 μm diameters (G28, G10), and streptavidin modified beads with 2.8 μm and 1.0 μm diameters (S28, S10). They indicated that streptavidin coated magnetic beads provided adequate binding sites, as well as binding strength (dissociation constant, $K_d = 10^{-15}$) for biotinylated primary antibodies. Also, streptavidin coated magnetic beads had the easiest protocol for binding the antibodies onto them. They concluded that application of this method of detection reduced the assay time from a few days to a few hours; however the detection limit could be improved by enhancing the capture ability of the magnetic beads [13].

A rapid and sensitive chemiluminescent immunoassay for quantitative detection of vitellogenin (Vg) was proposed by Soh *et al.* [5]. They reported that other researchers had studied this antigen utilizing electroimmunoassay, radioimmunoassay, and enzyme-

linked immuno-sorbent assay. The latter assay, the ELISA method that employs a microtiter plate, is commonly used because of its safety and simplicity. However, methods utilizing microtiter plates are very time-consuming. Their immunoassay consisted of primary anti-Vg antibodies immobilized on magnetic beads, the antigen solution containing Vg, and the secondary antibodies that were labeled with horseradish peroxidase (HRP). The response was measured by a chemiluminescence detector upon the reaction between luminol, hydrogen peroxide (H_2O_2), p-iodophenol, and HRP [5]. A schematic representation of their method is shown in Figure 9.

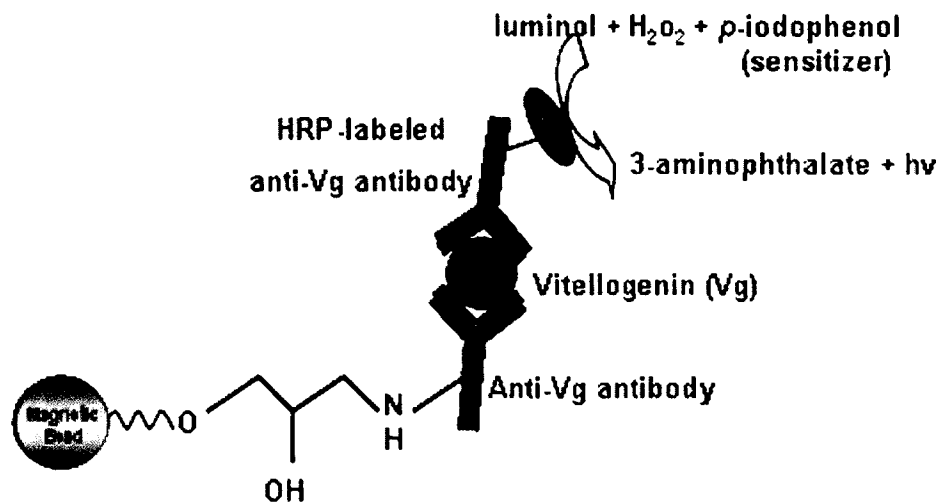


Figure 9. Schematic illustration of the determination of Vg based on the sandwich chemiluminescent immunoassay on magnetic beads. Modified from original [5].

By employing a magnetic chemiluminescent immunoassay, Soh *et al.* were able to obtain a more rapid and slightly more sensitive detection limit of about 2 ng/ml of Vg antigen [5].

For rapid detection of *E. coli*, Gehring *et al.* [14] applied enzyme-linked immuno-magnetic chemiluminescent (ELIMCL). They reported that many methods had been used by other researchers for detection of *E. coli* such as: enzyme-linked immuno-magnetic colorimetry, immuno-magnetic electro-chemiluminescence, polymerase chain reaction with agarose gel electrophoresis, and flow cytometry immuno-magnetic bead separation. However, the ELIMCL method has shown higher sensitivity, as well as a faster assay compared with previously mentioned assays. Their work involved sandwiching the antigen (*E. coli*) between the antibody-coated magnetic beads and the secondary alkaline phosphatase labeled antibodies. Upon the addition of chemiluminescent substrate for the enzyme, the light emitted was measured by a luminometer to quantify the amount of *E. coli* [14]. A schematic representation of this assay is shown in Figure 10.

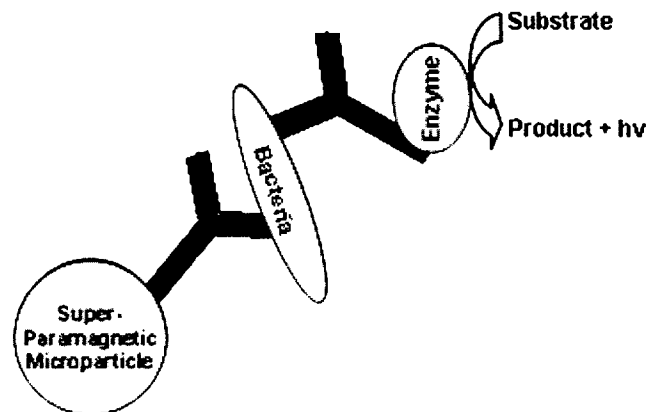


Figure 10. Schematic representation of the enzyme-linked immuno-magnetic chemiluminescent assay. Modified from original [14].

Gehring *et al.* were able to detect about 7.6×10^3 live *E. coli* cells/ml with an assay time of approximately 75 minutes. Their result using this technique was favorably comparable with results applying other techniques [14].

Kim *et al.* [15] utilized laser induced fluorescence magnetic immunoassay (LIFMIA) to detect prion protein diseases (PrP^{Sc}) that are fatal neurodegenerative disorders caused by accumulation of an abnormal prion protein in the central nervous system. Their assay consisted of primary antibodies bounded on magnetic beads mixed with a solution containing the antigen (PrP^{Sc}) and secondary Alexa Flour labeled antibodies. Upon formation of the sandwich immunoassay, the amount of fluorescence could be read by the spectrofluorometer to further quantify the amount of antigen present in the solution [15]. Figure 11 illustrates the diagram of this assay.

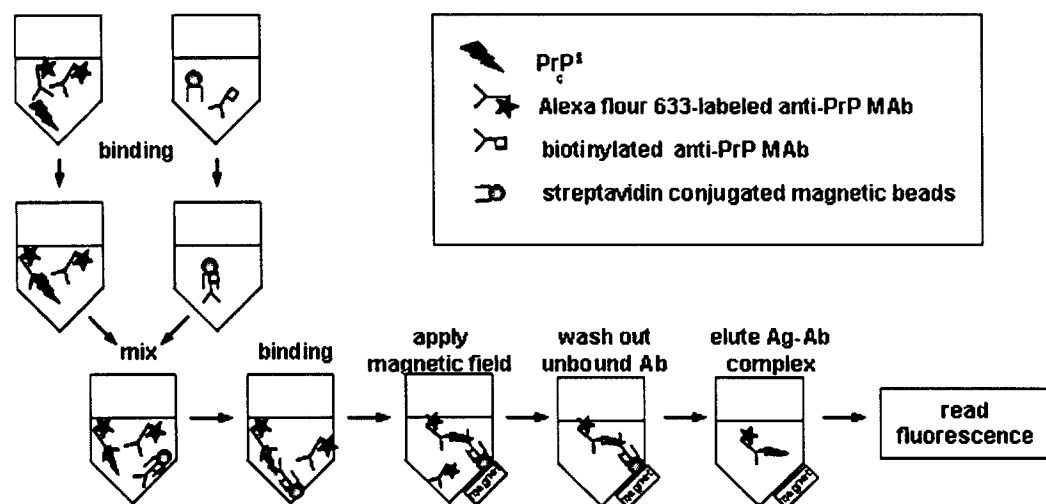


Figure 11. Experimental protocol for LIFMIA. Modified from original [15].

They reported that utilizing the LIFMIA technique increased the specificity, reliability, and rapidity of PrP^{Sc} quantification. They were able to detect 2 ng/ml of antigen (PrP^{Sc}) during a 3 to 4 hour assay time. They included that employing magnetic beads made the assay much faster and easier to handle, resulting in a more prompt diagnostic of the diseases [15].

A novel technique to detect amyloid- β -derived diffusible ligands (ADDLs) was recently developed by Georganopoulou *et al.* [16], which is a soluble pathogenic marker in Alzheimer's disease (AD). The concentrations of this marker are extremely low in the cerebrospinal fluid (CSF) in the early stages of AD, and so they can not be accurately determined by the conventional ELISA method. Their technique was based on a nanoparticle-based detection bio-barcode assay. This assay consisted of magnetic micro particles (MMP) coated with primary antibodies. Then, the antigen (ADDL) to be detected was added, along with gold (Au) nanoparticles (NP). The NPs are pre-coated with secondary antibodies, as well as DNA strands. These DNA strands were made by hybridization between thiolated DNA and bio-barcode DNA, which were complimentary to each other. After the sandwich complex was formed, high temperature was applied to fully dehybridize the bio-barcode DNA strands. These released bio-barcodes were then collected for further quantification by scanometric detection [16]. The schematic diagram of this assay is shown in Figure 12.

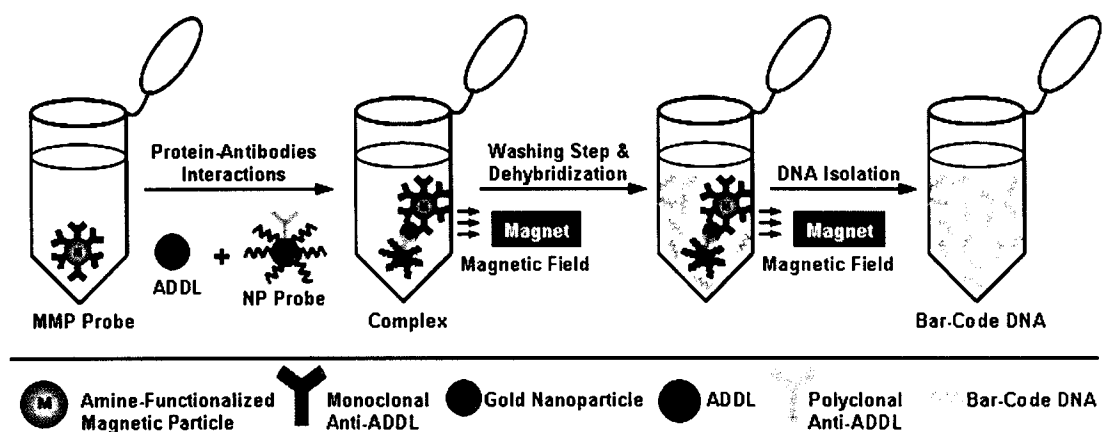


Figure 12. The bio-barcode amplification assay (BCA). Modified from original [16].

Scanometric detection was based on capturing the barcode DNA on a micro array with spots of oligonucleotides that were complementary to half of the barcode DNA sequence. NPs with oligonucleotides that were complementary to the other half of the barcode DNA were hybridized to the captured barcode strands. The signal was enhanced by using silver amplification, and the results were recorded with the Verigene ID system, which measured scattered light intensity from each spot [16,17]. Figure 13 shows schematic representation of this detection technique.

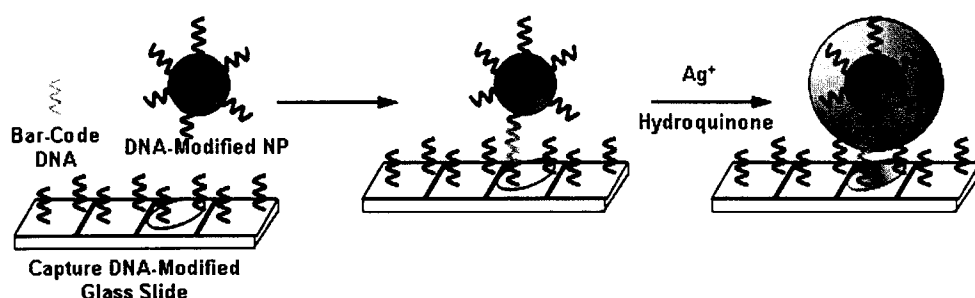


Figure 13. Scanometric detection. Modified from original [16].

Utilizing this unique technique, Georganopoulou *et al.* were able to successfully quantify very low amounts of ADDL for 30 different individuals. Half of them were diagnosed with AD and their results are displayed as squares on the left side in Figure 14. The other half was the negative control population and their results are displayed as triangles on the right side in Figure 14.

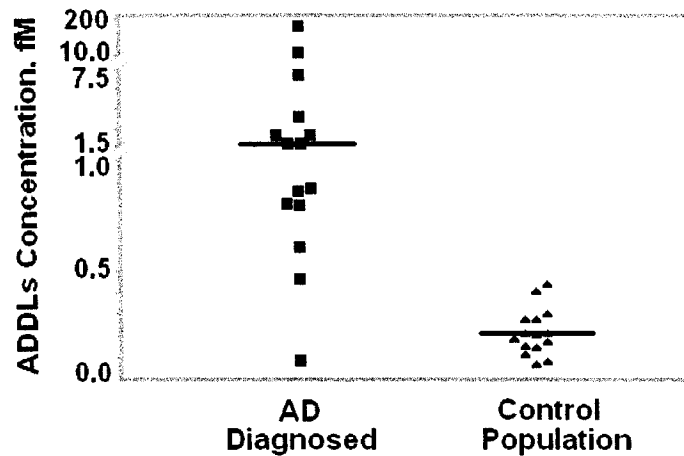
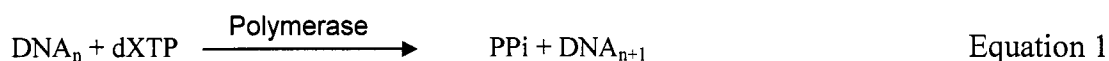


Figure 14. Scatter plot from the scanometric detection of barcode DNA released from the bio-barcode assay for 30 subjects. Modified from original [16].

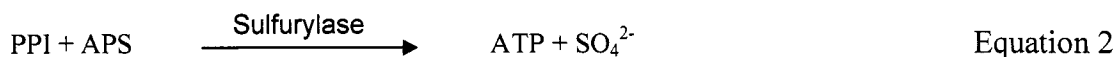
The experimental results of Georganopoulou *et al.* indicated that they were able to detect the ADDL concentration as low as 0.2 femto molar (fM). The highest ADDL concentration in the negative control population was found to be less than 0.5 fM. This immunoassay has several advantages over the conventional techniques. Since the assay was performed in homogenous suspension, faster kinetics for proteins to bind could be obtained. Moreover, the bio-barcode DNA strands were separated from the main sample, so they could be detected by different methods such as gel electrophoresis or electrochemistry. Due to the high sensitivity of this assay, a more reliable and low cost detection for early diagnosis of AD can be achieved. The most important benefit is that the assay has the potential to simultaneously detect and quantify different proteins in CSF [16,17].

2.3 Pyrosequencing Method

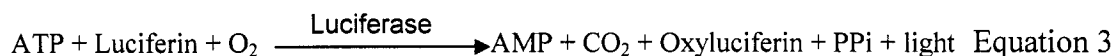
DNA sequencing, which is the analysis of genes at the nucleotide level, has become a robust technique in the field of molecular biology. Sanger DNA sequencing was the first sequencing technique performed around two decades ago. Due to the limitation of this technique regarding its throughput, as well as cost, several other methods have been proposed. These include sequencing by synthesis, sequencing by hybridization, and parallel bead array. Recently, Ronaghi *et al.* [6] invented a new technique for DNA sequencing called pyrosequencing. This technique is currently one of the fastest methods for DNA sequencing. This real-time bioluminometric method consists of a series of enzymatic reactions. Two different types of pyrosequencing have been proposed by Ronaghi, which include the three-enzyme system and four-enzyme system [6]. In the four-enzyme system, an inorganic pyrophosphate (PPi) is released due to the nucleic acid polymerization. Equation 1 is the corresponding reaction, where dXTP is deoxynucleotide triphosphate.



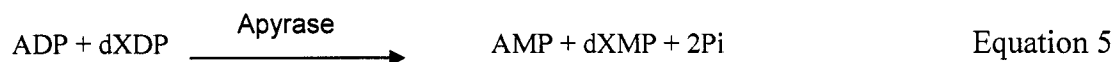
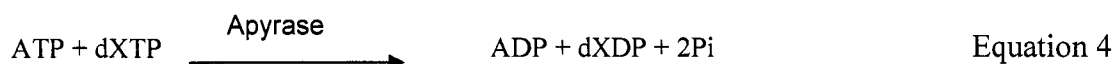
The released PPi is then converted to ATP by Sulfurylase. This reaction is shown in Equation 2, where APS is adenosine phosphosulfate.



The generated ATP is sensed by Luciferase, which produces light energy that is directly proportional to the amount of incorporated nucleotides. Equation 3 is the corresponding reaction, where AMP is adenosine monophosphate.



Un-reacted nucleotides and the generated ATP are degraded by Apyrase for further stepwise addition of nucleotides to the reaction. These reactions are shown in Equations 4 and 5, where Pi is inorganic phosphate.



Ronaghi *et al.* reported that the overall reaction takes place within 4 seconds, while 1 pmol of DNA at 560 nanometers wavelength, releases 6×10^9 photons. Since the added nucleotide is known, the sequence of the template can be determined [6]. Figure 15 shows the schematic representation of pyrosequencing technique.

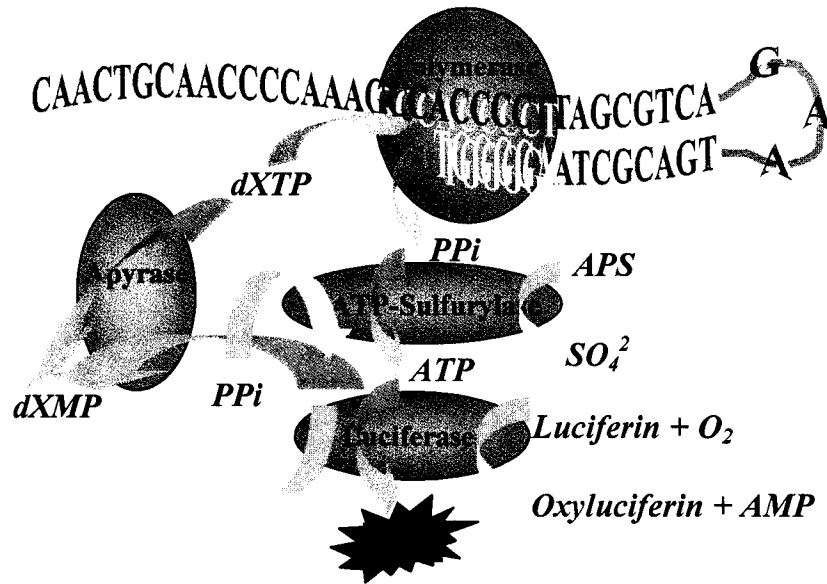


Figure 15. Schematic representation of the progress of four-enzyme system.

Figure 16 illustrates the results Ronaghi *et al.* obtained from the pyrosequencing software, where the generated light from the third reaction is detected and recorded in a form of a peak signal [6]. Consequently, the unknown sequence was determined by the magnitude of each recorded signal.

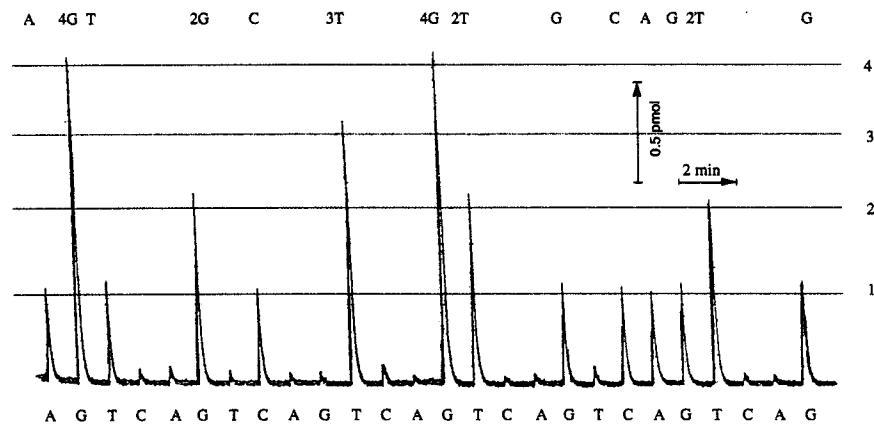


Figure 16. Pyrogram of the raw data obtained from four-enzyme pyrosequencing. Modified from original [6].

According to Figure 15, the unknown sequence to be identified is: 5'-CAACTGCAACCCCAAAGCCACCCCT. During the pyrosequencing technique, the reverse complementary sequence of the unknown sequence is synthesized as shown in Figure 16, which is: 3'-GTTGACGTTGGGGTTTCGGTGGGGA. By knowing the complementary sequence, the unidentified sequence can be easily determined. Pyrosequencing technique yields very quantitative signals, which can be used for different applications such as genotyping, resequencing of diseased genes, and determining sequence of difficult secondary DNA structure [6,18].

2.4 Summary

Different sandwich immunoassays with different detection techniques were discussed by reviewing available and nearly related literatures. However, one common topic that most of the reviewed literatures lacked was the potential for multi-plexing. Only one type of antigen per each assay could be detected and quantified. A novel method that has not been studied was considered within the scope of this research. Sandwich complexes of antigens between matching antibodies were captured on magnetic beads, and pyrosequencing technique was employed to quantitatively detect the antigen type. This method allows for multi-plexing through the use of individual pyro-tags for different antigens captured between different matching antibodies.

CHAPTER THREE RESEARCH HYPOTHESIS AND OBJECTIVES

3.1 Research Hypothesis

The hypothesis of this study is that the intensity of light produced during pyrosequencing onto specific pyro-tags will vary quantitatively with the amount of captured antigen if such pyro-tags are attached to the secondary antibody of a sandwich immunocomplex. Thus, the generated light intensity can be measured to quantify the concentration of captured antigen.

3.2 Research Objectives

The first objective of this research is to develop an assay in which primary antibodies will be captured onto the surface of magnetic beads. These will be referred to as capturing complexes. In the second objective, unique pyro-tags will be attached to secondary antibodies through binding median molecules. These will be referred to as detection complexes. The third objective will be to form immunocomplexes by capturing the antigens between capturing complexes and detection complexes. Pyrosequencing technique will be used to detect and quantify the captured antigen.

Throughout the assay, a key objective will be to optimize the process of constructing immunocomplexes in order to produce a high signal response with minimum

background noise. Maximizing the signal-to-noise ratio will be a crucial factor in detecting low concentration of antigens.

Multiple immunocomplexes for capturing multiple antigens will be made in one solution. Pyrosequencing technique will be used for simultaneous detection and quantification of multiple antigens. This will be referred to as multi-plexing, and will be the final objective of this research.

CHAPTER FOUR EXPERIMENTAL METHODS AND MATERIALS

The overall scope of this thesis is to quantitatively detect single and multiple proteins by pyrosequencing technique. Numerous experimental steps were taken that progressed into the main method. The accomplished methods are described in detail in the subsequent sections; however, the prior steps are briefly mentioned in Appendix A. Each experiment was designed based on the results of previous experiments. First, the Multiple Applications (MA) pyrosequencing machine was employed for quantitative detections of IL-8, IL-4, and IL-10 proteins. Next, multi-plex detections between three different combinations of the mentioned protein pairs were performed. The MA pyrosequencing machine was replaced by the High Sensitivity (HS) pyrosequencing machine to enhance assay sensitivity. Employing the HS pyrosequencing machine, single quantitative detection of IL-8 was carried out to obtain the best possible results.

4.1 Materials and Methods

4.1.1 Single Human IL-8 Detection Using MA Pyrosequencing Machine

The experiment of this section was designed to detect and quantify the human IL-8 antigen. This protein plays an important role in tumor growth, angiogenesis, and metastasis, and thus the initial experimental results would be of interest.

4.1.1.1 Experimental Design for Detecting IL-8 Using MA Machine

The experiment to quantitatively detect IL-8 was conducted according to Table 1. In this design, all samples had 50 pmol of capturing antibody. This amount was determined in accordance to the initial tests detailed in Appendix A. For each sample, different antigen concentrations were tested to measure the generated signal intensities in hopes of obtaining a quantitative correlation. In run 3, the amount of detection antibody was decreased while the antigen concentration was kept constant to determine how much detection antibody could be saved in order to lower the assay cost without sacrificing a drop in signal intensity. 160 ng/ml of antigen concentration was tested in runs 1, 2, 4, and 5 to determine the reproducibility of the assay. Run 3 was not included in testing the repeatability because different detection antibody levels were being tested with constant antigen concentration. Experiments in which no antigen was present were conducted to find the background noise signal. All runs were performed separately on different days.

Table 1. Experimental design to determine signal intensities for quantitatively detecting IL-8 antigen.

Run No.	Capturing Ab (Mole)	Ag (Mole)	Ag Concentration	Detection Ab (Mole)	Light Intensity
1	50 pmol	2 pmol	160 ng/ml	50 pmol	✓
		0.5 pmol	40 ng/ml		✓
		0.25 pmol	20 ng/ml		✓
2	50 pmol	10 pmol	800 ng/ml	50 pmol	✓
		2 pmol	160 ng/ml		✓
3	50 pmol	2 pmol	160 ng/ml	50 pmol	✓
				25 pmol	✓
				10 pmol	✓
				5 pmol	✓
4	50 pmol	2 pmol	160 ng/ml	10 pmol	✓
5	50 pmol	2 pmol	160 ng/ml	10 pmol	✓
6	50 pmol	0 pmol	0 ng/ml	50 pmol	✓

4.1.1.2 Materials for Detecting IL-8 Using MA Machine

- Dynabeads M-270 carboxylic acid super paramagnetic beads (DynaL Biotech)
- Human IL-8 monoclonal antibody (Pierce)
- Human IL-8 monoclonal antibody, biotin-labeled (Pierce)
- Recombinant human IL-8, MW ~8 kilo Dalton (Pierce)
- N-hydroxysuccinimide: NHS, MW 115.09 (Sigma-Aldrich)
- 1-ethyl-3-(3-dimethylaminopropyl) carbodiimide hydrochloride (EDC) MW 191.7 (Sigma-Aldrich)
- 25 mM MES buffer (2-[N-Morpholino] ethanesulfonic acid), MW 213.25, pH 5 (Sigma)
- 0.01 M Phosphate Buffered Saline (PBS), (0.138 M NaCl, 0.0027 M KCl) with 1% Bovine Serum Albumin (BSA), pH 7.4 (Sigma)

- 0.01 M Phosphate Buffered Saline (PBS), (0.138 M NaCl, 0.0027 M KCl), pH 7.4 (Sigma)
- 1.0 M Tris acetate EDTA buffer (TAE), pH 7.6
- 0.02 % (w/v) sodium azide
- Pyro-tag Sequence: 100 μ M Oligo in Tris-EDTA Buffer
 - 5' Biotin C6CCCCCTTTTGGGGGCCCCCGTCGTTTTACAACGGAAC
GTTGTAAAACGACGG: b-CTGC (Stanford Genome Technology Center)
- Streptavidin (Sigma-Aldrich)
- Bovine Serum Albumin (BSA)
- Pyrosequencing Reagents: Enzyme mixture, Substrate mixture, Nucleotides (Pyrosequencing AB)

4.1.1.3 Experimental Procedures for Detecting IL-8 Using MA Machine

To prepare the capturing complex, Dynabeads M-270 carboxylic acid super paramagnetic beads with 2.8 μ m diameter were used as the surface. These beads can be manipulated when a magnetic field is applied. They need to be activated with a carbodiimide followed by coupling of an amine containing ligand, which results in a stable amide bond between the ligand and the bead. The beads were supplied in an aqueous suspension containing 2×10^9 beads per ml (approximately 30 mg/ml). According to the manufacturer's protocol, 20 μ g of protein can be coated onto the surface of 1 mg of beads. This ratio was confirmed by calculating the theoretical limit of

antibody to bead ratio, as detailed in Appendix B. Capturing complexes were always prepared in big batches of 100 μ l, 200 μ l or more, depending on the number of samples (each sample needs 12.5 μ l). Theoretically, each 100 μ l batch should be enough for eight samples; however, due to pipetting loss each 100 μ l is enough for only seven samples. So, to make a batch of 100 μ l capturing complex, 100 μ l of beads were transferred into a microcentrifuge tube, which was then placed on a Dynal MPC (magnetic particle concentrator). The supernatant was removed by a pipette while the tube remained on the magnet. Next, the beads were washed twice with 100 μ l of 25mM MES buffer for ten minutes and the supernatant was decanted. Immediately before use, EDC and NHS were dissolved in cold 25 mM MES to a concentration of 50 mg/ml. 50 μ l of EDC solution and 50 μ l of NHS solution were added to the washed beads. The sample was mixed well and incubated for 30 minutes on the tube rotator. After incubation the sample was placed on the magnet for four minutes and the supernatant was removed. Next, the beads were washed twice with 100 μ l MES and then they were activated and ready to be coated with the capturing antibody. As calculated in Appendix B, 60.2 μ l of human IL-8 monoclonal antibody (60 μ g or 400 pmol) with concentration of 0.996 mg/ml plus 39.8 μ l MES buffer were added to the beads. The beads were vortexed to ensure proper mixing, and then the sample was incubated for at least 30 minutes on the tube rotator. After incubation the tube was placed on the magnet for four minutes and the supernatant was removed. The beads were washed a total of four times with the PBS-BSA and TAE buffers and resuspended in 100 μ l of PBS-BSA buffer. As a bacteriostatic agent, 1 μ l sodium azide (0.02 % w/v) was added to the sample. The capturing complex batch was

then refrigerated until further use. A simple representation of this complex is shown in Figure 17.

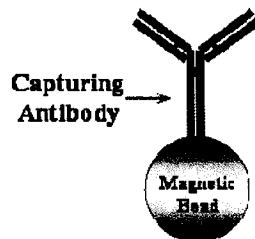


Figure 17. Capturing complex.

In order to make the detection complex, b-CTGC pyro-tags were attached to the detection antibody through streptavidin (SA), which acted as an intermediate binding molecule. Considering the molecular size and structure of the antibody, SA, and pyro-tag, the optimized molar ratio to construct the detection complex was determined to be 1:2:10 respectively to allow for the likelihood of having three pyro-tags per each antibody. As indicated in Table 1, for each run a batch of detection complex specific for that run was prepared. For example, all samples of run 1 had 50 pmol of detection antibody, whereas in run 3 the detection antibody was decreased for each sample. To make a detection complex with 50 pmol of detection antibody, 15 μ l biotinylated human IL-8 monoclonal antibody (50 pmol) with concentration of 0.5 mg/ml was mixed with 5 μ l SA (100 pmol) that had been dissolved in the PBS buffer with concentration of 20 μ M. This mixture was placed into a microcentrifuge tube and incubated for 30 minutes on the tube rotator. Afterward, 5 μ l of b-CTGC (500 pmol) was added to the mixture and the sample was incubated for one hour on the tube rotator. Thus, the remaining biotin binding sites of the SA were used to couple b-CTGC pyro-tags making the detection

complex ready for use. Note that in a previous method, described in Appendix A, free biotin was added to the capturing and detection complexes. Streptavidin has a high binding affinity for biotin, and was present in both complexes. The capturing antibodies used in the previous method were biotinylated. Therefore free biotin was added to ensure that all biotin binding sites of streptavidin molecules were coupled with biotin and non-specific bindings between the complexes would be prevented. However, in this method the magnetic beads were coated with carboxylic acid and the capturing antibodies were not biotinylated. Thus, the addition of free biotin to the complexes was no longer required. A schematic representation of the detection complex is shown in Figure 18.

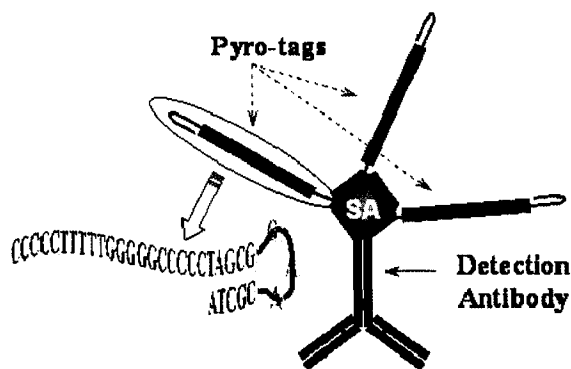


Figure 18. Detection complex.

The whole immunocomplex was formed by adding the solution that contained the antigen to the capturing complex, followed by the addition of the detection complex. The antigen was then captured and sandwiched between the two antibodies and detected by the pyrosequencing technique. The capturing complex batch was divided in a manner to obtain 50 pmol of capturing antibody in each sample. To accomplish this, 12.5 μ l of the capturing complex was transferred into a tube, placed on the magnet, and washed twice for five minutes with 100 μ l of PBS buffer. The recombinant human IL-8 antigen was

supplied with a 25 $\mu\text{g}/\text{ml}$ concentration and was diluted in the PBS-1%BSA buffer. For the first sample of run 2, 8 μl of the antigen with concentration of 10 $\mu\text{g}/\text{ml}$ (10 pmol) mixed with 92 μl PBS buffer was added to the washed capturing complex and the mixture was incubated for one hour on the tube rotator. For the rest of the samples, the antigen solution was prepared in a serial dilution to the desired concentrations. Note that for each sample, the total volume of antigen with PBS buffer was always kept at 100 μl to keep the sample volume constant throughout all experiments. The tube was placed on the magnet for four minutes and the beads were washed a total of three times with 100 μl of PBS buffer. For samples that had 50 pmol of detection antibody, 25 μl of the prepared detection complex was added to the beads. The sample volume was increased to 100 μl by adding 75 μl of PBS buffer, and the mixture was incubated for one hour on the tube rotator. For samples that had less than 50 pmol of detection antibody, lower volume of the detection complex was added; however, the total volume was always kept at 100 μl with the addition of PBS buffer. Finally, the sample was placed on the magnet, washed once with 100 μl of PBS buffer, washed once more with 100 μl of DI water, and resuspended in 40 μl of DI water. Figure 19 illustrates the whole immunocomplex captured on magnetic beads.

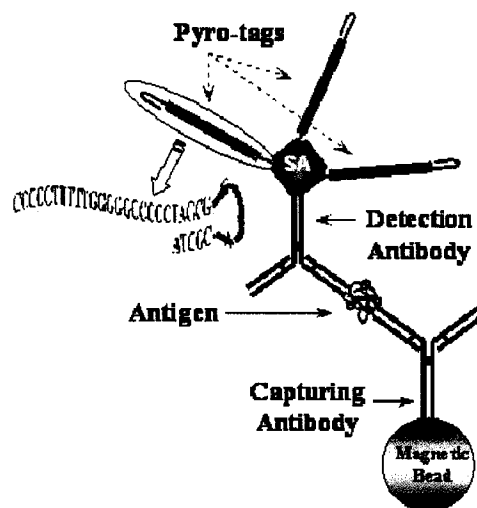


Figure 19. Immunocomplex captured on magnetic beads.

A 40 μl solution containing the immunocomplex captured on magnetic beads was transferred into a single well of a 96-well microtiter plate. Next, 5 μl of substrate mixture (Luciferin, Adenosine 5' Phosphosulfate) and 5 μl of enzyme mixture (DNA Polymerase, ATP Sulfurylase, Luciferase, Apyrase) were added to each well. An inkjet cartridge was filled with 50 μl of nucleotides (dATP α S, dGTP, dCTP, dTTP) and was inserted into the pyrosequencing machine along with the microtiter plate. The machine's software program was then adjusted to the desired settings and the run was performed.

4.1.2 Single Human IL-4 Detection Using MA Pyrosequencing Machine

The experiment of this section was designed to detect and quantify the human IL-4 antigen. The IL-4 antibody-antigen system had to be tested to be employed in the multi-plexing experiments. This protein has many actions on a variety of cell types, such

as endothelial cells, T cells, B cells, monocytes, and fibroblasts. It also regulates the inflammatory response.

4.1.2.1 Experimental Design for Detecting IL-4 Using MA Machine

The experiment to quantitatively detect IL-4 was conducted according to Table 2. In this design, all samples had 50 pmol of capturing antibody as it was found to be a convenient amount according to earlier experiments. For each sample, different antigen concentrations were tested to measure the generated signal intensities in hopes of obtaining a quantitative correlation. In run 3, the amount of detection antibody was decreased while the antigen concentration was kept constant to determine how much detection antibody could be saved in order to lower the assay cost without sacrificing a drop in signal intensity. 280 ng/ml of antigen concentration was tested in runs 1, 2, 4, and 5 to determine the reproducibility of the assay. Run 3 was not included in testing the repeatability because different detection antibody levels were being tested with constant antigen concentration. Experiments in which no antigen was present were conducted to find the background noise signal. All runs were performed separately on different days.

Table 2. Experimental design to determine signal intensities for quantitatively detecting IL-4 antigen.

Run No.	Capturing Ab (Mole)	Ag (Mole)	Ag Concentration	Detection Ab (Mole)	Light Intensity
1	50 pmol	2 pmol	280 ng/ml	50 pmol	✓
		1 pmol	140 ng/ml		✓
		0.5 pmol	70 ng/ml		✓
2	50 pmol	50 pmol	7000 ng/ml	50 pmol	✓
		2 pmol	280 ng/ml		✓
3	50 pmol	2 pmol	280 ng/ml	50 pmol	✓
				25 pmol	✓
				10 pmol	✓
				5 pmol	✓
4	50 pmol	2 pmol	280 ng/ml	25 pmol	✓
5	50 pmol	2 pmol	280 ng/ml	25 pmol	✓
6	50 pmol	0 pmol	0 ng/ml	50 pmol	✓

4.1.2.2 Materials for Detecting IL-4 Using MA Machine

- Monoclonal anti-human IL-4 antibody (R&D Systems)
- Biotinylated anti-human IL-4 antibody (R&D Systems)
- Recombinant human IL-4, MW ~14 kilo Dalton (R&D Systems)
- Tris Buffered Saline (20 mM Trizma base, 150 mM NaCl) with 0.1% BSA, pH 7.3
- Pyro-tag Sequence: 100 μ M Oligo in Tris-EDTA Buffer
 - 5'BiotinC6CCCCCTTTTCCCCCAAAAACCGTCGTTTTACAACGGAAC
GTTGTAAAACGACGG: b-CTCA (Stanford Genome Technology Center)

Except for the antibody-antigen pair and the pyro-tag, all other reagents used were the same as the reagents mentioned in section 4.1.1.2.

4.1.2.3 Experimental Procedures for Detecting IL-4 Using MA Machine

IL-4 capturing complex was prepared exactly the same way as IL-8 capturing complex, except for the addition of the capturing antibody. The IL-4 capturing antibody had a 500 µg/ml concentration; therefore, for each batch of 100 µl capturing complex, 120 µl of human IL-4 monoclonal antibody (60 µg or 400 pmol) was added to the beads.

In order to make the detection complex, b-CTCA pyro-tags were attached to the detection antibody through streptavidin, with the molar ratio of Ab:SA:b-CTCA as 1:2:10 respectively. The biotinylated human IL-4 monoclonal antibody was provided in a lyophilized form and reconstituted in Tris buffered saline to 100 µg/ml concentration. As indicated in Table 2, for each run a batch of detection complex specific for that run was prepared. For example, all samples of run 1 had 50 pmol of detection antibody, whereas in run 3 the detection antibody was decreased for each sample. To make a detection complex with 50 pmol of detection antibody, 75 µl biotinylated human IL-4 monoclonal antibody (50 pmol) was mixed with 5 µl SA (100 pmol). This mixture was placed into a microcentrifuge tube and incubated for 30 minutes on the tube rotator. Next, 5 µl b-CTCA (500 pmol) was added to the mixture and the sample was incubated for one hour on the tube rotator.

The whole IL-4 immunocomplex was constructed exactly the same way as the IL-8 immunocomplex, which is explained in section 4.1.1.3. The recombinant human IL-4

antigen was supplied in lyophilized condition and was reconstituted in a PBS buffer with 0.3% BSA to 10 $\mu\text{g/ml}$ concentration. For the first sample of run 2, 70 μl of the antigen with concentration of 10 $\mu\text{g/ml}$ (50 pmol) mixed with 30 μl PBS buffer was added to the washed capturing complex and the mixture was incubated for one hour on the tube rotator. For the rest of the samples, the antigen solution was prepared in a serial dilution to the desired concentrations. Again, the total volume of antigen with PBS buffer was kept constant at 100 μl . The tube was placed on the magnet for four minutes and the beads were washed a total of three times with 100 μl of PBS buffer. For samples that had 50 pmol of detection antibody, 85 μl of the prepared detection complex was added to the beads, the sample volume was increased to 100 μl by adding 15 μl of PBS buffer, and the mixture was incubated for one hour on the tube rotator. For samples that had less than 50 pmol of detection antibody, lower volume of the detection complex was added; however, the total volume was always kept at 100 μl with the addition of PBS buffer. Finally, the sample was placed on the magnet, washed once with 100 μl of PBS buffer, washed once more with 100 μl of DI water, and resuspended in 40 μl of DI water. The rest of the procedure was performed the same as the procedure explained in section 4.1.1.3.

4.1.3 Single Human IL-10 Detection Using MA Pyrosequencing Machine

The experiment of this section was designed to detect and quantify the human IL-10 antigen. The IL-10 antibody-antigen system had to be tested to be employed in the

multi-plexing experiments. This protein stimulates growth of B cells, mast cells, and thymocytes. It also regulates the immune response.

4.1.3.1 Experimental Design for Detecting IL-10 Using MA Machine

The experiment for detection and quantification of IL-10 was conducted according to Table 3. For consistency with previous experiments, all samples had 50 pmol of capturing antibody. For each sample in run 1, different antigen concentrations were tested to measure the generated signal intensities in hopes of obtaining a quantitative correlation. As indicated in the last column of run 1, each sample was tested twice with the exception of 744 ng/ml antigen concentration that was tested four times to determine the reproducibility of the assay. In run 2, the amount of detection antibody was decreased while the antigen concentration was kept constant to determine how much detection antibody could be saved in order to lower the assay cost without sacrificing a drop in signal intensity. Experiments in which no antigen was present were conducted to find the background noise signal. All runs were performed separately on different days.

Table 3. Experimental design to determine signal intensities for quantitatively detecting IL-10 antigen.

Run No.	Capturing Ab (Mole)	Ag (Mole)	Ag Concentration	Detection Ab (Mole)	Light Intensity
1	50 pmol	100 pmol	18600 ng/ml	50 pmol	✓(2)
		50 pmol	9300 ng/ml		✓(2)
		25 pmol	4650 ng/ml		✓(2)
		10 pmol	1860 ng/ml		✓(2)
		4 pmol	744 ng/ml		✓(4)
		2 pmol	372 ng/ml		✓(2)
		1 pmol	186 ng/ml		✓(2)
		0.5 pmol	93 ng/ml		✓(2)
		2	50 pmol		2 pmol
25 pmol	✓				
10 pmol	✓				
5 pmol	✓				
3	50 pmol	0 pmol	0 ng/ml	50 pmol	✓

4.1.3.2 Materials for Detecting IL-10 Using MA Machine

- Human IL-10 monoclonal antibody (Pierce)
- Anti-human IL-10, monoclonal antibody, biotin-labeled (Pierce)
- Recombinant human IL-10, MW ~18.6 kilo Dalton (Pierce)
- Pyro-tags Sequences: 100 μ M Oligo in Tris-EDTA Buffer
 - 5'BiotinC6CCCCCTTTTTCCCCCAAAAACCGTCGTTTTACAACGGAAC
GTTGTAAAACGACGG: b-CTCA (Stanford Genome Technology Center)
 - 5'BiotinC6CCCCCTTTTTGGGGGCCCCCGTCGTTTTACAACGGAAC
GTTGTAAAACGACGG: b-CTGC (Stanford Genome Technology Center)

Except for the antibody-antigen pair and the pyro-tags, all other reagents used were the same as the reagents mentioned in section 4.1.1.2.

4.1.3.3 Experimental Procedures for Detecting IL-10 Using MA Machine

IL-10 capturing complex was prepared exactly the same way as the other capturing complexes except for the addition of the capturing antibody. The IL-10 capturing antibody had a 1.04 mg/ml concentration; therefore, for each batch of 100 μ l capturing complex, 57.7 μ l of human IL-10 monoclonal antibody (60 μ g or 400 pmol) was added to the beads.

To make the detection complex, b-CTCA pyro-tag was used for runs 1 and 2, and b-CTGC pyro-tag was used for run 3. The molar ratio of Ab:SA:b-pyro-tag was 1:2:10 respectively. As indicated in Table 3, for each run a batch of detection complex specific for that run was prepared. For example, all samples of runs 1 and 3 had 50 pmol of detection antibody, whereas in run 2 the detection antibody was decreased for each sample. To make a detection complex with 50 pmol of detection antibody, 15 μ l biotinylated of human IL-10 monoclonal antibody (50 pmol) with concentration of 0.5 mg/ml was mixed with 5 μ l SA (100 pmol). This mixture was placed into a microcentrifuge tube and incubated for 30 minutes on the tube rotator. Next, 5 μ l biotinylated pyro-tag (500 pmol) was added to the mixture and the sample was incubated for one hour on the tube rotator.

The whole IL-10 immunocomplex was constructed exactly the same way as the other immunocomplexes. The recombinant human IL-10 antigen was supplied in

lyophilized condition and was reconstituted first in DI water and then diluted in a PBS buffer with 1% BSA to 50 $\mu\text{g/ml}$ concentration. For the first sample of run 3, 37.2 μl of the antigen with concentration of 50 $\mu\text{g/ml}$ (100 pmol) mixed with 62.8 μl PBS buffer was added to the washed capturing complex and the mixture was incubated for one hour on the tube rotator. For the rest of the samples, the antigen solution was prepared in a serial dilution to the desired concentrations. The total volume of antigen with PBS buffer was kept constant at 100 μl . The tube was placed on the magnet for four minutes and the beads were washed a total of three times with 100 μl of PBS buffer. For samples that had 50 pmol of detection antibody, 25 μl of the prepared detection complex was added to the beads, the sample volume was increased to 100 μl by adding 75 μl of PBS buffer, and the mixture was incubated for one hour on the tube rotator. For samples that had less than 50 pmol of detection antibody, lower volume of the detection complex was added; however, the total volume was always kept at 100 μl with the addition of PBS buffer. Finally, the sample was placed on the magnet, washed once with 100 μl PBS buffer, washed once more with 100 μl DI water, and resuspended in 40 μl of DI water. The rest of the procedure was performed the same as the procedure explained in section 4.1.1.3.

4.1.4 Multi Protein Detection of IL-8 and IL-4 Using MA Pyrosequencing Machine

The experiment of this section was designed to quantitatively detect multiple proteins in a single sample. As stated in chapter one of this thesis, simultaneous detection and quantification of multiple proteins is the true significance of this research.

This experiment is the first multi-plexing experiment in which the combination of IL-8 and IL-4 proteins was tested.

4.1.4.1 Experimental Design for Multi-plexing IL-8 and IL-4 Using MA Machine

The experiments for simultaneous detection and quantification of IL-8 and IL-4 antigens were conducted according to Tables 4 and 5. In Table 4, samples (a) and (d) were single-plex detection of the proteins. In sample (a), 2 pmol of IL-8 antigen was added to the IL-8 capturing complex, and then IL-8 detection complex was added to detect the antigen. In sample (d), 2 pmol of IL-4 antigen was added to the IL-4 capturing complex, and then IL-4 detection complex was added to detect the antigen. Samples (b) and (c) were control samples to check for cross reactivity. For example, in sample (b), 2 pmol of IL-8 antigen was added to the IL-4 capturing complex, and then IL-4 detection complex was added to detect the occurrence of cross reactivity. Other permutations were omitted as seen in Table 4. Sample (e) was the multi-plex detection of the proteins.

Table 4. Experimental design to determine signal intensities and cross reactivities for multi-plex detection of IL-8 and IL-4 antigens.

Ag IL-8 (2 pmol)	Detection Complex IL-8 (10 pmol)	Detection Complex IL-4 (25 pmol)
Capturing Complex IL-8 (50 pmol)	✓(+) ^a	
Capturing Complex IL-4 (50 pmol)		✓(-) ^b
Ag IL-4 (2 pmol)	Detection Complex IL-8 (10 pmol)	Detection Complex IL-4 (25 pmol)
Capturing Complex IL-8 (50 pmol)	✓(-) ^c	
Capturing Complex IL-4 (50 pmol)		✓(+) ^d
Ag IL-8 (2 pmol) + Ag IL-4 (2 pmol)	Detection Complex IL-8 (10 pmol)	Detection Complex IL-4 (25 pmol)
Capturing Complex IL-8 (50 pmol)	✓(Multi-Plex) ^e	
Capturing Complex IL-4 (50 pmol)		

In Table 5, samples (a) and (h) were single-plex detection of the proteins, whereas samples (b) through (g) were all control samples to check for cross reactivity. Finally, sample (i) was the multi-plex detection of the proteins. All capturing and detection antibody amounts were based on the single detection experiments. The generated signal intensities were measured in all samples to detect and quantify both antigens simultaneously.

Table 5. Experimental design to determine signal intensities and all combinations of cross reactivity for multi-plex detection of IL-8 and IL-4 antigens.

Ag IL-8 (2 pmol)	Detection Complex IL-8 (10 pmol)	Detection Complex IL-4 (25 pmol)
Capturing Complex IL-8 (50 pmol)	✓(+) a	✓(-) b
Capturing Complex IL-4 (50 pmol)	✓(-) c	✓(-) d
Ag IL-4 (2 pmol)	Detection Complex IL-8 (10 pmol)	Detection Complex IL-4 (25 pmol)
Capturing Complex IL-8 (50 pmol)	✓(-) e	✓(-) f
Capturing Complex IL-4 (50 pmol)	✓(-) g	✓(+) h
Ag IL-8 (2 pmol) + Ag IL-4 (2 pmol)	Detection Complex IL-8 (10 pmol)	Detection Complex IL-4 (25 pmol)
Capturing Complex IL-8 (50 pmol)	✓(Multi-Plex) i	
Capturing Complex IL-4 (50 pmol)		

4.1.4.2 Experimental Procedures for Multi-plexing IL-8 and IL-4 Using MA Machine

The procedure of making all capturing and detection complexes precisely followed the procedures explained in previous sections. b-CTGC pyro-tags were attached to the IL-8 detection complex and b-CTCA pyro-tags were attached to the IL-4 detection complex. Samples (e) in Table 4 and sample (i) in Table 5 were the multi-plex detection of the proteins. To make these samples, 2 pmol of both antigens were added to both capturing complexes in a single tube, and after incubation and washing steps, both detection complexes were added to detect and quantify both antigens.

4.1.5 Multi Protein Detection of IL-4 and IL-10 Using MA Pyrosequencing Machine

The experiment of this section was designed to quantitatively detect multiple proteins in a single sample. This experiment is the second multi-plexing experiment in which the combination of IL-4 and IL-10 proteins was tested.

4.1.5.1 Experimental Design for Multi-plexing IL-4 and IL-10 Using MA Machine

The experiment for simultaneous detection and quantification of IL-4 and IL-10 antigens was conducted according to Table 6. In Table 6, samples (a) and (h) were single-plex detection of the proteins. In sample (a), 2 pmol of IL-4 antigen was added to the IL-4 capturing complex, and then IL-4 detection complex was added to detect the antigen. In sample (h), 10 pmol of IL-10 antigen was added to the IL-10 capturing complex, and then IL-10 detection complex was added to detect the antigen. Samples (b) through (g) were control samples to check for cross reactivity. For example, in sample (b), 2 pmol of IL-4 antigen was added to the IL-4 capturing complex, and then IL-10 detection complex was added to detect the occurrence of cross reactivity. Sample (i) was the multi-plex detection of the proteins. All capturing and detection antibody amounts were based on the single detection experiments. The generated signal intensities were measured in all samples to detect and quantify both antigens simultaneously.

Table 6. Experimental design to determine signal intensities and cross reactivities for multi-plex detection of IL-4 and IL-10 antigens.

Ag IL-4 (2 pmol)	Detection Complex IL-4 (25 pmol)	Detection Complex IL-10 (50 pmol)
Capturing Complex IL-4 (50 pmol)	✓(+) ^a	✓(-) ^b
Capturing Complex IL-10 (50 pmol)	✓(-) ^c	✓(-) ^d
Ag IL-10 (10 pmol)	Detection Complex IL-4 (25 pmol)	Detection Complex IL-10 (50 pmol)
Capturing Complex IL-4 (50 pmol)	✓(-) ^e	✓(-) ^f
Capturing Complex IL-10 (50 pmol)	✓(-) ^g	✓(+) ^h
Ag IL-4 (2 pmol) + Ag IL-10 (10 pmol)	Detection Complex IL-4 (25 pmol)	Detection Complex IL-10 (50 pmol)
Capturing Complex IL-4 (50 pmol)	✓(Multi-Plex) ⁱ	
Capturing Complex IL-10 (50 pmol)		

4.1.5.2 Experimental Procedures for Multi-plexing IL-4 and IL-10 Using MA Machine

The procedure of making all capturing and detection complexes precisely followed the procedures explained in previous sections. b-CTCA pyro-tags were attached to the IL-4 detection complex and b-CTGC pyro-tags were attached to the IL-10 detection complex. Sample (i) was the multi-plex detection of both IL-4 and IL-10 proteins. To make this sample, 2 pmol of IL-4 antigen and 10 pmol of IL-10 antigen were added to both capturing complexes in a single tube, and after incubation and washing steps, both detection complexes were added to detect and quantify both antigens.

4.1.6 Multi Protein Detection of IL-8 and IL-10 Using MA Pyrosequencing Machine

The experiment of this section was designed to quantitatively detect multiple proteins in a single sample. This experiment is the third multi-plexing experiment in which the combination of IL-8 and IL-10 proteins was tested.

4.1.6.1 Experimental Design for Multi-plexing IL-8 and IL-10 Using MA Machine

The experiment for simultaneous detection and quantification of IL-8 and IL-10 antigens was conducted according to Table 7. In Table 7, samples (a) and (h) were single-plex detection of the proteins. In sample (a), 2 pmol of IL-8 antigen was added to the IL-8 capturing complex, and then IL-8 detection complex was added to detect the antigen. In sample (h), 10 pmol of IL-10 antigen was added to the IL-10 capturing complex, and then IL-10 detection complex was added to detect the antigen. Samples (b) through (g) were control samples to check for cross reactivity. For example, in sample (b), 2 pmol of IL-8 antigen was added to the IL-8 capturing complex, and then IL-10 detection complex was added to detect the occurrence of cross reactivity. Sample (i) was the multi-plex detection of the proteins. All capturing and detection antibody amounts were based on the single detection experiments. The generated signal intensities were measured in all samples to detect and quantify both antigens simultaneously.

Table 7. Experimental design to determine signal intensities and cross reactivities for multi-plex detection of IL-8 and IL-10 antigens.

Ag IL-8 (2 pmol)	Detection Complex IL-8 (10 pmol)	Detection Complex IL-10 (50 pmol)
Capturing Complex IL-8 (50 pmol)	✓(+) ^a	✓(-) ^b
Capturing Complex IL-10 (50 pmol)	✓(-) ^c	✓(-) ^d
Ag IL-10 (10 pmol)	Detection Complex IL-8 (10 pmol)	Detection Complex IL-10 (50 pmol)
Capturing Complex IL-8 (50 pmol)	✓(-) ^e	✓(-) ^f
Capturing Complex IL-10 (50 pmol)	✓(-) ^g	✓(+) ^h
Ag IL-8 (2 pmol) + Ag IL-10 (10 pmol)	Detection Complex IL-8 (10 pmol)	Detection Complex IL-10 (50 pmol)
Capturing Complex IL-8 (50 pmol)	✓(Multi-Plex) ⁱ	
Capturing Complex IL-10 (50 pmol)		

4.1.6.2 Experimental Procedures for Multi-plexing IL-8 and IL-10 Using MA Machine

The procedure of making all capturing and detection complexes precisely followed the procedures explained in previous sections. b-CTCA pyro-tags were attached to the IL-8 detection complex and b-CTGC pyro-tags were attached to the IL-10 detection complex. Sample (i) was the multi-plex detection of both IL-8 and IL-10 proteins. To make this sample, 2 pmol of IL-8 antigen and 10 pmol of IL-10 antigen were added to both capturing complexes in a single tube, and after incubation and washing steps, both detection complexes were added to detect and quantify both antigens.

4.1.7 Multi DNA Detection Using b-CTGC and b-CTCA Pyro-tags as Templates Employing MA Pyrosequencing Machine

After observing the multi-plexing results, this experiment was designed to determine the quantitative results from pyrosequencing in the case of having two different pyro-tags mixed in a single test tube without the presence of any proteins.

4.1.7.1 Experimental Design for Multi-plexing b-CTGC and b-CTCA Pyro-tags

The design of this experiment was to have 1 pmol of b-CTGC pyro-tag in the first sample, 1 pmol of b-CTCA pyro-tag in the second sample, and 1 pmol each of both pyro-tags in the third sample.

4.1.7.2 Experimental Procedures for Multi-plexing b-CTGC and b-CTCA Pyro-tags

1 μ l of b-CTGC with concentration of 1 μ M (1 pmol) mixed with 39 μ l of DI water was transferred into the first well of microtiter plate. 1 μ l of b-CTCA with concentration of 1 μ M (1 pmol) mixed with 39 μ l of DI water was transferred into the second well of microtiter plate. 1 μ l of b-CTGC (1 pmol) and 1 μ l of b-CTCA (1 pmol) mixed with 38 μ l of DI water was transferred into the third well of microtiter plate. 5 μ l of enzyme and 5 μ l of substrate were added to each well and then pyrosequencing was performed as described in previous sections.

4.1.8 Switching from MA to HS Pyrosequencing Machine

At this point of the experiments a decision was made to switch the pyrosequencing from the MA machine to HS machine. It was claimed that the HS machine had a higher sensitivity and consumed lower amounts of reagents mainly due to a more sensitive CCD camera. Moreover, since the HS machine needed much lower volume, a second experiment was performed to optimize the final volume of each sample by adjusting the volume of DI water.

4.1.8.1 Experimental Design for Switching from MA to HS Machine

The experiment for comparing the MA and HS machines was conducted according to Table 8. In this design, samples of 1 pmol and 5 pmol of b-CTGC pyro-tag were simultaneously tested in the MA and HS pyrosequencing machines. Each sample had three replicates.

Table 8. Experimental design for comparison of light intensity between MA and HS machines.

b-CTGC	Pyrosequencing Machine (MA)	Pyrosequencing Machine (HS)
1 pmol	✓ (3)	✓ (3)
5 pmol	✓ (3)	✓ (3)

The experiment for adjusting the final sample volume in the HS machine was conducted according to Table 9. In this design, while the number of moles of the first

and second samples was kept the same the concentration of the second sample was decreased. Conversely, while the concentration of first and third samples was kept the same the number of moles of the third sample was increased. Each sample had three replicates and the signal intensities were measured to study the effect of different moles and different concentrations on the generated signals.

Table 9. Experimental design for comparison of light intensity for different sample concentrations and different moles.

b-CTGC		
No. of Moles	Concentration	Light Intensity
1 pmol	$0.1 \times 10^{-6} \text{ M}$	✓(3)
1 pmol	$(0.1/1.6) \times 10^{-6} \text{ M}$	✓(3)
1.6 pmol	$0.1 \times 10^{-6} \text{ M}$	✓(3)

4.1.8.2 Experimental Procedures for Switching from MA to HS Machine

To perform experiments in Table 8 the following procedure was performed: 1 μl of b-CTGC (1 pmol) mixed with 39 μl of DI water was transferred into the first well of MA microtiter plate, and 5 μl of b-CTGC (5 pmol) mixed with 35 μl of DI water was transferred into the second well of MA microtiter plate. So, the final volume of each sample was kept at 40 μl as in previous experiments. 5 μl of enzyme and 5 μl of substrate were added to each well. The inkjet cartridge was filled with 50 μl of nucleotides and was inserted into the MA machine and the MA pyrosequencing was performed as described in previous sections. Both samples had three replicate tests.

Simultaneously, 1 μl of b-CTGC (1 pmol) mixed with 5 μl of DI water was transferred into the first well of HS pyrosequencing plate, and 5 μl of b-CTGC (5 pmol) mixed with 1 μl of DI water was transferred into the second well of HS plate. So, the final volume of each sample was kept as 6 μl . 2 μl of enzyme and 2 μl of substrate were added to each well of the HS plate and the capillary dispensing tips (CDT) were filled with 50 μl of nucleotides and were inserted into the CDT holder. The plate and the CDT holder were inserted into the HS machine and pyrosequencing was performed as described in previous sections. Both samples had three replicate tests.

To perform the experiment mentioned in Table 9 the following procedure was executed: 1 μl of b-CTGC (1 pmol) mixed with 5 μl of DI water was transferred into the first well of HS plate. 1 μl of b-CTGC (1 pmol) mixed with 11 μl of DI water was transferred into the second well of HS plate. 1.6 μl of b-CTGC (1.6 pmol) mixed with 10.4 μl of DI water was transferred into the third well of HS plate. So, the number of moles of first and second samples was kept the same, whereas the concentration of first and third samples was kept the same. 2 μl of enzyme and 2 μl of substrate were added to each well and then HS pyrosequencing was performed.

4.1.9 Single Human IL-8 Detection Using HS Pyrosequencing Machine

The experiment of this section was designed to exclusively detect and quantify human IL-8 antigen employing the higher sensitive pyrosequencing machine. The intent

was to gather sufficient data to compare the single protein detection results from the method used in this thesis with the well established ELISA method.

4.1.9.1 Experimental Design for Detecting IL-8 Using HS Machine

The experiment for detection and quantification of IL-8 antigen was conducted according to Table 10. Different antigen concentrations were tested in each run to measure the generated signal intensities and all runs were performed separately on different days. All samples of run 1 and run 2 were made by using capturing complex batch 1 (C.C.1). Samples of run 3 were prepared by using capturing complex batch 2 (C.C.2). Samples of run 4 were made by using two different capturing complex batches (C.C.2 and C.C.3). All samples of run 5 were prepared by using capturing complex batch 3 (C.C.3). Antigen concentration levels were repeated in different runs to check the reproducibility of data, and were decreased with each new run to find the limit of detection. Several control samples in which no antigen was present, were tested in run 5 to find the background noise signal.

Table 10. Experimental design to quantitatively detect IL-8 antigen.

Run 1			
Antigen (pmol)	Antigen (ng/ml)	No. of Samples	Light Intensity
50	4000	I _(C.C.1)	✓
25	2000	II _(C.C.1)	✓
10	800	II _(C.C.1)	✓
4	320	II _(C.C.1)	✓
2	160	II _(C.C.1)	✓
1	80	II _(C.C.1)	✓
0.5	40	II _(C.C.1)	✓
0.25	20	II _(C.C.1)	✓
Run 2			
Antigen (pmol)	Antigen (ng/ml)	No. of Samples	Light Intensity
25	2000	II _(C.C.1)	✓
2	160	II _(C.C.1)	✓
0.25	20	I _(C.C.1)	✓
0.125	10	I _(C.C.1)	✓
Run 3			
Antigen (pmol)	Antigen (ng/ml)	No. of Samples	Light Intensity
1	80	I _(C.C.2)	✓
0.5	40	I _(C.C.2)	✓
0.125	10	I _(C.C.2)	✓
0.0625	5	II _(C.C.2)	✓
0.03125	2.5	I _(C.C.2)	✓
0.01563	1.25	II _(C.C.2)	✓
Run 4			
Antigen (pmol)	Antigen (ng/ml)	No. of Samples	Light Intensity
0.0625	5	I _(C.C.3) +I _(C.C.2)	✓
0.03125	2.5	I _(C.C.2)	✓
0.01563	1.25	I _(C.C.2)	✓
0.00781	0.625	I _(C.C.3) +I _(C.C.2)	✓
0.00391	0.3125	II _(C.C.3) +I _(C.C.2)	✓
0.00195	0.15625	II _(C.C.3) +I _(C.C.2)	✓
Run 5			
Antigen (pmol)	Antigen (ng/ml)	No. of Samples	Light Intensity
8	640	II _(C.C.3)	✓
4	320	I _(C.C.3)	✓
1	80	II _(C.C.3)	✓
0.5	40	I _(C.C.3)	✓
0.00195	0.15625	I _(C.C.3)	✓
0.00098	0.07813	II _(C.C.3)	✓
0	0	V _(C.C.3)	✓

4.1.9.2 Experimental Procedures for Detecting IL-8 Using HS Machine

Throughout this experiment, three batches of capturing complex were prepared as specified in Table 10. The procedure of making the capturing complex was the same as the procedure explained in section 4.1.1.3. All capturing complexes had 50 pmol capturing antibody.

In opposite to the capturing complex where some batches were used for several runs, the detection complex was always made fresh for each run. A total of five batches were prepared throughout this experiment. Each detection complex had 10 pmol detection antibody, and the molar ratio of detection antibody to streptavidin to pyro-tag (Ab: SA: b-CTGC) was kept at 1:2:10 respectively.

The immunocomplexes were prepared the same as before, by adding the antigen solutions to the capturing complexes, followed by the addition of the detection complexes. For each sample, 12.5 μl of the capturing complex was transferred into a tube, placed on the magnet, and washed twice for five minutes with 100 μl of PBS buffer. For the first sample of run 1, 20 μl of antigen with concentration of 20 $\mu\text{g/ml}$ (50 pmol) mixed with 80 μl of PBS buffer was added to the washed capturing complex, and the mixture was incubated for one hour on the tube rotator. For the rest of the samples, the antigen solution was prepared in serial dilutions to the desired concentrations. As previously described, the total volume of antigen with PBS buffer was always kept at 100

μl . The tube was placed on the magnet for four minutes and the beads were washed a total of three times with 100 μl of PBS buffer. Next, 5 μl of the prepared detection complex was added to the beads, the sample volume was increased to 100 μl by adding 95 μl of PBS buffer, and the mixture was incubated for one hour on the tube rotator. Finally, the sample was placed on the magnet, washed once with 100 μl PBS buffer, washed once more with 100 μl DI water, and resuspended in 40 μl of DI water.

Each sample was divided into at least three replicates of 6 μl immunocomplex solution mixed with 6 μl of DI water, and each replicate was transferred into a well of the HS pyrosequencing plate. 2 μl substrate and 2 μl enzyme mixture were added to each well. CDTs were filled with 150 μl of nucleotides and were inserted into the CDT holder. The plate and the CDT holder were placed into the HS machine and pyrosequencing was performed.

4.2 Equipment

4.2.1 Dynal Magnetic Particle Concentrator (MPC)

For several washing steps during the construction of the immunocomplex, a Dynal Magnetic Particle Concentrator (Dynal MPC) was used. Dynal MPC is equipped with strong magnets to maximize the separation of bead-bound targets. The supernatant

could be easily removed by aspiration with a pipette while the magnetic beads and the isolated target were left in the tube. Figure 20 shows the front view of this magnet.

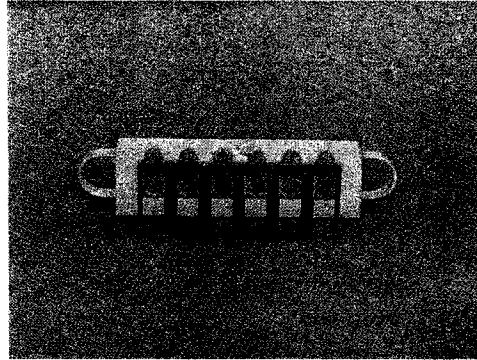


Figure 20. Front view of the dynal magnetic particle concentrator.

4.2.2 Tube rotator

During the incubation of reagents, a tube rotator was used to enhance the binding. The tube rotator has variable speed, ranging from 15 RPM to 80 RPM, as well as flexible magnetic tube holders to allow the user to place different size tubes on the rotating bar. Different speed controls allow for gentle or vigorous mixing motion as desired. Figure 21 displays a view of this equipment.

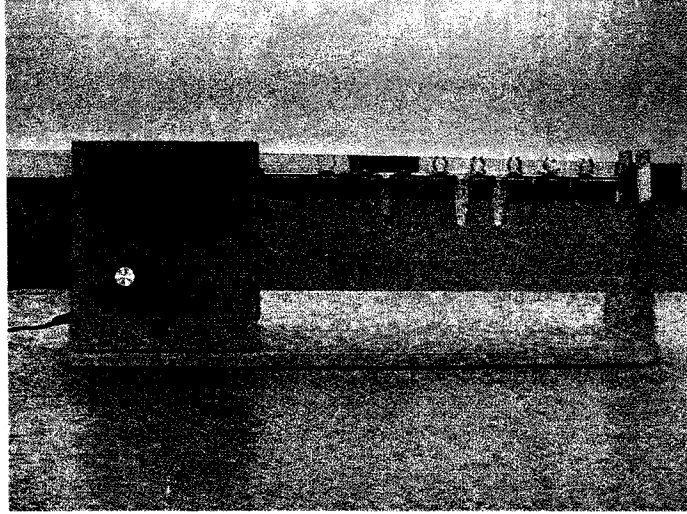


Figure 21. Tube rotator.

4.2.3 Pyrosequencing Instrument

Detection and quantification of the antigen was accomplished by the pyrosequencing instrument. Two models of this instrument were used in this research, the PSQ™96MA machine and the PSQ™HS 96A machine. Figure 22 shows the front view of the MA machine, and Figure 23 illustrates a view of the HS machine.



Figure 22. PSQ™96MA pyrosequencing instrument.

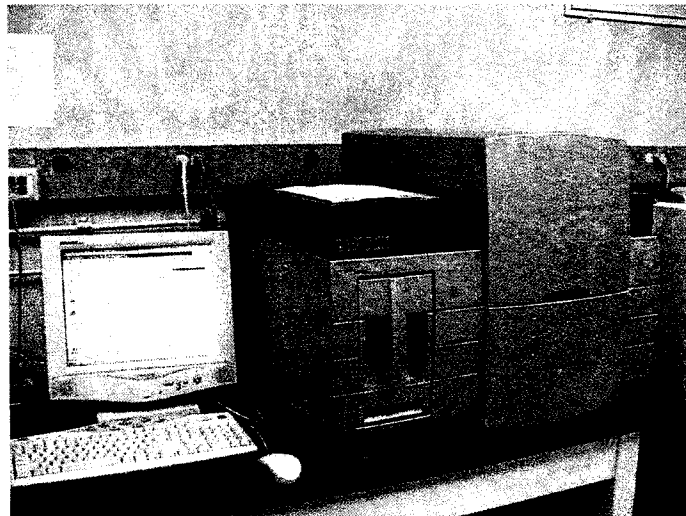


Figure 23. PSQ™HS 96A pyrosequencing instrument.

During pyrosequencing, the pyro-tags were synthesized into DNA through a series of enzymatic reactions and a light directly proportional to the amount of each incorporated nucleotide was generated. The generated light signal confirmed the presence of a specific antigen, and the intensity of the generated light quantified the

amount of antigen present. Prior to pyrosequencing in MA machine, the inkjet cartridge and the microtiter plate were mounted into the instrument, and in the HS machine the capillary dispensing tips (CDT) as well as the HS plate were inserted into the instrument. The inkjet cartridge and the CDT were loaded with the four nucleotides for exact dispensation of 200 nl volume into the pyrosequencing plate well according to the prespecified order. Figure 24 shows the MA plate and the inkjet cartridge used in MA machine, and Figure 25 shows the HS plate and the cartridge used in HS machine.



Figure 24. Microtiter plate and inkjet cartridge used in MA pyrosequencing.

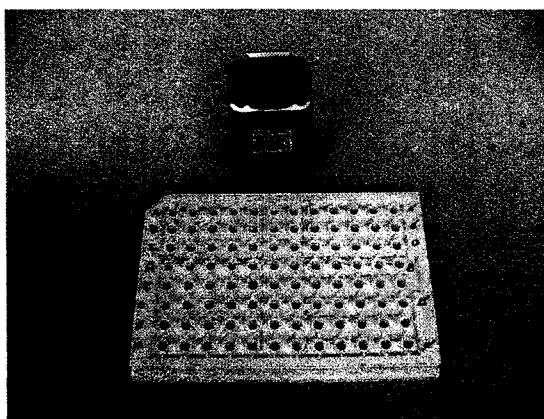


Figure 25. HS plate and cartridge used in HS pyrosequencing.

During the pyrosequencing run, the plate is under continuous agitation and controlled temperature to increase the rate of enzymatic reactions. A CCD camera that is located under the plate images the plate once every second and a computer that is connected to the machine saves the data graphically using pyrosequencing software. The PSQ HS 96A employs a much higher sensitive light detector than the PSQ™96MA during pyrosequencing reactions, resulting in much lower consumption of sample and reagents required per assay.

4.3 Data Analysis

Detection and quantification of antigens were obtained employing pyrosequencing by the unique pyro-tags (b-CTGC, and b-CTCA) attached to the detection antibodies. During pyrosequencing the presence of signals detected the antigens and the magnitude of signals quantified the antigens. In fact, the graphical surface area under each peak is the real signal intensity; however, since it was not easy to determine the area under each peak, the height of the peak was used for quantification. For instance, in the case of having b-CTGC pyro-tag, signals of G, C, A, and G were released, and then the height of the first peak (G signal) was used to quantify the antigen while the magnitude of the other three peaks were checked as references.

Furthermore, the nucleotides dispensation order during pyrosequencing was designed in a way that the G nucleotide was dispensed more than once to assure that all

of the C nucleotides in the pyro-tag were incorporated and depleted. In the case of having more than one peak for G, the heights of all peaks were added together for quantifying the amount of antigen present.

For the final results, the reproducibility of all data points was checked. Results were compared between different batches of capturing complexes, as well as between the same batch tested at different times (days). Several concentrations had more than one sample, and each sample had at least three replicates.

Standard curves were established for the concentrations of antigen versus the intensity of the generated signals by the pyro-tags. The standard deviation and the coefficient of variation were calculated to examine the reproducibility of the results. Equation 6 was used to calculate the standard deviation.

$$SD = \sqrt{\frac{(X - x_1)^2 + (X - x_2)^2 + \dots + (X - x_n)^2}{n - 1}} \quad \text{Equation 6}$$

Equation 7 was used to determine the coefficient of variation.

$$\%CV = \frac{SD}{\text{mean}} \times 100 \quad \text{Equation 7}$$

Finally, the noise level where no antigen was present in the solution was calculated using equation 8, and all data points below this level were omitted.

$$\text{Noise Level} = \text{Average} + 3 \times SD \quad \text{Equation 8}$$

CHAPTER FIVE RESULTS AND DISCUSSION

5.1 IL-8 Single-plexing Using MA Pyrosequencing Machine

For making the capturing complex, magnetic beads needed to be activated with EDC and NHS prior to coating the beads with capturing antibodies. The ratio of EDC to NHS and the amount of capturing antibody for coating the beads' surface were changed several times to find the optimal ratio for activating the beads and the maximum level of coating, respectively. The optimal molar ratio of EDC to NHS was determined to be 1:1, and the highest rate of coating was determined to be 60 μg of antibody per 100 μl of beads. Both results corresponded well with what was recommended in the Dynabeads protocol.

Figure 26 shows the results of IL-8 experiment that was conducted based on Table 1. Section (a) in this figure shows the pyrosequencing graphs for different concentrations of antigen. In all of these graphs the x-axis shows the sequential addition of the nucleotides, and the y-axis shows the detected light intensities by pyrosequencing. Section (b) in this figure is the generated light intensity verses antigen concentration. The x-axis is a logarithmic scale of antigen concentration (ng/ml) and the y-axis is the light intensity detected by pyrosequencing, which is displayed in arbitrary units (AU).

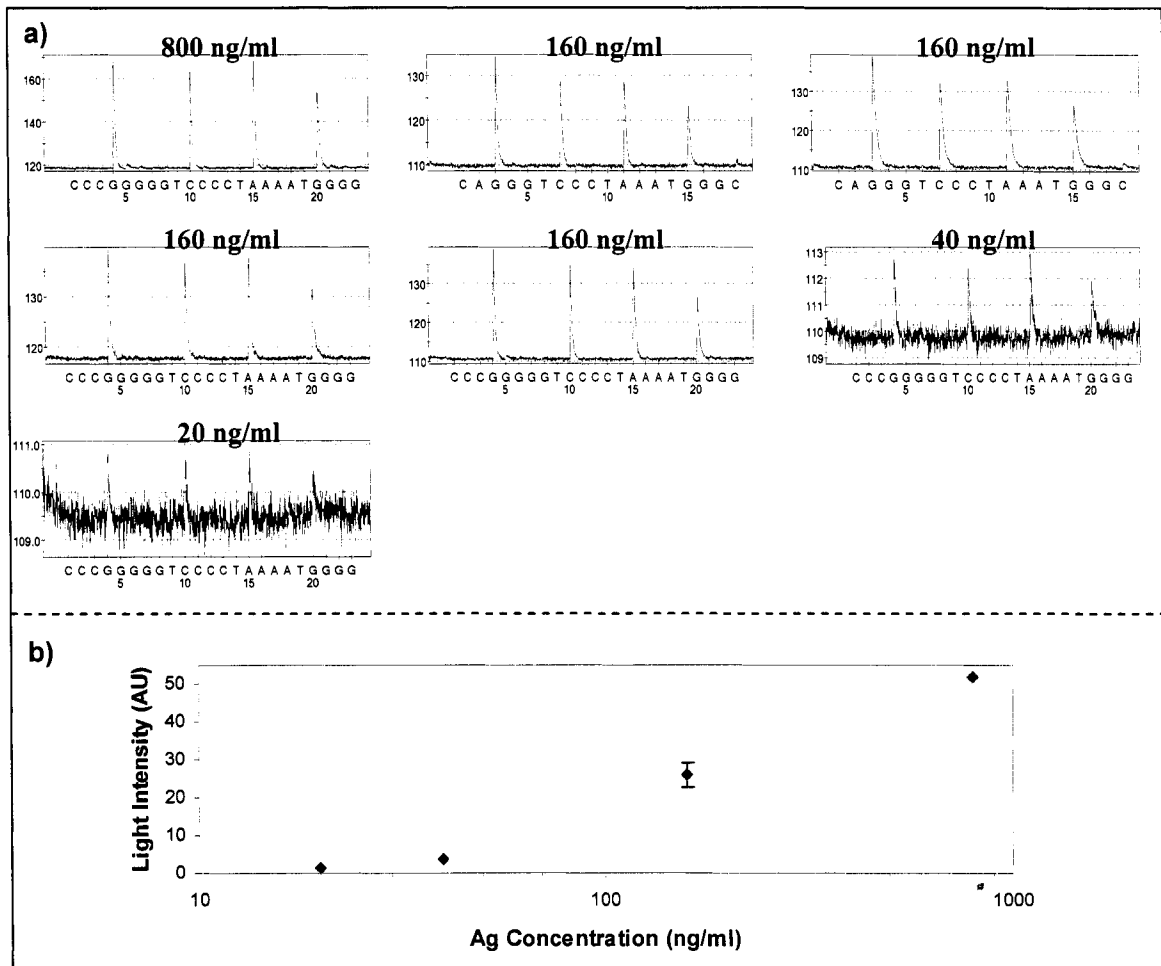


Figure 26. IL-8 Ag concentration versus light intensity generated by b-CTGC pyro-tag during pyrosequencing.

Based on the hypothesis of this research, when the amount of antigen increases more detection antibodies with attached pyro-tags will be present in the immunocomplex, and so during pyrosequencing the result will be a greater light intensity. As seen in Figure 26, the signal intensity increases as antigen concentration increases. This agrees well with the hypothesis. For a 160 ng/ml antigen concentration level, the signal intensity was the average of four individual samples that were prepared and tested on four separate days to check the reproducibility of the data. The error bar indicates one SD,

which was about 3.2 AU, and the percentage of coefficient of variation (CV) for this data point was about 12%. The limit of detection for IL-8 antigen was determined to be at 20 ng/ml antigen concentration level. Run 3 in Table 1 was performed to find the minimum amount of detection antibody in the immunocomplex while maintaining constant signal intensity. By decreasing the detection antibody from 50 pmol to 10 pmol, no drop in signal intensity was observed, which changed the ratio of capturing antibody to detection antibody from 1:1 to 1:0.2. This was significant in saving the antibodies and decreasing assay cost. Several control samples in which no antigen was present were prepared and tested on separate days. The results of these samples were all negative meaning that no significant signals were detected. The level of noise was found to be approximately 0.5 AU. This specifies the near absence of cross reactivity between the capturing and the detection complexes. Overall, the initial results of this experiment proved worthy of further testing, which was conducted and discussed in section 5.9 of this chapter.

5.2 IL-4 Single-plexing Using MA Pyrosequencing Machine

The IL-4 antigen was tested in hopes of utilizing a second antigen in a multiplexing experiment, according to the scope of this thesis. Figure 27 shows the results of IL-4 experiment that was carried out based on Table 2.

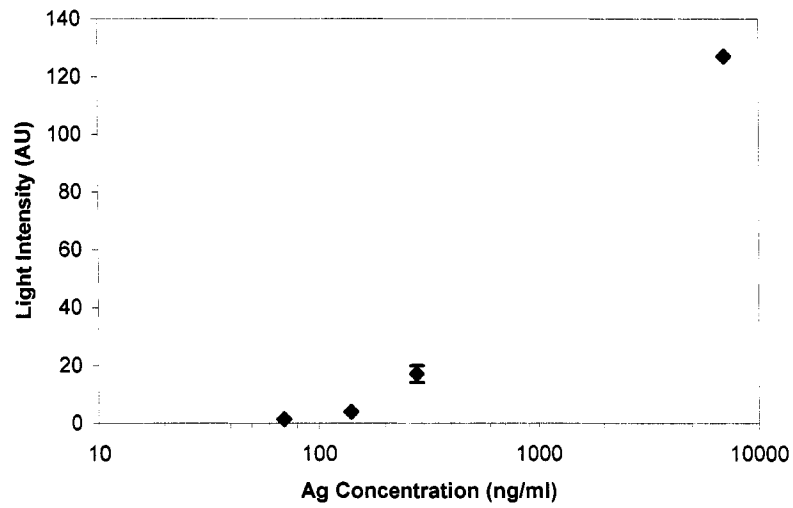


Figure 27. IL-4 Ag concentration versus light intensity generated by b-CTCA pyro-tag during pyrosequencing.

As seen in Figure 27, by increasing the antigen concentration, the signal intensity increases, which agrees with the hypothesis of this research. For a 280 ng/ml antigen concentration level, the signal intensity was the average of four individual samples that were prepared and tested on four separate days to check the reproducibility of the data. The error bar indicates one SD, which was about 3 AU, and the percentage of CV for this data point was about 17%. The limit of detection for IL-4 antigen was determined to be at 70 ng/ml antigen concentration level. Run 3 in Table 2 was performed to find the minimum amount of detection antibody in the immunocomplex while maintaining constant signal intensity. The lowest detection antibody amount was determined to be 25 pmol, which changed the ratio of capturing antibody to detection antibody from 1:1 to 1:0.5. The level of noise was found to be approximately 0.5 AU, indicating the near absence of cross reactivity between the capturing and the detection complexes. For the same antigen concentration level, IL-8 antigen generates higher signals than IL-4 antigen.

The sensitivity of IL-4 antigen was less than IL-8 antigen as indicated by their limits of detection. Furthermore, the ratio of capturing antibody to detection antibody for IL-4 (1:0.5) was not as significant as that of IL-8's ratio (1:0.2), resulting in less saving in assay cost. The overall comparative results favored the IL-8 antigen over the IL-4 antigen.

5.3 IL-10 Single-plexing Using MA Pyrosequencing Machine

The IL-10 antigen was tested in hopes of obtaining a superior candidate for a second antigen in a multi-plexing experiment, as compared to the IL-4 antigen. Figure 28 shows the results of IL-10 experiment that were performed based on run 1 of Table 3.

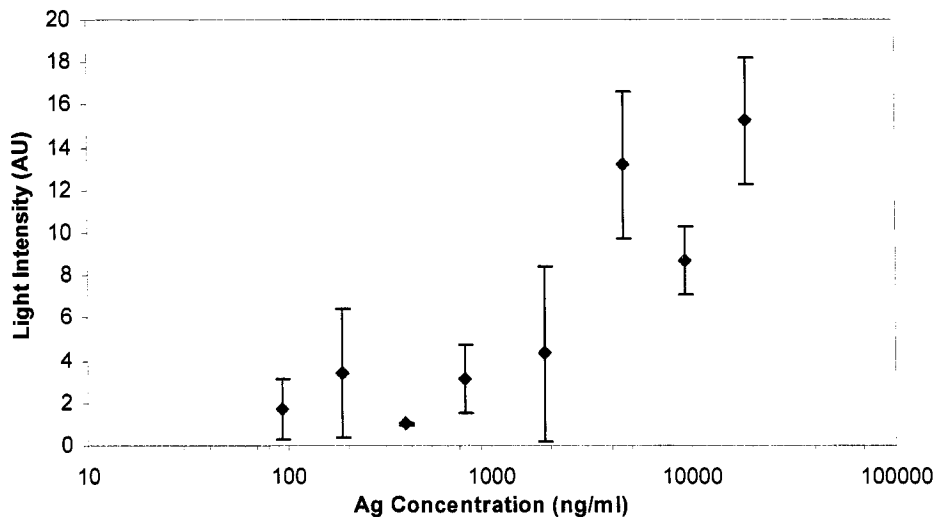


Figure 28. IL-10 Ag concentration versus light intensity generated by b-CTCA pyro-tag during pyrosequencing. The error bars represent one SD.

As seen in Figure 28, the overall trend of the graph shows increasing light intensity with increasing antigen concentration; however, the obtained results were very

inconsistent. Four samples were prepared at a 744 ng/ml antigen concentration level to test reproducibility, and all other concentrations had two replicates. The error bars represent one SD and the percentage of CV was significantly high for most of the points. The most likely reason for getting this inconsistency was due to the high amount of biotin per IL-10 detection antibody. During the construction of the detection complex, cloudiness was observed in the sample when streptavidin was added to the antibody. This was most likely due to the formation of macro-molecules between SA and antibody molecules. Technical support staff at Pierce indicated that the IL-10 detection antibody had a very high concentration of biotin, measuring 5 to 7 biotin per antibody, whereas IL-8 only had 1 to 2 biotin per antibody. Therefore, in the step of adding the detection complex, the concentration could not be distributed evenly between samples. The limit of detection for IL-10 antigen was determined to be at 93 ng/ml antigen concentration level. Run 2 in Table 3 was performed to find the minimum amount of detection antibody in the immunocomplex while maintaining constant signal intensity. The lowest detection antibody amount remained at 50 pmol, which kept the ratio of capturing antibody to detection antibody at 1:1. The level of noise was found to be approximately 0.5 AU, indicating the near absence of cross reactivity between the capturing and the detection complexes. Overall, the IL-10 antigen had the lowest sensitivity and was considered to be the most inferior antigen to be tested with respect to all the other tested antigens.

5.4 IL-8 and IL-4 Multi-plexing Using MA Pyrosequencing Machine

In this experiment two different types of antigen were mixed in a sample in order to be simultaneously detected and quantified by pyrosequencing. The results of this experiment that were performed according to Table 4 are demonstrated in Figure 29.

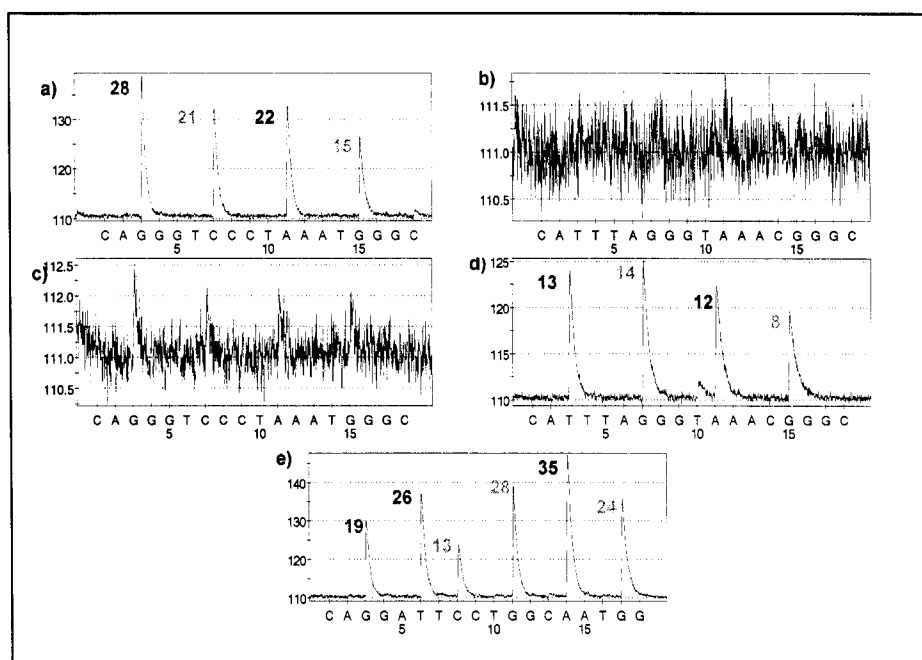


Figure 29. (a) Single detection of IL-8 Ag. (b) Control experiment of IL-8 Ag. (c) Control experiment of IL-4 Ag. (d) Single detection of IL-4 Ag. (e) Multi-plexing of IL-8 and IL-4 Ags.

As shown in graph (a), IL-8 antigen was detected by pyrosequencing and the GCAG signals were generated by the b-CTGC pyro-tags that were attached to the IL-8 detection complex. The magnitude of each signal is specified by a number next to each peak. The result of graph (b) indicates that there was no non-specific binding between the IL-8 antigen and IL-4 capturing and detection complexes. Graph (c) also shows that there was very minor non-specific binding between the IL-4 antigen and IL-8 capturing

and detection complexes. In graph (d), IL-4 antigen was detected by pyrosequencing and TGAG signals were generated by the b-CTCA pyro-tags that were attached to the IL-4 detection complex. Getting the results of (a), (b), (c), and (d), it was expected that when the two antigens were added together in sample (e), six individual peaks would be generated. The first two signals of G and C from IL-8 antigen and T and G from IL-4 antigen should have maintained the same magnitudes as graphs (a) and (d). The last two signals of A and G should have been the sum of signals of A and G from both IL-8 and IL-4 antigens. However, looking at the results in graph (e), the magnitude of G and C signals (first and third peaks) both decreased by about 32%, and the magnitude of T and G signals (second and fourth peaks) both increased by about 100%. The magnitudes of A and G signals (fifth and sixth peaks) changed accordingly to the expected results. This result obviously was only qualitative meaning that both antigens could be detected, but not in a quantitative manner.

Figure 30 illustrates the obtained results that were performed according to Table 5.

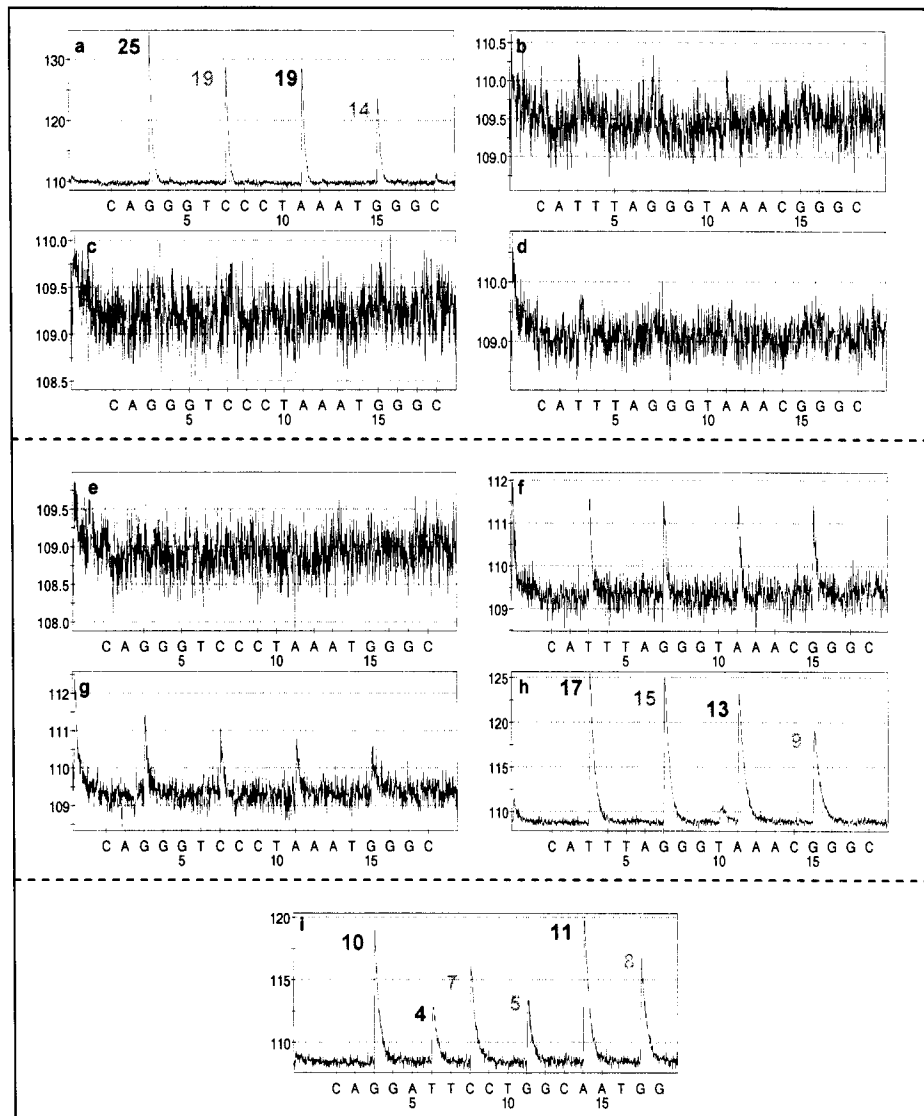


Figure 30. (a) Single detection of IL-8 Ag. (b), (c), (d) Control experiments of IL-8 Ag. (e), (f), (g) Control experiments of IL-4 Ag. (h) Single detection of IL-4 Ag. (i) Multi-plexing of IL-8 and IL-4 Ags.

In this experiment, all possible combinations of control samples that were not included in the previous experiment were considered to find the source of non-specific bindings that might have resulted in obtaining the inconsistent result of the previous multi-plexing experiment. As shown in Figure 30, single IL-8 and IL-4 antigens were

detected as demonstrated in graphs (a), and (h). Minor non-specific binding between IL-4 antigen and IL-8 capturing complex was present; however, the result of multi-plexing was still very inconsistent. As seen in graph (i), the magnitude of G and C signals both decreased about 62% and the magnitude of T and G signals both decreased about 72%. The exact reason for getting this variation could not be determined, but it was most likely due to intermolecular interactions between the two antigens and their corresponding capturing and detection complexes.

Although, the magnitudes of the signals were not consistent between the single-plex and multi-plex experiments, the percent difference between the signal peaks remained consistent. The magnitudes of A signal (third peak) and C signal (second peak) were equal in graph (a), and the magnitude of A signal (third peak) was about 87% of G signal (second peak) in graph (h). Therefore, in graph (i), the magnitude of A signal (fifth peak) should be equivalent to the sum of C signal (third peak) and 87% of G signal (fourth peak). Furthermore, in graph (a), the magnitude of G signal (fourth peak) was about 74% of C signal (second peak), and in graph (h), the magnitude of G signal (fourth peak) was about 60% of G signal (second peak). Thus, in graph (i), the magnitude of G signal (sixth peak) should be equivalent to the sum of 74% of C signal (third peak) and 60% of G signal (fourth peak). This correlation remained consistent for both A signal (fifth peak) and G signal (sixth peak) in graph (i). The result in graph (i) was certainly qualitative, in that both proteins could be simultaneously detected, but a quantitative correlation could not be established.

5.5 IL-4 and IL-10 Multi-plexing Using MA Pyrosequencing Machine

Figure 31 demonstrates the obtained results of multi-plexing of IL-4 and IL-10 antigens that were conducted according to Table 6.

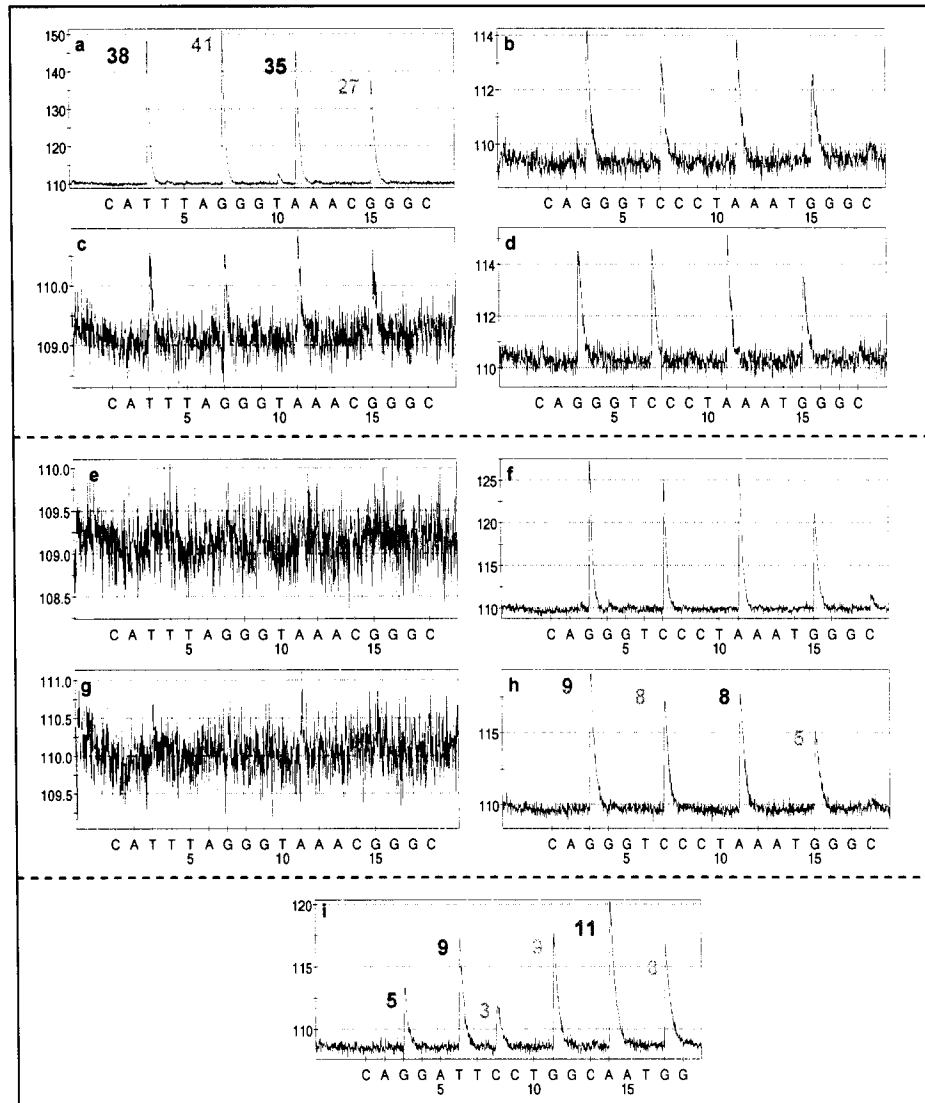


Figure 31. (a) Single detection of IL-4 Ag. (b), (c), (d) Control experiments of IL-4 Ag. (e), (f), (g) Control experiments of IL-10 Ag. (h) Single detection of IL-10 Ag. (i) Multi-plexing of IL-8 and IL-4 Ags.

Graph (a) shows single IL-4 antigen detection. The intensities of signals are more than twice that of IL-4 from the previous experiment. The IL-4 detection antibody that was used in this experiment was from a new batch and was freshly reconstituted in Tris buffered saline. The sensitivity of IL-4 detection antibody was very high upon receipt, but it degraded rapidly. In only three days time, the signal intensity of IL-4 decreased by one-half. As shown in Figure 31 non-specific bindings were present in most of the control samples. The IL-4 antigen had non-specific bindings to IL-10 capturing and detection complexes. Graph (h) shows single IL-10 antigen detection, which used 10 pmol, in contrast to 2 pmol of IL-4 antigen, because of its low sensitivity. Graph (f) illustrates that IL-10 antigen had huge non-specific bindings with IL-4 capturing complex. Again, the result in graph (i) was not consistent with the results from single detection of each antigen. In graph (i), IL-4 signals decreased in magnitude more than twice as much as IL-10 signals decreased. Although, the magnitudes of the signals were not consistent between the single-plex and multi-plex experiments, the percent difference between the signal peaks remained consistent. In graph (i), the intensity of A signal (fifth peak) should be the sum of 85% of G signal (fourth peak) plus C signal (third peak). The intensity of G signal (sixth peak) should be equivalent to the sum of 60% of C signal (third peak) and 70% of G signal (fourth peak). This correlation remained consistent for both A signal (fifth peak) and G signal (sixth peak) in graph (i). The six generated signals in the multi-plexing experiment confirmed that both proteins could be detected simultaneously but not quantified.

5.6 IL-8 and IL-10 Multi-plexing Using MA Pyrosequencing Machine

Figure 32 demonstrates the obtained results of multi-plexing of IL-8 and IL-10 that were conducted according to Table 7.

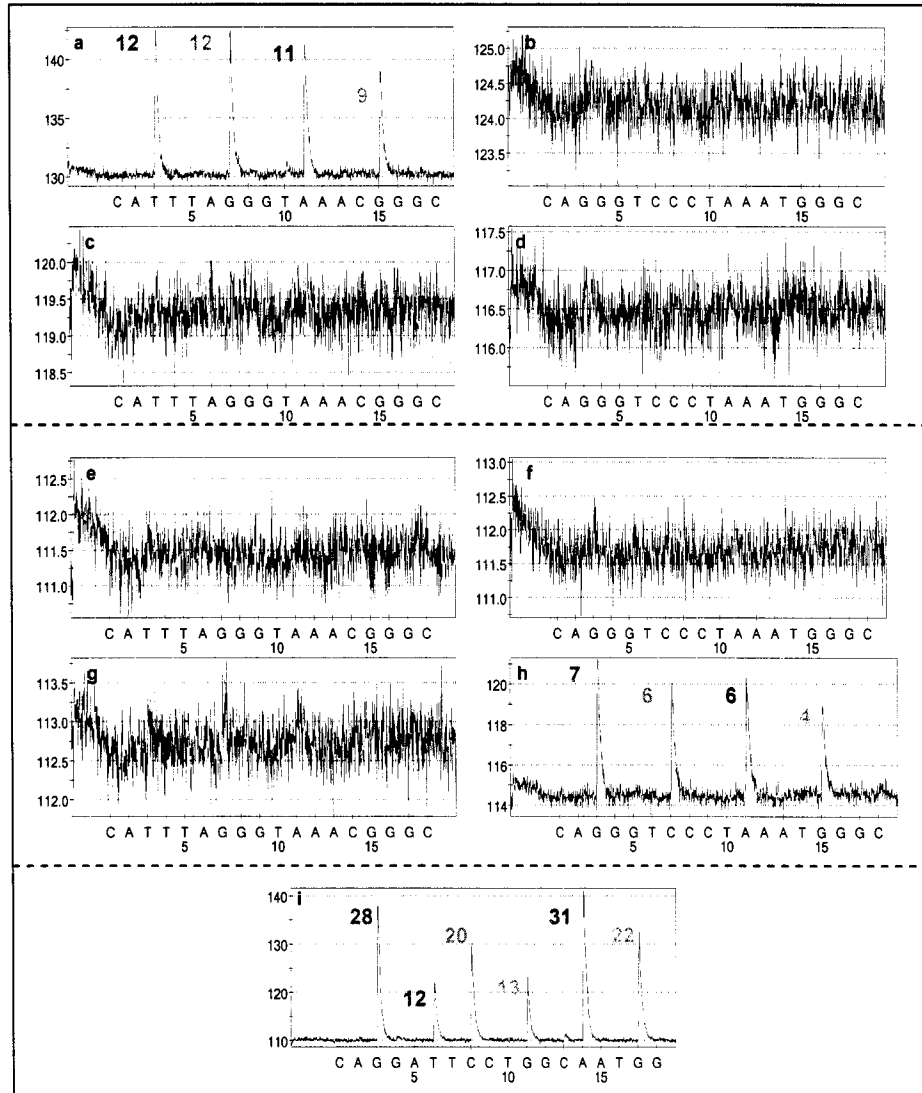


Figure 32. (a) Single detection of IL-8 Ag. (b), (c), (d) Control experiments of IL-8 Ag. (e), (f), (g) Control experiments of IL-10 Ag. (h) Single detection of IL-10 Ag. (i) Multi-plexing of IL-8 and IL-10 Ags.

Graph (a) shows single IL-8 antigen detection, where the signal intensities were about half that of IL-8 signals shown in section 5.4. This was most likely due to degradation of the reagents. As demonstrated in Figure 32 the IL-8 and IL-10 proteins did not have any cross reactivity and so no non-specific binding was present between the samples. Graph (h) shows single IL-10 antigen detection, which also had a lower signal intensity compared to the previous experiment. This was also due to the degradation of the reagents. The result of multi-plexing is shown in graph (i), where the magnitude of signals generated by IL-8 antigen stayed constant and the magnitude of released signals from IL-10 antigen increased about four times. This was an unexpected as well as inconsistent result when compared with the results from single detection of each antigen; however, the percent difference between the signal peaks remained consistent. In graph (i), the intensity of A signal (fifth peak) should be equivalent to the sum of 90% of G signal (fourth peak) plus C signal (third peak). The intensity of G signal (sixth peak) should be equivalent to the sum of 75% of G signal (fourth peak) and 66% of C signal (third peak). This correlation remained consistent for both A signal (fifth peak) and G signal (sixth peak) in graph (i). This result and the results of the previous multi-plexing experiments were consistently qualitative. Nonetheless, two different proteins were simultaneously detected with the same sample volume required to detect just one protein. This reduction in assay volume can be represented in the reduction of assay time instead, as the two different proteins were detected in half the time it would have taken to detect the proteins individually.

Table 11, compares the percent difference between the signal intensity of single antigen detection versus multi antigen detection. The multi-plexing results produced signal intensities that were mostly inconsistent with those produced in single antigen detection experiments.

Table 11. Percent difference between signal intensity of single antigen detection versus multi antigen detection.

Single Detection	Multi-Plexing Experiment			
	"IL-8 + IL-4"	"IL-8 + IL-4"	"IL-4 + IL-10"	"IL-8 + IL-10"
"IL-8" Ag	(32%) ↓	(60%) ↓		(0%) ↔
"IL-4" Ag	(100%) ↑	(77%) ↓	(76%) ↓	
"IL-10" Ag			(40%) ↓	(300%) ↑

Based on the multi-plexing results, the IL-8 antigen produced the most consistent generated signal values.

5.7 b-CTGC and b-CTCA Multi-plexing Using MA Pyrosequencing Machine

This experiment was conducted according to the design mentioned in section 4.1.7.1. Figure 33 shows the obtained results.

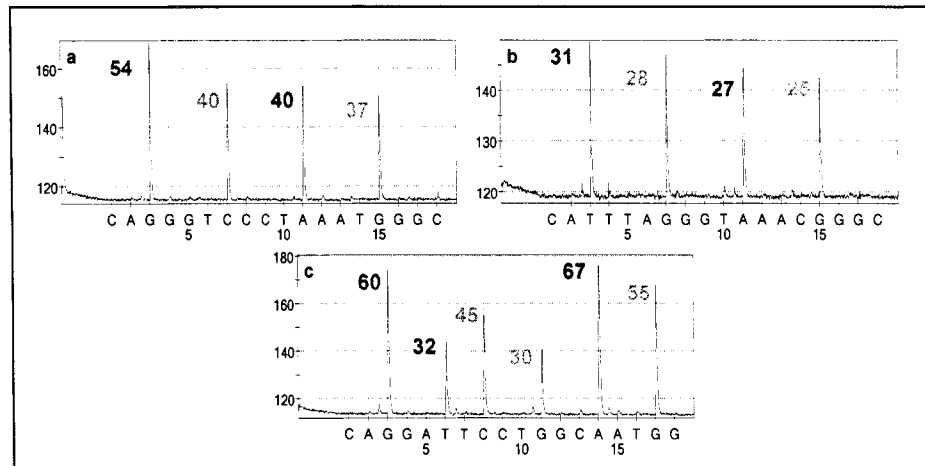


Figure 33. (a) 1 pmol b-CTGC pyro-tag. (b) 1 pmol b-CTCA pyro-tag. (c) 1 pmol b-CTGC plus 1 pmol b-CTCA pyro-tags.

Graph (a) shows the GCAG signals generated from 1 pmol of b-CTGC pyro-tag during DNA synthesis, and graph (b) illustrates the TGAG signals generated from 1 pmol of b-CTCA pyro-tag during DNA synthesis. The signals in graph (c) were the light intensities generated from 1 pmol of both pyro-tags. As seen in this graph, the magnitudes of G, T, C and G signals all slightly increased, which was most likely due to both pipetting error and instrumentation error. The magnitudes of A signal (fifth peak) and G signal (sixth peak) in graph (c) were nearly equivalent to the sum of the two A signals (third peaks) and the two G signals (fourth peaks) from graphs (a) and (b). This was certainly a qualitative as well as a quantitative result and its consistency was significantly better than the results obtained from multi protein detection. Therefore, the results showed that the discrepancies in the previous results were not due to the interactions between the two pyro-tags. Instead, the discrepancies were due to the intermolecular interactions between the two antigens and their capturing and detection

complexes. This experiment was repeated three times and reproducibility was obtained with CV of less than 10%.

5.8 MA Pyrosequencing Machine Versus HS Pyrosequencing Machine

By employing the HS pyrosequencing machine for protein detection, the sensitivity was expected to increase significantly. The obtained result from the first experiment indicated that for the same amount of pyro-tag, the intensities of generated signals from the HS machine were about 40 times greater than the signals from the MA machine. This was a major step in assay improvement. By increasing the sensitivity of the detection technique, the limit of detection could be lowered by orders of magnitude.

Due to higher sensitivity of the HS machine, the final sample size could be divided into replicates of 6 μl of immunocomplex to be transferred into the HS plate. The addition of 2 μl of enzyme and 2 μl of substrate would increase the total volume to 10 μl , which was not enough to sufficiently cover the entire bottom surface of the plate well, causing non-homogeneous mixing. To solve this problem, the experimental design in Table 9 was designed. Comparing the first and second samples in this table, the number of moles was kept the same for both samples (1 pmol), while the concentration of the second sample was decreased by adding more water ($(0.1/1.6)\times 10^{-6}$ M). Conversely, the third sample had greater number of moles than the first sample (1.6 pmol), but the concentration was kept constant (0.1×10^{-6} M). By designing this experiment, it was

expected to obtain higher light intensities for the third sample since it contained more moles. The key point was to discover the difference in signal intensities between the first and second sample. The results are summarized in Table 12.

Table 12. Comparison of light intensity for different sample concentrations and different moles.

b-CTGC					
No. of Moles	Concentration	No. of Samples	Light Intensity (AU)		
			Average	SD	%CV
1 pmol	$0.1 \times 10^{-6} \text{ M}$	III	1398.8	51.9	3.7
1 pmol	$(0.1/1.6) \times 10^{-6} \text{ M}$	III	1659.4	10.9	0.7
1.6 pmol	$0.1 \times 10^{-6} \text{ M}$	III	2913.3	104.9	3.6

As shown in Table 12, the third sample had much higher signal intensity than the first two samples, which was as expected. Interestingly, the second sample with the same amount of moles and lower concentration generated greater light intensities than the first sample with lower SD and percentage of CV. This was due to the fact that by adding water, the bottom surface of the well was sufficiently covered, which enhanced homogenous mixing during pyrosequencing. This result was used to optimize the assay volume in protein detection experiments.

5.9 IL-8 Single-plexing Using HS Pyrosequencing Machine

Run 1 in Table 10 was designed to achieve quantitative results for detection of IL-8 antigen. Table 13 and Figure 34, show the obtained results.

Table 13. Reproducibility of IL-8 result: same batch, same run.

Ag (ng/ml)	No. of Samples	Light Intensity (AU)		
		Average	SD	%CV
4000	I _(C.C.1)	272.0	20.0	7.4
2000	II _(C.C.1)	268.0	19.2	7.2
800	II _(C.C.1)	234.9	19.0	8.1
320	II _(C.C.1)	168.9	9.6	5.7
160	II _(C.C.1)	87.0	8.8	10.1
80	II _(C.C.1)	39.2	8.8	22.3
40	II _(C.C.1)	18.7	3.0	15.8
20	II _(C.C.1)	19.2	4.7	24.3

The obtained data for each antigen concentration in Table 13 was the average of at least three replicates from each sample. All the concentrations, except 4000 ng/ml, were tested twice as indicated in the number of samples column. For example, at 2000 ng/ml the average light intensity, SD, and CV were obtained considering eight individual data points: two samples each with four replicates.

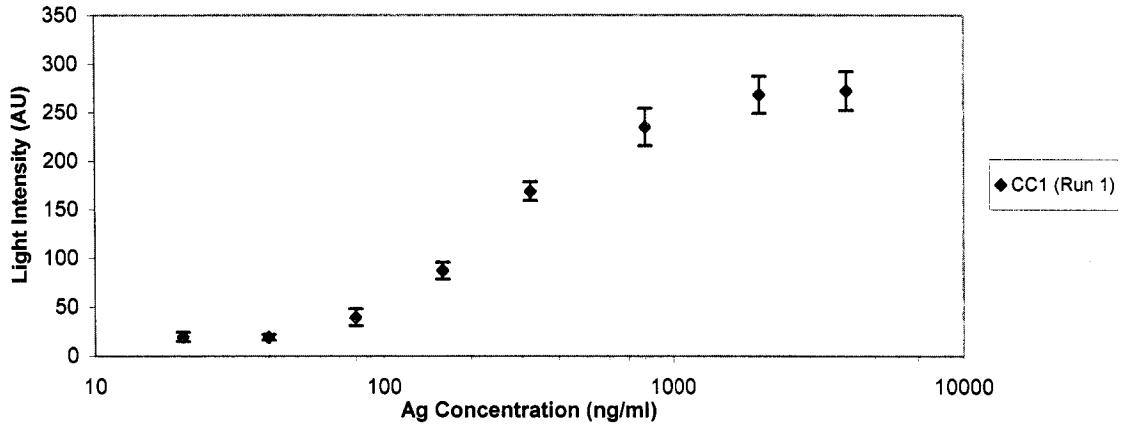


Figure 34. Reproducibility of IL-8 result: same batch, same run.

As shown in Figure 34, the curve started to flatten at the two highest antigen concentration values. By doubling the antigen concentration from 2000 ng/ml to 4000 ng/ml the light intensity did not increase significantly. This is most likely due to the cascade of enzymatic reactions in pyrosequencing beginning to saturate at 2000 ng/ml antigen concentration. This could limit the generated light intensity. In the middle portion of the curve the light intensity corresponded well with the change in antigen concentration levels, producing a region with a quantitative correlation. In the lower portion of the curve the percentage of CV began to increase and the quantitative correlation was no longer valid.

Run 2 in Table 10 was designed to determine the reproducibility for detection of IL-8 antigen between different runs, where each run was performed on different days. Table 14 and Figure 35 compare the obtained results.

Table 14. Reproducibility of IL-8 result: same batch, different runs.

Ag (ng/ml)	CCI (Run 1)				CCI (Run 2)			
	No. of Samples	Light Intensity (AU)			No. of Samples	Light Intensity (AU)		
		Average	SD	%CV		Average	SD	%CV
4000	I _(C.C.1)	272.0	20.0	7.4				
2000	II _(C.C.1)	268.0	19.2	7.2	II _(C.C.1)	250.0	22.4	9.0
800	II _(C.C.1)	234.9	19.0	8.1				
320	II _(C.C.1)	168.9	9.6	5.7				
160	II _(C.C.1)	87.0	8.8	10.1	II _(C.C.1)	60.91	6.92	11.36
80	II _(C.C.1)	39.2	8.8	22.3				
40	II _(C.C.1)	18.7	3.0	15.8				
20	II _(C.C.1)	19.2	4.7	24.3	I _(C.C.1)	14.45	2.29	15.84
10					I _(C.C.1)	12.58	1.63	12.96

Three data points were compared between the different runs. In run 2 an additional data point was tested at a lower antigen concentration to determine the limit of quantitative detection.

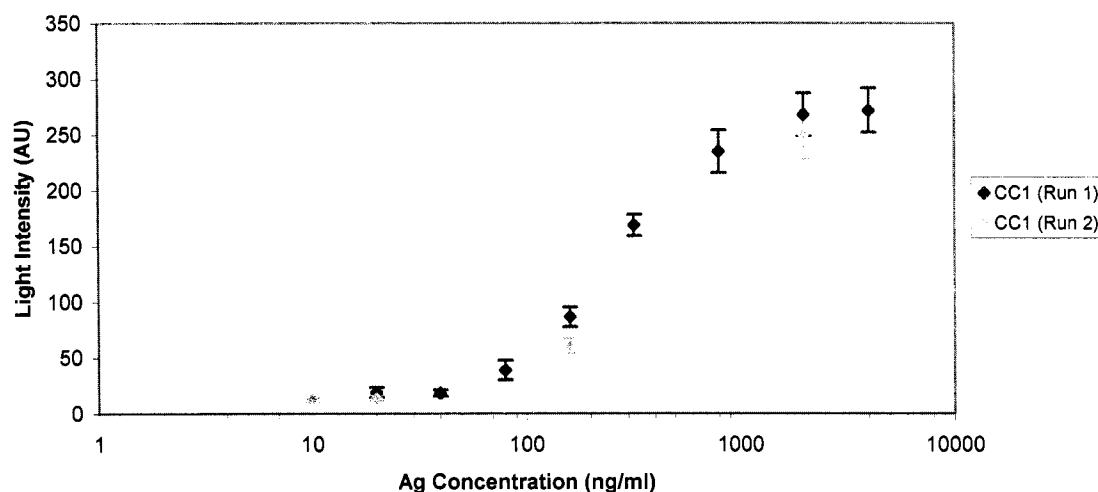


Figure 35. Reproducibility of IL-8 result: same batch, different runs.

In Figure 35 the data points from run 2 were compared with the data points from run 1. At 2000 ng/ml concentration, the different data points compared had overlapping error bars, which indicates a reproducible result. At 160 ng/ml concentration, the different data points compared showed a greater discrepancy, which could be due to experimental error that required further testing. The graph illustrates that there was a consistent shift of lower light intensity in the data set of run 2, indicating that run 2 by itself produced quantitative results. Furthermore, at 10 ng/ml concentration (lowest point), a detectable signal was produced in run 2, thus further testing was required to determine the limit of detection.

Run 3 in Table 10 had two purposes. The first purpose was to determine the limit of detection of IL-8 antigen. The second purpose was to check the reproducibility for detection of IL-8 antigen between different batches of capturing complexes. Table 15 and Figure 36 illustrate the results.

Table 15. IL-8 result: different capturing complex batches, different runs.

Ag (ng/ml)	CC2 (Run 3)				CC1 (Run 1 and Run 2)			
	No. of Samples	Light Intensity (AU)			No. of Samples	Light Intensity (AU)		
		Average	SD	%CV		Average	SD	%CV
80	I _(C.C.2)	19.4	1.1	5.5	II _(C.C.1)	39.2	8.8	22.3
40	I _(C.C.2)	8.9	1.1	12.0	II _(C.C.1)	18.7	3.0	15.8
20					III _(C.C.1)	16.8	4.5	26.9
10	I _(C.C.2)	7.5	0.8	11.0	I _(C.C.1)	12.6	1.6	13.0
5	II _(C.C.2)	8.8	2.5	27.9				
2.5	I _(C.C.2)	7.7	1.0	12.6				
1.25	II _(C.C.2)	10.2	2.7	26.4				

Because all of capturing complex batch CC1 was consumed in previous runs, a new capturing complex batch, CC2, was prepared and used in run 3. To determine the limit of detection, samples were tested down to 1.25 ng/ml concentration level. All data points from run 1, run 2, and run 3 with matching antigen concentration levels were used to check the reproducibility between the two different capturing complex batches.

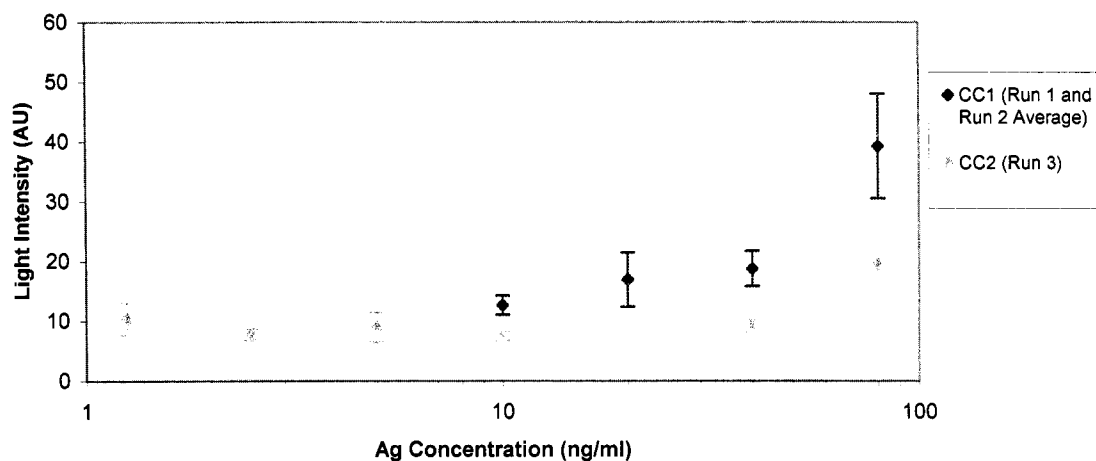


Figure 36. IL-8 result: different capturing complex batches, different runs.

In Figure 36 the light intensity results of run 3 did not correspond quantitatively to the level of antigen concentration, but the presence of the antigen was still detected. At the lowest antigen concentration level a signal was still detected requiring further testing to determine the limit of detection. Comparing the data points of batch CC1 and batch CC2 the results did not show reproducibility. Also, batch CC2 data showed consistently lower light intensity results than CC1, which indicated an inferior capturing complex batch. This could have been due to poor activation of the magnetic beads during preparation of the capturing complex, which would result in having a lower antibody count in the CC2 capturing complex as compared to the CC1 capturing complex. A third capturing complex batch needed to be made and tested to determine the limit of detection, as well as to determine the quality of batch CC2.

Run 4 in Table 10 was designed to determine the limit of detection of IL-8 antigen, and to check the quality of different batches of capturing complexes. Table 16 and Figure 37 illustrate the results.

Table 16. IL-8 result: different capturing complex batches, same run.

Ag (ng/ml)	CC2 (Run 4)				CC3 (Run 4)			
	No. of Samples	Light Intensity (AU)			No. of Samples	Light Intensity (AU)		
		Average	SD	%CV		Average	SD	%CV
5	I _(C.C.2)	7.3	1.5	20.7	I _(C.C.3)	10.1	0.9	8.8
2.5	I _(C.C.2)	7.6	0.3	4.3				
1.25	I _(C.C.2)	7.1	1.0	13.6				
0.625	I _(C.C.2)	9.5	0.9	9.0	I _(C.C.3)	6.9	1.2	17.0
0.3125	I _(C.C.2)	4.7	1.6	33.2	II _(C.C.3)	13.4	5.9	44.3
0.15625	I _(C.C.2)	6.5	1.0	16.0	II _(C.C.3)	6.3	0.5	8.3

In run 4 two different capturing complex batches were tested. A data point at 5 ng/ml concentration was used to measure the quality of batch CC2 with respect to batch CC3. This concentration level was chosen because it was the highest level of batch CC2 that was tested, but not compared with a different capturing complex batch. Three data points that had matching antigen concentration levels below 1 ng/ml were used to determine the limit of detection.

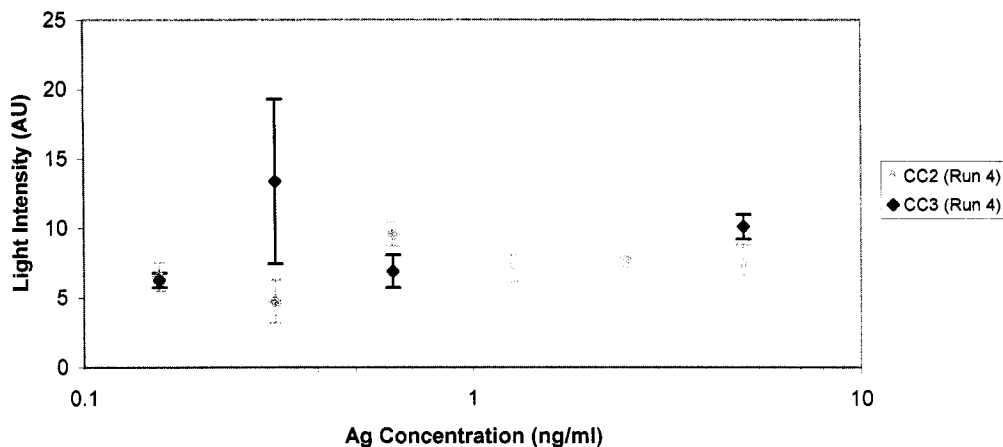


Figure 37. IL-8 result: different capturing complex batches, same run.

In Figure 37 the light intensity results of run 4 for 5 ng/ml concentration level showed the difference between capturing complex batch CC2 and batch CC3. Batch CC2 had a significantly lower light intensity than batch CC3. The lower light intensity of CC2 was consistent with the comparison to batch CC1 at different concentration values shown earlier in Figure 36. This result confirmed the inferior quality of batch CC2. At the lower antigen concentration levels of less than 1 ng/ml a signal was still detected, but the results were very inconsistent with varying standard deviations. The background noise signal (control experiment) for IL-8 antigen using the MA pyrosequencing machine was determined in earlier experiments; however, further testing was required to determine the background noise signal for IL-8 with the new HS pyrosequencing machine, so that the limit of detection could be extrapolated.

Run 5 in Table 10 was designed with several purposes in mind using capturing complex batch CC3. The first purpose was to determine the background noise signal

when no antigen was present in the solution. The second purpose was to find the limit of detection. The third purpose was to test several antigen concentration levels to check the reproducibility of data points in the quantitative region of Figure 34. Table 17 displays the results to determine both the background noise signal and find the limit of detection.

Table 17. IL-8 result: Limit of detection and noise level.

Ag (ng/ml)	CC3 (Run 5)			
	No. of Samples	Light Intensity (AU)		
		Average	SD	%CV
0.15625	$I_{(C,C,3)}$	6.70	0.22	3.32
0.078125	$II_{(C,C,3)}$	10.09	3.19	31.61
0	$V_{(C,C,3)}$	5.82	0.86	14.71

As shown in Table 17, five samples each with five replicates were tested to measure the background noise signal when no antigen was present. The average noise signal was determined to be 5.82 AU with a standard deviation of 0.86 AU. Equation 8 from section 4.3 was used to calculate the background noise level, which equaled 8.4 AU. Therefore, any data points with a light intensity of 8.4 AU or lower had to be omitted. Note that the background noise signal of 5.82 AU must be subtracted from all generated signals in order to obtain the true magnitude of the signals. At the lowest tested antigen concentration level (0.078125 ng/ml) the light intensity signal was above the noise level. This data point was tested in two samples, each with five replicates, and only one sample produced a signal higher than the noise level. Although, the IL-8 antigen was detected at 0.078125 ng/ml the signal was not consistently reproducible. Due to limited experimental reagents no further testing could be conducted to confirm the repeatability

of this data point, nor to test lower antigen concentration levels. The lowest antigen concentration level that could be detected confidently was shown to be at 5 ng/ml in run 4. All average light intensities generated above 5 ng/ml antigen concentration levels were consistently greater than the background noise level, and all lower concentration levels did not produce repeatable results. This was most likely due to errors in the signal intensities that were of the same magnitude as the real detected signals at low antigen concentration levels, which caused the detected signals to be less than the background noise. In this thesis, the lowest limit of detection for IL-8 antigen was found to be at 0.078125 ng/ml (78 pg/ml), and the lowest reproducible limit of detection was found to be at 5 ng/ml.

At this point a comparison could be made between the limit of detection of IL-8 antigen using the MA pyrosequencing machine (20 ng/ml) and the HS pyrosequencing machine (78 pg/ml). The limit of detection using the HS machine improved by 2.4 orders of magnitude; however, the signal to noise ratio (S/N) at the limits of detection remained the same (about 2). Thus, the sensitivity of the HS machine improved without sacrificing signal quality.

The final purpose of run 5 was to check the reproducibility of data points in the quantitative region of Figure 34. Table 18 and Figure 38 compare the results of run 5 with the average of run 1 and run 2.

Table 18. IL-8 result: different capturing complex batches, different runs.

Ag (ng/ml)	CC1 (Run 1 and Run 2)				CC3 (Run 5)			
	No. of Samples	Light Intensity (AU)			No. of Samples	Light Intensity (AU)		
		Average	SD	%CV		Average	SD	%CV
4000	I _(C.C.1)	272.0	20.0	7.4				
2000	IV _(C.C.1)	265.3	24.5	9.2				
800	II _(C.C.1)	234.9	19.0	8.1				
640					II _(C.C.3)	220.7	27.3	12.4
320	II _(C.C.1)	168.9	9.6	5.7	I _(C.C.3)	172.9	13.2	7.7
160	IV _(C.C.1)	73.9	14.3	19.4				
80	II _(C.C.1)	39.2	8.8	22.3	II _(C.C.3)	41.94	2.65	6.31
40	II _(C.C.1)	18.0	2.5	14.1	I _(C.C.3)	15.2	1.6	10.2

Run 1 and run 2 both used capturing complex batch CC1 and had data points in the quantitative range of antigen concentration. Run 5 used capturing complex batch CC3 with data points in the same quantitative region, which included the 640 ng/ml antigen concentration level to increase the data set of this region.

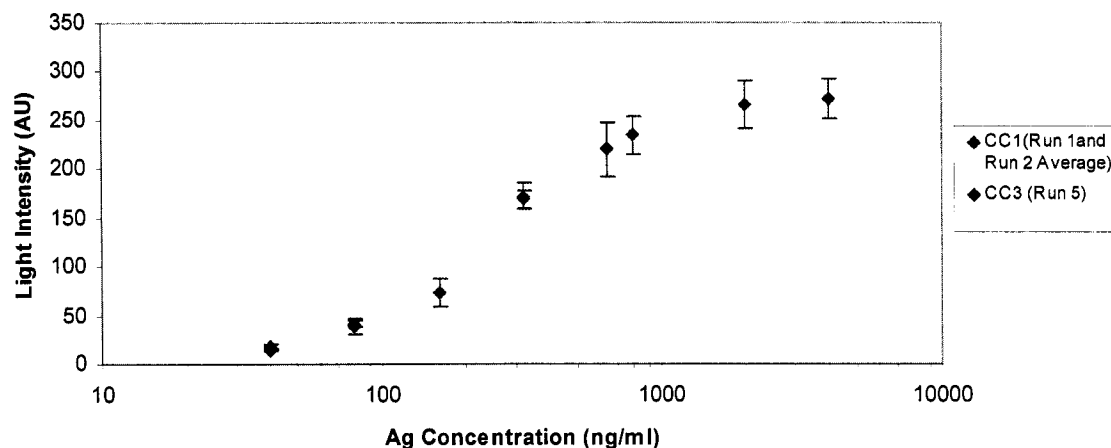


Figure 38. IL-8 result: different capturing complex batches, different runs.

As illustrated in Figure 38 the data set in the quantitative region was highly reproducible with low percentage of CV. All data from runs 1, 2, and 5 confirmed that

the quantitative region was between 40 ng/ml and 4,000 ng/ml concentration levels of IL-8 antigen. The dominating factor for non-quantitative results below 40 ng/ml concentration was most likely due to the constant noise signal caused by non-specific binding between the capturing and detection antibodies. At higher concentration levels of antigen this noise signal was relatively small, and contributed only a few percentage points of variation. At lower concentration levels of antigen this noise signal had a significant effect on the accuracy of the generated signal, which caused large percentage points of variation.

Figure 39 illustrates the average of all data sets from the five runs discussed in this section excluding any data points obtained using capturing complex batch CC2, due to its inferior quality. The data set includes all results with light intensities greater than the noise level. The dynamic range is noted, where the results are quantitative.

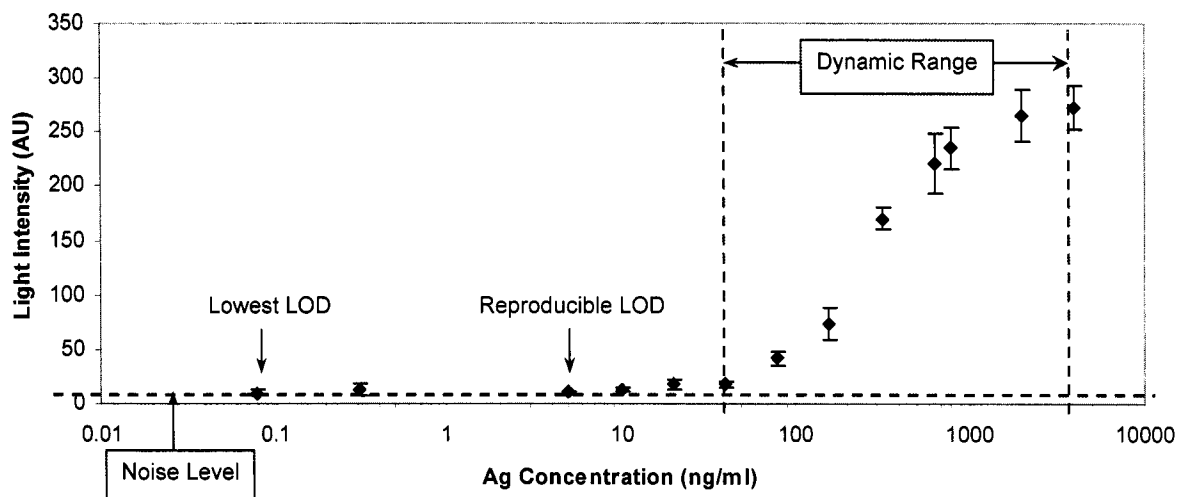


Figure 39. Comprehensive results of IL-8 antigen.

The dynamic range results of IL-8 antigen displayed increasing light intensity with increasing antigen concentration, where the light intensity of each data point was proportional to the matching antigen concentration. The percentage of CV of the data points in the dynamic range were between 7% and 19%, with an average of less than 12%. This confirmed reproducibility of the results.

The final result for quantitative detection of IL-8 produced a dynamic range that covered two orders of magnitude from 40 to 4,000 ng/ml antigen concentration. The limit of detection for this protein was found to be 78 pg/ml. It is reported in the Pierce catalog that the dynamic range for the same IL-8 protein using the ELISA method covers less than two orders of magnitude, from 25.6 pg/ml to 1,000 pg/ml with a limit of detection of 2 pg/ml.

CHAPTER SIX CONCLUSIONS

In this research a novel method for quantitative protein detection was studied. Magnetic beads coated with the capturing antibodies were mixed with a sample containing the antigen. Detection antibodies carrying self primed oligonucleotides (pyro-tags) were added to the sample forming sandwich immunocomplexes. Pyrosequencing was used to detect and quantify the captured antigen.

Single protein detection experiments were performed by employing the MA pyrosequencing machine on three different antigens: IL-8, IL-4, and IL-10. The IL-8 antigen produced the highest stability and sensitivity with a 20 ng/ml limit of detection.

The other antigens were used to conduct three different combinations of multiplexing experiments. In all multi-plexing experiments the antigens could be simultaneously detected but not quantified. Multi-plexing experiment of pure pyro-tags had a quantitative and consistent result. This indicated that the discrepancy in the multiplex protein detection was most likely due to the intermolecular interactions between the two antigens and their capturing and detection complexes.

The obtained results for single protein detection using the MA machine were all quantitative; however, the experiments tested few antigen concentration levels and lacked

sufficient replicates. The main reason for this limited data was due to relatively large sample volumes required by the MA machine, which would increase the assay cost.

Next, the more sensitive HS pyrosequencing machine was employed to decrease sample volumes and to allow more extensive experiments. These experiments were performed with the IL-8 antigen. The final assay volume had to be optimized to ensure proper mixing of reagents inside the HS plate during pyrosequencing runs. The sample volume was reduced to approximately one third of that used in the MA machine (16 μ l:50 μ l), and the volume of pyrosequencing reagents (substrate and enzyme) was also reduced by a factor of 2.5 (4 μ l:10 μ l).

The dynamic range for detection of IL-8 covered two orders of magnitude. The limit of detection for this protein using the HS machine was found to be 78 pg/ml, which was 2.4 orders of magnitude better than the MA machine result. The percentage of CV within the dynamic range of IL-8 was between 7% and 19%. These results are nearly comparable with the well established ELISA method. Nonetheless, by employing different pyro-tags in this research simultaneous detection of multiple proteins was achieved. The ELISA method is only capable of single protein detection, but with this technique two different proteins were detected in the same assay volume and assay time as single protein detection. Moreover, this technique has the potential for multi-plexing, where multiple proteins can be both detected and quantified simultaneously. This could greatly reduce assay volume, time, and overall cost.

CHAPTER SEVEN FUTURE STUDY

Simultaneous detection and quantification of proteins is very important for rapid disease diagnosis as well as new drug designs. This can be achieved with multi-plexing as described in this thesis. The initial results were limited due to low quality antigen samples (IL-4 and IL-10), and the multi-plexing results were only valid for the simultaneous detection of two antigens. Clinically relevant results for the detection and quantification of a single antigen were obtained using a good quality antigen (IL-8) and a more sensitive pyrosequencing machine (HS). To achieve true multi-plexing, the logical next step is to find a second good quality antibody-antigen system (stable without cross reactivity) and to conduct quantitative experiments together with IL-8. Upon successful results, a third antibody-antigen system can be confirmed and employed in multi-plexing. By following this step-by-step approach, the number of antigens to be simultaneously detected and quantified can be increased to implement large scale multi-plexing.

REFERENCES

1. M. McNeil, ChE-192 Lecture Notes, Introduction to Biochemical Engineering Course at San Jose State University (Fall 2003).
2. M.L. Shuler and F. Kargi, *Bioprocess Engineering*, 2nd ed. (Prentice-Hall, Inc., New Jersey, U.S.A., 2002), pp. 26-46.
3. Introduction to Antibodies [Online] Available at <http://www.chemicon.com/resource/ANT101/a1.asp> (accessed 30 March 2006).
4. J.P. Gosling, Immunoassays [Online] Available at <http://www.wiley-vch.de/books/emcbmm2/samples/Immunoassays.pdf> (accessed 20 February 2005).
5. N. Soh, H. Nishiyama, Y. Asano, T. Imato, T. Masadome and Y Kurokawa, "Chemiluminescence sequential injection immunoassay for vitellogenin using magnetic microbeads," *Talanta*, **64**, pp. 1160-1168 (December 2004).
6. M. Ronaghi, "Pyrosequencing sheds light on DNA sequencing," *Genome Research*, **11**, 3-11 (January 2001).
7. A. Agah, M. Aghajan, F. Mashayekhi, S. Amini, R.W. Davis, J.D. Plummer, M. Ronaghi and P.B. Griffin, "A multi-enzyme model for pyrosequencing," *Nucleic Acids Research*, **32**, pp. 1-14 (October 2004).
8. Principles of ELISA [Online] Available at <http://www.iuk.edu/faculty/cchauret/L321/L321series4.htm> (accessed 10 March 2005).
9. H.A.H. Rongen, H.M. van der Horst, A.J.M. van Oosterhout, A. Bult and W.P. van Bennekom, "Application of xanthine oxidase-catalyzed luminol chemiluminescence in a mouse interleukin-5 immunoassay," *Journal of Immunological Methods*, **197**, pp. 161-169 (1996).
10. L.D. Ciana, G. Bernacca, C. De Nitti and A. Massaglia, "Highly sensitive amperometric enzyme immunoassay for α -fetoprotein in human serum," *Journal of Immunological Methods*, **193**, pp. 51-62 (June 1996).
11. S.G. Gundersen, I. Haagensen, T.O. Jonassen, K.J. Figenschau, N. de Jonge and A.M. Deelder, "Magnetic bead antigen capture enzyme-linked immunoassay in

- microtiter trays for rapid detection of schistosomal circulating anodic antigen,*" Journal of Immunological Methods, **148**, pp. 1-8 (1992).
12. T. Alefantis, P. Grewal, J. Ashton, A.S. Khan, J.J. Valdes and V.G. Del Vecchio, "*A rapid and sensitive magnetic bead-based immunoassay for the detection of staphylococcal enterotoxin B for high-throughput screening,*" Molecular and Cellular Probes, **18**, pp. 379-382 (December 2004).
 13. Y. Che, Y. Li and M. Slavik, "*Detection of Campylobacter jejuni in poultry samples using an enzyme-linked immunoassay coupled with an enzyme electrode,*" Biosensors and Bioelectronics, **16**, pp. 791-797 (December 2001).
 14. A.G. Gehring, P.L. Irwin, S.A. Reed, S. Tu, P.E. Andreotti, H. Akhavan-Tafti and R.S. Handley, "*Enzyme-linked immunomagnetic chemiluminescent detection of Escherichia coli O157:H7,*" Journal of Immunological Methods, **293**, pp. 97-106 (October 2004).
 15. J. Kim, C. Wang, S. Kuizon, J. Xu, D. Barendolts, P.C. Gray and R. Rubenstein, "*Simple and specific detection of abnormal prion protein by a magnetic bead-based immunoassay coupled with laser-induced fluorescence spectrofluorometry,*" Journal of Neuroimmunology, **158**, pp. 112-119 (January 2005).
 16. D.G. Georganopoulou, L. Chang, J. Nam, C. Shad Thaxton, E.J. Mufson, W.L. Klein and C.A. Mirkin, "*Nanoparticle-based detection in cerebral spinal fluid of a soluble pathogenic biomarker for Alzheimer's disease,*" PNAS, **102**, pp. 2273–2276 (February 15, 2005).
 17. C.D. Keating, "*Nanoscience enables ultrasensitive detection of Alzheimer's biomarker,*" PNAS, **102**, pp. 2263–2264 (February 15, 2005).
 18. T. Langae and M. Ronaghi, "*Genetic variation analyses by Pyrosequencing,*" Fundamental and Molecular Mechanisms of Mutagenesis, **573**, pp. 96-102 (June 2005).
 19. G.B. Sigal, M. Mrksich and G.M. Whitesides, "*Effect of Surface Wettability on the Adsorption of Proteins and Detergents,*" J. Am. Chem. Soc., **120**, pp. 3464–3473 (1998).
 20. K.-P.S. Dancil, D.P. Greiner and M.J. Sailor, "*A Porous Silicon Optical Biosensor: Detection of Reversible Binding of IgG to Protein A-Modified Surface,*" J. Am. Chem. Soc., **121**, pp. 7925–7930 (1999).

21. Y. Li, Y.T.H. Cu and D. Luo, “*Multiplexed detection of pathogen DNA with DNA-based fluorescence nanobarcodes*,” *Nature Biotechnology*, **23**, pp. 885–889 (June 2005).
22. G. Zheng, F. Patolsky, Y. Cui, W.U. Wang and C.M. Lieber, “*Multiplexed electrical detection of cancer markers with nanowire sensor arrays*,” *Nature Biotechnology*, **23**, pp. 1294–1301 (2005).
23. E.P. Kartalov¹, J.F. Zhong¹, A. Scherer, S.R. Quake, C.R. Taylor¹ and W.F. Anderson¹, “*High-throughput multi-antigen microfluidic fluorescence immunoassays*,” *BioTechniques*, **40**, pp. 85–90 (January 2006).
24. S.F. Kingsmore, “*Multiplexed protein measurement: technologies and applications of protein and antibody arrays*,” *Nature Reviews Drug Discovery*, **5**, pp. 310–321 (April 2006).
25. C.Y. Yang, E. Brooks, Y. Li, P. Denny, C.M. Ho, F. Qi, W. Shi, L. Wolinsky, B. Wu, D. Wong and C.D. Montemagno, “*Detection of picomolar levels of interleukin-8 in human saliva by SPR*,” *Lab on a Chip*, **5**, pp. 1017–1023 (August 2005).

APPENDIX A EXPERIMENTAL STEPS PRIOR TO THE MAIN APPROACH

In this thesis, the sandwich immunocomplex captured on magnetic beads was constructed step by step incorporating different approaches, which finally led to the main approach. These steps were needed to produce a robust method mentioned in Chapter Four, although several of these steps did not give precise and reproducible results. All experiments discussed in this section were performed using the MA pyrosequencing machine. These experimental steps are mentioned below in the order in which they were executed.

1. In the first step, pyrosequencing was performed on different biotinylated pyro tags with different number of moles. Figure A1 shows a basic structure of a pyro-tag.



Figure A1. Basic structure of a pyro-tag.

To summarize, only one type of pyro-tag is discussed. 100 μM biotinylated pyro-tag in Tris EDTA buffer with the sequence b-CTGC was used as a template during pyrosequencing. To test 1 pmol of pyro-tag, b-CTGC was diluted to a concentration of 1 μM in DI water. Next, 1 μl b-CTGC mixed with 39 μl of DI water was transferred into a well of a 96-well microtiter plate. To test 5 pmol of pyro-tag, 5 μl b-CTGC mixed with 35 μl of DI water was transferred into another well of the microtiter plate. Next, 5 μl pyrosequencing substrate mixture (Luciferin, Adenosine 5' Phosphosulfate) and 5 μl pyrosequencing enzyme mixture (DNA Polymerase, ATP Sulfurylase, Luciferase,

Apyrase) were added to each well. The inkjet cartridge was filled with 50 μ l of nucleotides (dATP α S, dGTP, dCTP, dTTP) and was inserted into the pyrosequencing machine along with the microtiter plate. The machine's software program was then adjusted to the desired settings and the run was performed. During the run, signals corresponding to the b-CTGC pyro-tag were generated, which are shown in Figures A2 and A3.

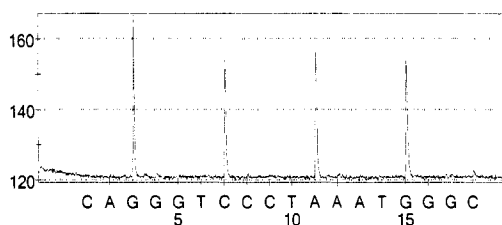


Figure A2. 1 pmol b-CTGC.

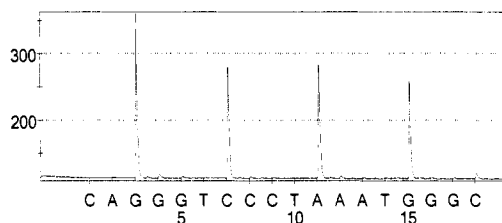


Figure A3. 5 pmol b-CTGC.

As shown in both graphs, during pyrosequencing the complimentary sequences were synthesized and the GCAG signals were generated. The intensity of the signals in Figure A3 is approximately 5 times greater than the signals in Figure A2, which corresponds to the amount of pyro-tag being five times greater in the second sample.

2. In the Second step, streptavidin-coated magnetic beads were coated with a specific biotinylated pyro-tag and pyrosequencing was performed to detect the attached pyro-tag. Figure A4 shows a simple representation of this experiment.

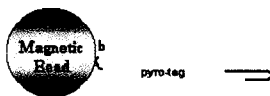


Figure A4. Biotinylated pyro-tag is attached to magnetic bead.

Dynabeads M-280 streptavidin super paramagnetic beads (DynaL Biotech) with 2.8 μm diameter were used as the surface for capturing the pyro-tag. These beads could be manipulated when a magnetic field was applied. Streptavidin is a tetrameric protein that has high affinity binding ($KD = 10^{-15}$) for biotin. The beads were supplied as a suspension containing 10 mg beads per ml that had been dissolved in phosphate buffered saline (PBS) containing 0.1% BSA. According to the manufacturer's protocol, one milligram of Dynabeads binds to 200 pmol biotinylated oligonucleotides (pyro-tags). To make two different samples with 20 pmol and 50 pmol biotinylated pyro-tags attached to the beads, 10 μl and 25 μl of the beads were transferred into two microcentrifuge tubes, and the tubes were placed on the magnet for two minutes. The supernatants were removed by a pipette while the tubes remained on the magnet. Next, the beads were washed with 20 μl and 50 μl binding and washing buffer (B&W), (10 mM Tris-HCl, 1 mM EDTA, 2.0 M NaCl), pH 7.5 respectively, and resuspended in 20 μl and 50 μl of B&W buffer. To ensure that all the biotin sites of the beads were coated with the pyro-tags, twice the amount of needed pyro-tags were added to the beads. 0.4 μl (40 pmol) biotinylated pyro-tag with the sequence of b-C (Stanford Genome Technology Center)

mixed with 19.6 μ l of DI water was added to the first tube, and 1 μ l (100 pmol) b-C mixed with 49 μ l of DI water was added to the second tube. Both samples were incubated for one hour on the tube rotator. After incubation, both tubes were placed on the magnet and washed two times with 40 μ l and 100 μ l of B&W buffer respectively, four times with DI water, and resuspended in 40 μ l DI water. The remainder of the procedure of transferring the samples to the pyrosequencing machine was identical to step 1 of this section. During the run, signals corresponding to the b-C were generated, which are shown in Figures A5 and A6.

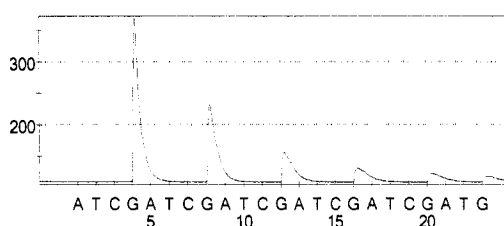


Figure A5. 20 pmol b-C is attached on magnetic beads.

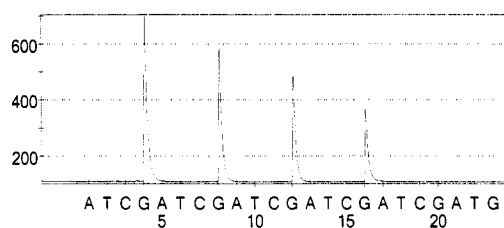


Figure A6. 50 pmol b-C is attached on magnetic beads.

As shown in both graphs, during pyrosequencing the complimentary sequences were synthesized and the G signals were generated. The magnitude of the signals in Figure A6 is about 2.5 times greater than the signals in Figure A5, which corresponds well with the amount of the attached pyro-tags to the beads (50 pmol : 20 pmol).

3. In the third step, the streptavidin-coated magnetic beads were coated with a specific biotinylated pyro-tag, and then free biotin was added to block the remaining biotin binding sites of the beads. Next, another kind of biotinylated pyro-tag was added and then pyrosequencing was performed to check for the signals generated only from the first attached pyro-tag. A simple representation of this experiment is shown in Figure A7.

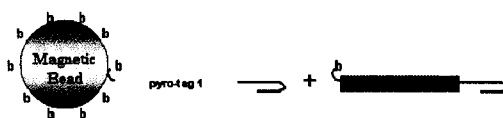


Figure A7. A specific biotinylated pyro-tag is attached to the magnetic bead, the rest of the beads' biotin sites are blocked with free biotin, and then another type of biotinylated pyro-tag is added to the sample.

To attach 50 pmol b-G pyro-tag (Stanford Genome Technology Center) to the beads, 25 μ l of beads was transferred into a microcentrifuge tube and the tube was placed on the magnet for two minutes. The supernatant was removed by a pipette while the tube remained on the magnet. Next, the beads were washed with 50 μ l B&W buffer and resuspended in 50 μ l B&W buffer. 1 μ l (100 pmol) b-G mixed with 49 μ l DI water was added to the beads' tube, and the sample was incubated for one hour on the tube rotator. After incubation, the tube was placed on the magnet and the supernatant was removed. According to the manufacturer's protocol, one milligram of Dynabeads binds to 700 pmol of free biotin. To ensure that all the remaining biotin sites of the beads were blocked with the free biotin, twice the needed amount of free biotin was added to the beads. 35 μ l (350 pmol) free biotin solution with the concentration of 10 μ M and 65 μ l B&W buffer were added to the beads, and the sample was incubated for 30 minutes on

the tube rotator. After incubation the beads were washed three times with 100 μ l B&W buffer and resuspended in 50 μ l B&W buffer. Next 1 μ l (100 pmol) b-C mixed 49 μ l DI water were added to the sample, and the sample was incubated for another one hour on the tube rotator. Finally the tube was placed on magnet and the beads were washed two times with 100 μ l B&W buffer, four times with 100 μ l DI water, and resuspended in 40 μ l DI water. The remainder of the procedure of transferring the sample to the pyrosequencing machine was identical to step 1 of this section. The result of this experiment is shown in Figures A8.

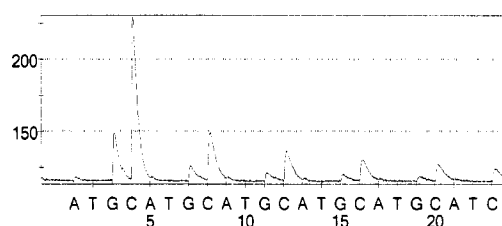


Figure A8. 50 pmol b-G is attached to magnetic beads, biotin is added to block the free biotin sites of the beads, and then 50 pmol b-C is added to the beads.

The C signals generated during pyrosequencing correspond to the attached b-G pyro-tag. Since free biotin was added to the beads, there should not be any free biotin binding sites available on the beads for the next added pyro-tag to attach. However, as shown in Figure A8, the released G signals verify the presence of b-C pyro-tag that has attached to the beads.

To enhance the results, another experiment was performed, where all the steps were kept the same as the previous steps, except the step in which the free biotin was added. Instead of adding 35 μ l (350 pmol) free biotin with concentration of 10 μ M, 35 μ l

(35,000 pmol) of free biotin with the concentration of 1mM solution was added. This was done to ensure that sufficient biotin was added to the beads, and therefore no biotin binding site was available for the second pyro-tag. Figure A9 demonstrates the results of this experiment.

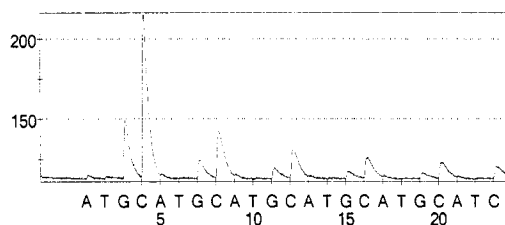


Figure A9. 50 pmol b-G is attached to magnetic beads, biotin is added to block the free biotin sites of the beads, and then 50 pmol b-C is added to the beads.

As shown in Figure A9, the G signal was still generated. This indicates that the b-C pyro-tag was present in the solution and was not washed out from the sample. Since the beads were fully coated with the first pyro-tag and free biotin, then the only spot that the b-C pyro-tag could be attached to was the b-G pyro-tag. The b-G pyro-tag has 20 G nucleotides in a row and so there is a possibility that the b-C pyro-tag with 20 C nucleotides in a row had hybridized to it.

The next experiment was designed to have the same procedure as the previous experiment up to the point of adding the second pyro-tag. The second pyro-tag was not a biotinylated oligonucleotide; instead it was a Thiol-C pyro-tag with 20 C nucleotides in a row. Figure A10 illustrates the results of this experiment.

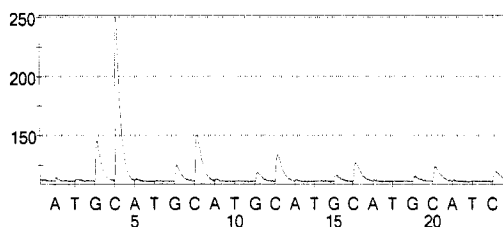


Figure A10. 50 pmol b-G is attached to magnetic beads, biotin is added to block the free biotin sites of the beads, and then 50 pmol Thiol-C is added to the beads.

As shown in Figure A10, the G signals were generated during pyrosequencing. Since the Thiol-C pyro-tag was not biotinylated, it could not have been attached to the beads, and so this is a strong indication that the Thiol-C pyro-tag due to having 20 C nucleotides in a row had hybridized to the b-G pyro-tag. To confirm this conclusion, b-CTGC was used as the second pyro-tag for the following experiment. Figure A11 shows the obtained results.

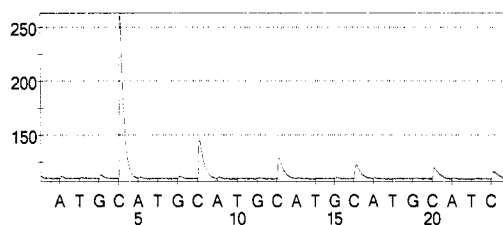


Figure A11. 50 pmol b-G is attached to magnetic beads, biotin is added to block the free biotin sites of the beads, and then 50 pmol b-CTGC is added to the beads.

The b-CTGC pyro-tag has only five replicates of each nucleotide in a row, so the chance of hybridization of this oligonucleotide to the b-G pyro-tag was very weak, which corresponds well to the achieved results. As shown in the graph no GCAG signals were generated.

4. In the fourth step, the streptavidin-coated magnetic beads were coated with a biotinylated Ab, and then a specific biotinylated pyro-tag was added. Next, free biotin was added to the sample to block the remaining biotin binding sites of the beads, and finally pyrosequencing was performed to detect the attached pyro-tag. Throughout this experiment, the ratio of the biotinylated antibody to the biotinylated pyro-tag was varied in a way as to maximize the amount of antibody coated on the beads with enough biotinylated pyro-tag to detect a signal. This complex was referred to as the capturing complex. The capturing complex was labeled with a pyro-tag for the purpose of locating the specific position of the whole immunocomplex within a magnetic bead micro-array. This was based on the design potential to allow multi-plexing of different antigens using a magnetic bead micro-array. A simple representation of this experiment is shown in Figure A12.

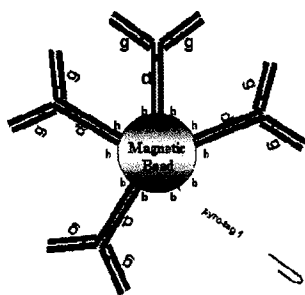


Figure A12. Biotinylated antibodies and biotinylated pyro-tags are coated on a magnetic bead.

Polyclonal biotinylated anti-goat IgG antibody produced in donkey: b-(dag)Ab (R&D Systems) was used to coat the surface of the beads. The b-(dag)Ab was supplied in a lyophilized form and was reconstituted in Tris buffered saline (20 mM Trizma base, 150 mM NaCl) with 0.1% BSA, pH 7.3 (TBS). According to the manufacturer's

protocol, 1 mg of Dynabeads binds to 5-10 μg of biotinylated antibody. 25 μl of beads (0.25 mg) was transferred into a microcentrifuge tube and the tube was placed on the magnet for two minutes. The supernatant was removed by a pipette while the tube remained on the magnet. Next, the beads were washed with 50 μl PBS buffer and resuspended in 50 μl PBS buffer. 5 μl b-(d α g) antibody (1.25 μg) with concentration of 250 $\mu\text{g}/\text{mL}$ mixed with 45 μl PBS buffer was added to the beads' tube and the sample was incubated for 30 minutes on the tube rotator. After incubation, the tube was placed on the magnet and the beads were washed four times with 100 μl PBS buffer and then resuspended in 50 μl B&W buffer. 1 μl (100 pmol) b-G mixed with 49 μl DI water was added to the beads' tube, and the sample was incubated for one hour on the tube rotator. After incubation, the tube was placed on the magnet and the supernatant was removed. 35 μl free biotin solution and 65 μl B&W buffer were added to the beads, and the sample was incubated for 30 minutes on the tube rotator. Finally the tube was placed on the magnet and the beads were washed two times with 100 μl B&W buffer, four times with 100 μl DI water, and resuspended in 40 μl DI water. The remainder of the procedure of transferring the sample to the pyrosequencing machine was identical to step 1 of this section. Four more experiments were executed in parallel, which everything was kept the same except the amount of the added b-(d α g)Ab. The added antibody in these four experiments ranged from 2.5 μg to 5 μg to 7.5 μg to 10 μg . Figures A13 through A17 show the obtained results.

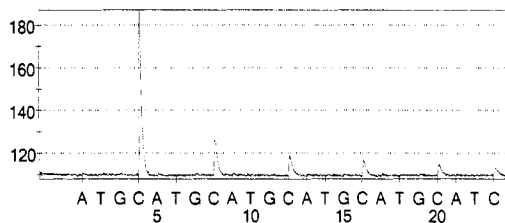


Figure A13. 1.25 μg b-(dag)Ab, 50 pmol b-G and free biotin are coated on magnetic beads.

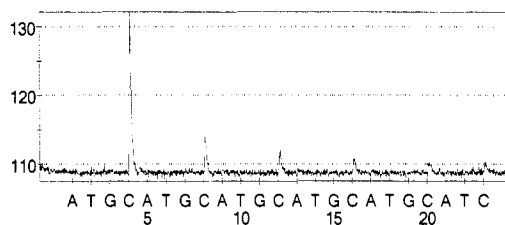


Figure A14. 2.5 μg b-(dag)Ab, 50 pmol b-G and free biotin are coated on magnetic beads.

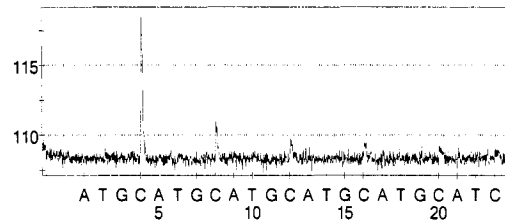


Figure A15. 5 μg b-(dag)Ab, 50 pmol b-G and free biotin are coated on magnetic beads.

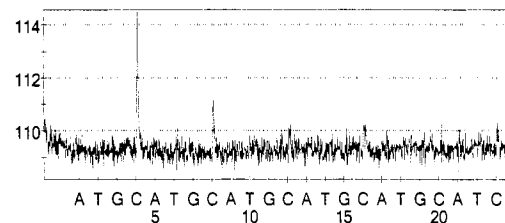


Figure A16. 7.5 μg b-(dag)Ab, 50 pmol b-G and free biotin are coated on magnetic beads.

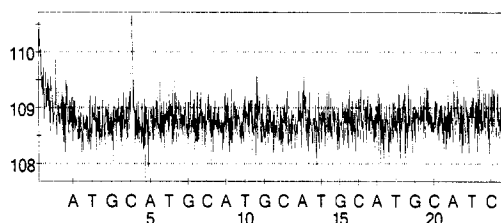


Figure A17. 10 μg b-(dag)Ab, 50 pmol b-G and free biotin are coated on magnetic beads.

The objective of this experiment was to attach as much as possible biotinylated Ab to the beads with only enough biotinylated pyro-tag to get a detectable signal. As shown throughout Figures A13 to A17, the generated C signals were decreased by increasing the amount of added biotinylated antibody, which satisfied the objectives. The C signal in Figure A17 is very close to the noise level of the machine, therefore the desired amount of biotinylated antibody to be attached to the beads to make the capturing complex, was found to be 7.5 μg (50 pmol), which is shown in Figure A16.

5. In the fifth step, another type of biotinylated Ab was used to make a secondary complex. The capturing complex and the secondary complex were added together and pyrosequencing was performed to detect the generated signals from the pyro-tags. Figure A18 shows a basic representation of this experiment.

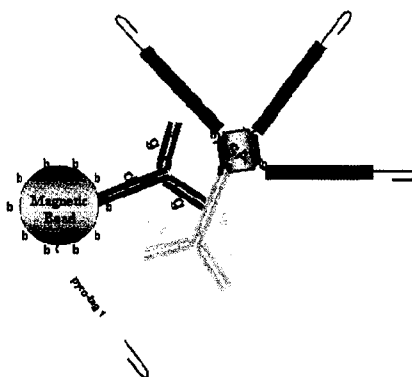


Figure A18. A biotinylated Ab is used to make the secondary complex. The capturing complex and the secondary complex are added together.

The capturing complex was prepared according to step 4 with 7.5 μg (50 pmol) b-(dag)Ab coated on the beads. Biotinylated anti-rabbit IgG antibody produced in goat: b-(gar)Ab (R&D Systems) was used to make the secondary complex. The b-(gar)Ab was supplied in a lyophilized form and was reconstituted in Tris buffered saline (20 mM Trizma base, 150 mM NaCl) with 0.1% BSA, pH 7.3 (TBS). To make the secondary complex, b-CTGC pyro-tags were attached to the b-(gar)Ab through streptavidin (SA), which acted as an intermediate binding molecule. Considering the molecular size and structure of the Ab, SA, and pyro-tag, the molar ratio in which they were added was decided to be 1:2:10 respectively. 60 μl b-(gar)Ab (100 pmol) and 10 μl SA (200 pmol) that had been dissolved in the PBS buffer with concentration of 20 μM were added into a microcentrifuge tube and the tube was incubated for 30 minutes on the tube rotator. Next, 10 μl b-CTGC (1000 pmol) was added to the mixture and the sample was incubated for one hour on the tube rotator. Thus, the remaining biotin binding sites of the SA were used to couple b-CTGC pyro-tags. Finally, the sample was incubated for

another 30 minutes with free biotin to ensure that there were no biotin binding sites available on the SA, making the secondary complex ready for use.

After the capturing complex was ready, the sample was placed on the magnet and the beads were washed twice with 100 μ l B&W buffer. Next, the secondary complex was added to the capturing complex and the sample was incubated for one hour on the tube rotator. Finally the tube was placed on the magnet and the beads were washed six times with 100 μ l DI water, and resuspended in 40 μ l DI water. The remainder of the procedure of transferring the sample to the pyrosequencing machine was identical to step 1 of this section. The result of this experiment is shown in Figure A19.

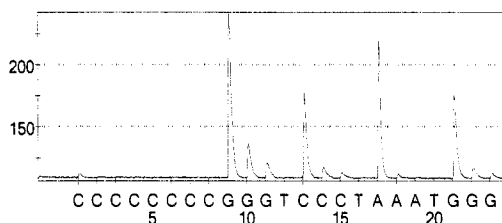


Figure A19. Secondary complex is made by having 15 μ g (100 pmol) b-(gar)Ab, 200 pmol SA, and 1000 pmol b-CTGC. The capturing complex is then added to the secondary complex and the binding occurrence is checked by pyrosequencing.

The b-G pyro-tag was attached to the capturing complex and the b-CTGC pyro-tag was attached to the secondary complex. Theoretically, if the b-(dag)Ab and the b-(gar)Ab were bounded together, then during pyrosequencing the corresponding signals from the attached pyro-tags would be generated. As illustrated in Figure A19, first there is a very low C signal generated from the b-G pyro-tag, and then there are much higher GCAG signals released from the b-CTGC pyro-tag. This result confirms the binding

between the two Abs and consequently the two complexes, which fulfilled the objective of this experiment.

6. In the sixth step, b-(dag)Ab was used to make the detection complex. Anti-rabbit IgG antibody produced in goat (gar)Ab (R&D Systems) was used instead of an antigen and is referred to as Ag throughout this section. The capturing complex and the Ag were added together, followed by the addition of the detection complex to make the whole immunocomplex. Pyrosequencing was performed to detect the captured Ag. A control experiment in which the Ag was not present in the sample was carried out simultaneously. Figure A20 represents a schematic representation of this experiment.

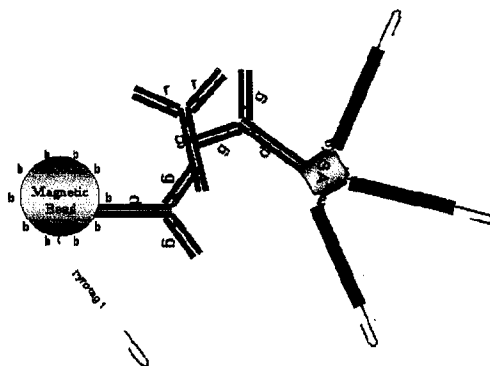


Figure A20. Whole immunocomplex is captured on magnetic bead.

The capturing complex was prepared according to step 4 with 7.5 μg (50 pmol) b-(dag)Ab. To make the detection complex, b-CTGC pyro-tags were attached to the b-(dag)Ab through streptavidin (SA), which acted as an intermediate binding molecule. Considering the molecular size and structure of the Ab, SA, and pyro-tag, the molar ratio in which they were added was decided to be 1:2:10 respectively. The molar ratio in which the capturing complex, Ag, and the detection complex were added together, were

chosen to be 1:2:4 in the positive run and 1:0:4 in the control run. To make the detection complex, 120 μl b-(d α g)Ab (200 pmol) and 20 μl SA (400 pmol) that had been dissolved in the PBS buffer with concentration of 20 μM were added into a microcentrifuge tube and the tube was incubated for 30 minutes on the tube rotator. Next, 20 μl b-CTGC (2000 pmol) was added to the mixture and the sample was incubated for one hour on the tube rotator. Thus, the remaining biotin binding sites of the SA were used to couple b-CTGC pyro-tag. Finally, the sample was incubated for another 30 minutes with free biotin to ensure that there was no biotin binding site available on the SA, making the detection complex ready for use. The detection complex was prepared for two samples in a bigger batch.

After the capturing complex was ready, the sample was placed on the magnet and the beads were washed twice with 100 μl B&W buffer. The capturing complex was also prepared for two samples in a bigger batch. The (g α r)Ab was supplied in a lyophilized form and was reconstituted in the PBS buffer. 30 μl (g α r)Ab (100 pmol) was added to the capturing complex and the sample was incubated for one hour on the tube rotator. After incubation, the tube was placed on the magnet and the beads were washed six times with 100 μl DI water, and resuspended in 40 μl DI water. The remainder of the procedure of transferring the sample to the pyrosequencing machine was identical to step 1 of this section. For the control run, the step of addition of (g α r)Ab to the capturing complex was skipped. Only the detection complex was added to the capturing complex. Figures A21 and A22 demonstrate the obtained results of this experiment.

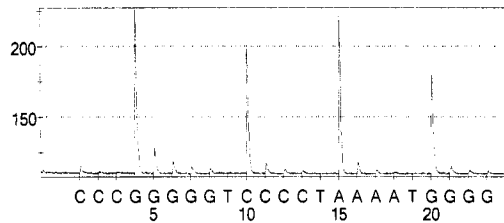


Figure A21. Whole immunocomplexes are captured on magnetic beads. Molar ratio of capturing complex to Ag to detection complex is 1:2:4, and molar ratio within the detection complex is 1:2:10.

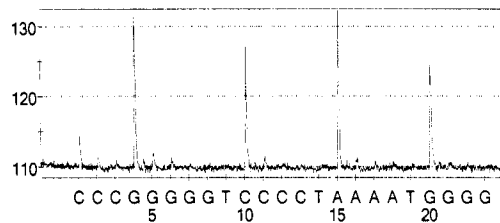


Figure A22. Capturing complex and detection complex are added together (control experiment). Molar ratio of capturing complex to Ag to detection complex is 1:0:4, and molar ratio within the detection complex is 1:2:10.

Since the antigen was present in the first sample, it was anticipated that the capturing complex and the detection complex would bind to it and therefore during pyrosequencing, signals corresponding to the attached pyro-tags would be generated. Result of Figure A21 confirms this statement by showing a low C signal generated from the attached b-G to the capturing complex and much higher GCAG signals released from the attached b-CTGC to the detection complex. In the control experiment, since no Ag was present in the solution, theoretically no bindings should have occurred between the capturing and the detection complexes since the detection complex should have been washed out from the sample. Therefore, during pyrosequencing no signals from the attached b-CTGC to the detection complex should have been detected. However, the result of Figure A22 illustrates the generated GCAG signals, which confirms the

existence of the detection complex in the solution. This means that the detection complex had been bounded to the capturing complex even though the antigen was not present. The intensity of this background noise signal was much lower than the positive signal, but the overall result is poor. The signal to noise ratio (S/N) was determined to be 5.3 in this experiment.

7. In the seventh step, the molar ratio in which the capturing complex, antigen, and the detection complex were added together, were changed to 1:2:1 in the positive run and 1:0:1 in the control run. Pyrosequencing was performed to detect the captured antigen. A schematic representation of this experiment is shown in Figure A23.

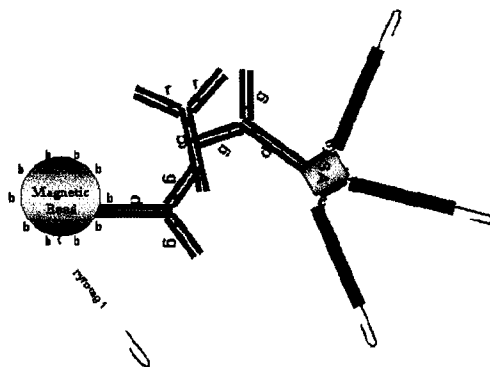


Figure A23. Whole immunocomplex is captured on magnetic bead.

The capturing complex was prepared according to step 4 except that the PBS-1%BSA buffer was used during the washing steps instead of the PBS buffer. To make the detection complex, 30 μ l b-(d α g)Ab (50 pmol) and 5 μ l SA (100 pmol) that had been dissolved in the PBS buffer with concentration of 20 μ M were added into a microcentrifuge tube and incubated for 30 minutes on the tube rotator. Next, 5 μ l b-CTGC (500 pmol) was added to the mixture and the sample was incubated for one hour

on the tube rotator. Thus, the remaining biotin binding sites of the SA were used to couple b-CTGC pyro-tag. Finally, the sample was incubated for another 30 minutes with free biotin to ensure that there was no biotin binding site available on the SA, making the detection complex ready for use. The detection complex was prepared for two samples in a bigger batch.

After the capturing complex was ready, the sample was placed on the magnet and the beads were washed twice with 100 μ l B&W buffer. The capturing complex was also prepared for two samples in a bigger batch. Next, 30 μ l (gar)Ab (100 pmol) was added to one of the capturing complex and the sample was incubated for one hour on the tube rotator. After the incubation, the tube was placed on the magnet and the beads were washed six times with 100 μ l DI water, and resuspended in 40 μ l DI water. The remainder of the procedure of transferring the sample to the pyrosequencing machine was identical to step 1 of this section. For the control run, the step of addition of (gar)Ab to the capturing complex was skipped. Only the detection complex was added to the capturing complex. Figures A24 and A25 demonstrate the obtained results of this experiment.

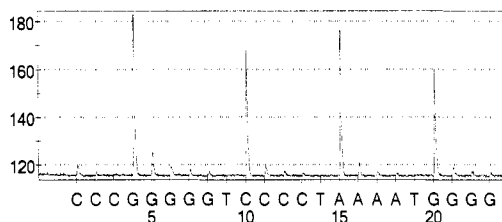


Figure A24. Whole immunocomplexes are captured on magnetic beads. Molar ratio of capturing complex to Ag to detection complex is 1:2:1, and molar ratio within the detection complex is 1:2:10.

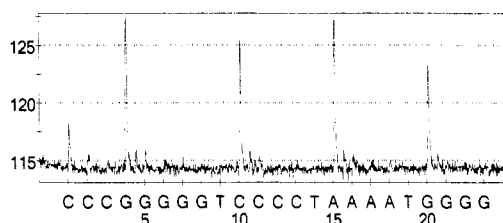


Figure A25. Capturing complex and detection complex are added together (control experiment). Molar ratio of capturing complex to Ag to detection complex is 1:0:1, and molar ratio within the detection complex is 1:2:10.

The result of the positive experiment indicates that the whole immunocomplex was formed and the signals corresponding to the attached pyro-tags were generated. The result of the control run, shows that the background noise signal still exists, although less detection complex was used. The signal to noise (S/N) ratio is approximately 5.1 in this experiment. This is almost the same as the previous experiment. The intensity of the signals slightly decreased as compared to the previous experiment. This might be due to a lower amount of detection complex and therefore less b-CTGC was available in the sample. The non-specific interactions between the two complexes could not be eliminated despite the presence of the blocking agent BSA in the PBS buffer during the washing steps.

8. In the eighth step, the construction of the detection complex changed in a way that the molar ratio of b-Ab to SA to b-CTGC was changed to 1:2:2. The capturing complex and the antigen were added together, followed by the addition of the detection complex. Pyrosequencing was performed to detect the captured antigen. A control experiment in which the antigen was not present in the sample was carried out simultaneously. The

molar ratio in which the capturing complex, antigen, and the detection complex were added were chosen to be 1:2:1 in the positive run and 1:0:1 in the control run. A schematic representation of this experiment is shown in Figure A26.

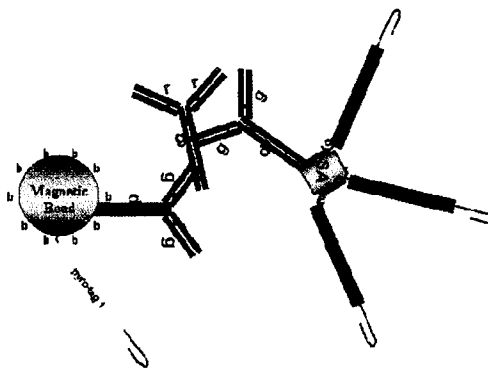


Figure A26. Whole immunocomplex is captured on magnetic bead.

The capturing complex was prepared according to step 7. To make the detection complex, 30 μl b-(dag)Ab (50 pmol) and 5 μl SA (100 pmol) that had been dissolved in the PBS buffer with concentration of 20 μM were added into a microcentrifuge tube and the tube was incubated for 30 minutes on the tube rotator. Next, 1 μl b-CTGC (100 pmol) was added to the mixture and the sample was incubated for one hour on the tube rotator. Thus, the remaining biotin binding sites of the SA were used to couple b-CTGC pyro-tag. Finally, the sample was incubated for another 30 minutes with free biotin to ensure that there was no biotin binding site available on the SA, making the detection complex ready for use. The detection complex was prepared for two samples in a bigger batch.

After the capturing complex was ready, the sample was placed on the magnet and the beads were washed twice with 100 μl B&W buffer. The capturing complex was also

prepared for two samples in a bigger batch. Next, 30 μl (g α r)Ab (100 pmol) was added to the capturing complex and the sample was incubated for one hour on the tube rotator. After the incubation, the tube was placed on the magnet and the beads were washed six times with 100 μl DI water, and resuspended in 40 μl DI water. The remainder of the procedure of transferring the sample to the pyrosequencing machine was identical to step 1 of this section. For the control run, the step of the addition of (g α r)Ab to the capturing complex was skipped. Only the detection complex was added to the capturing complex. Figures A27 and A28 demonstrate the obtained results of this experiment.

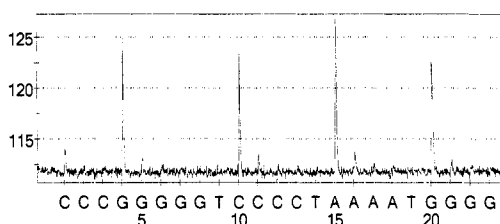


Figure A27. Whole immunocomplexes are captured on magnetic beads. Molar ratio of capturing complex to Ag to detection complex is 1:2:1, and molar ratio within the detection complex is 1:2:2.

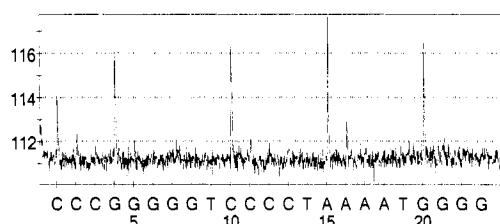


Figure A28. Capturing complex and detection complex are added together (control experiment). Molar ratio of capturing complex to Ag to detection complex is 1:0:1, and molar ratio within the detection complex is 1:2:2.

The ratio within the detection complex (Ab:SA:b-CTGC) was chosen to be 1:2:2 in this experiment. This means that the amount of b-CTGC pyro-tags decreased considerably in both positive and control samples. As illustrated in both A27 and A28

Figures, the intensity of all signals decreased significantly. The goal was to increase the signal to noise ratio as much as possible by decreasing the noise signal and increasing the positive signal. However, the obtained S/N in this experiment is only about 2.6, which is about half the previous results. This experiment verified that having 1:2:10 ratio within the detection complex was definitely a better alternative than having 1:2:2 ratio, and therefore decreasing the amount of b-CTGC pyro-tag did not produce an enhanced result.

9. In the ninth step, only the biotinylated pyro-tag was added to the capturing complex and pyrosequencing was performed. Figure A29 demonstrates a basic display of this experiment.

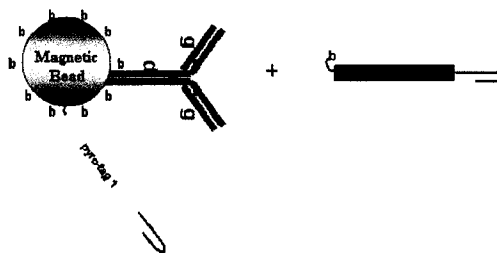


Figure A29. b-CTGC pyro-tag is added to the capturing complex.

The capturing complex was prepared according to step 7, washed twice with B&W buffer and resuspended in 50 μl B&W buffer. Next, 1 μl (100 pmol) b-CTGC mixed with 49 μl DI water was added to the beads' tube, and the sample was incubated for one hour on the tube rotator. After the incubation, the tube was placed on the magnet and the beads were washed six times with 100 μl DI water, and resuspended in 40 μl DI water. The remainder of the procedure of transferring the sample to the pyrosequencing machine was identical to step 1 of this section. Figures A30 shows the obtained result.

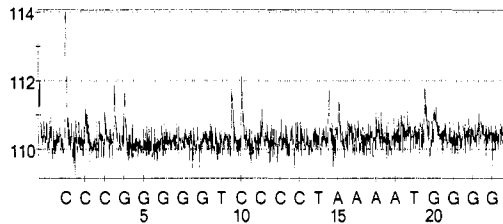


Figure A30. 100 pmol b-CTGC is added to the capturing complex.

As shown in the result, there is a low C signal generated from the attached b-G to the capturing complex, and then there are very low GCAG signals. Theoretically, the b-CTGC should not bind to the capturing complex, since all the biotin binding sites of the bead are blocked. Although, the intensity of the GCAG signals are very low, there is a possibility that by using a blocking agent the non-specific binding of b-CTGC to the capturing complex could be prevented.

10. In the tenth step, Tween-20 buffer was added to the capturing complex as the blocking agent, followed by the addition of biotinylated pyro-tag. A control experiment in which the Tween-20 was not present in the sample was also carried out. Figure A31 represents a simple schematic of this experiment.

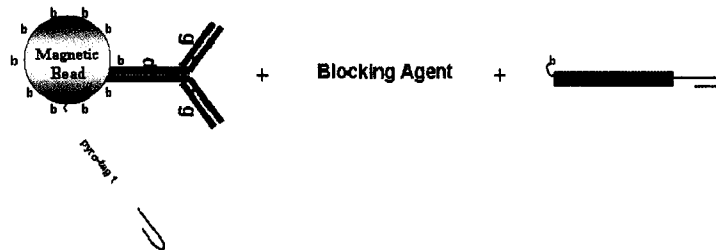


Figure A31. Blocking agent is added to the capturing complex followed by the addition of the b-CTGC pyro-tag.

A big batch of capturing complex (enough for four samples) was prepared according to step 7. Two of them were washed three times with 100 μ l PBS buffer containing 0.05% Tween-20, and the other two were washed as regular with 100 μ l B&W buffer. All four samples were resuspended in 50 μ l B&W buffer. Next, 1 μ l (100 pmol) b-CTGC mixed with 49 μ l DI water was added to two tubes (first tube that had been washed with the PBS-Tween-20 buffer and second tube that had been washed with the B&W buffer), and 5 μ l (500 pmol) b-CTGC mixed with 45 μ l DI water was added to the other two tubes (third tube that had been washed with the PBS-Tween-20 buffer and fourth tube that had been washed with the B&W buffer). All four samples were incubated for one hour on the tube rotator. After the incubation, the tubes were placed on the magnet and the beads were washed six times with 100 μ l DI water, and resuspended in 40 μ l DI water. The remainder of the procedure of transferring the samples to the pyrosequencing machine was identical to step 1 of this section. Figures A32 through A35 show the obtained results.

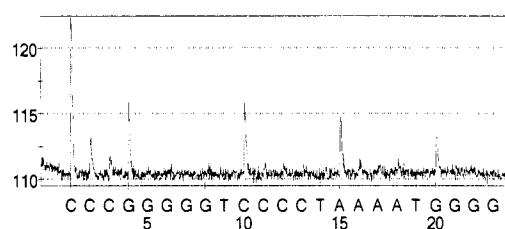


Figure A32. Capturing complex is washed with the Tween-20 (blocking agent) and then 100 pmol b-CTGC is added to the complex.

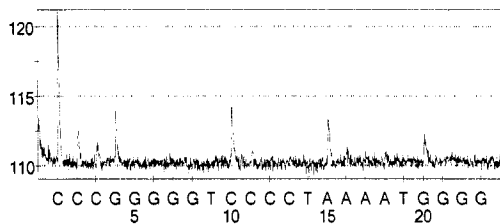


Figure A33. 100 pmol b-CTGC is added to the capturing complex.

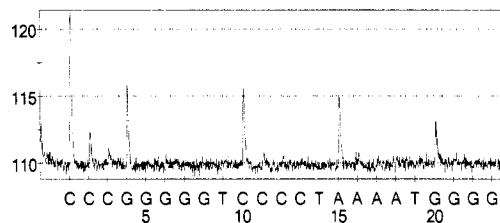


Figure A34. Capturing complex is washed with the Tween-20 (blocking agent) and then 500 pmol b-CTGC is added to the complex.

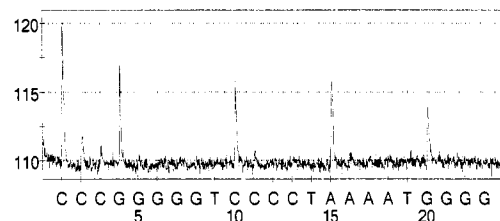


Figure A35. 500 pmol b-CTGC is added to the capturing complex.

The results indicate that the Tween-20 could not eliminate the noise GCAG signals. By increasing the b-CTGC from 100 to 500 pmol, the intensity of the GCAG signals did not increase considerably, which means that only a specific amount of the biotinylated pyro-tag can bind to the capturing complex. The intensity of the GCAG signals are much less in this experiment as compared to the experiment in which the b-CTGC pyro-tags were attached to the detection complex.

11. In the eleventh step, five samples were made in which two of them were identical to the 7th step's samples. In the third sample, the capturing and the detection complexes were added together with the presence of single stranded binding protein (SSB). For the fourth sample, a cocktail buffer was prepared with the following reagents' concentrations: 20 mM Hepes, 5 mM MgCl₂, 200 mM NaCl, 0.1 mM EDTA, 0.05% Tween-20, 1% BSA, 1% Sonicated Salmon Test DNA, and the buffer was named HMNETBS buffer. The capturing complex was washed in the cocktail HMNETBS buffer and then the capturing complex and the detection complex were added together in the presence of the HMNETBS buffer. In the fifth sample, MgCl₂ was added to the detection complex, and then the capturing and the detection complexes were added together with the presence of SSB. The molar ratio in which the capturing complex, Ag, and the detection complex were added in all the control experiments was chosen to be 1:0:1. The molar ratio within the detection complex in all samples was 1:2:10. Pyrosequencing was performed on all five samples. Figure A36 illustrates a basic representation of this experiment.

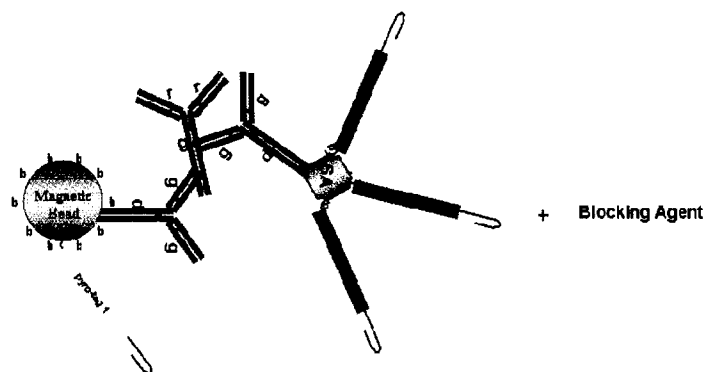


Figure A36. Whole immunocomplex is captured on magnetic bead along with the use of different blocking agents.

A big batch of the capturing complex (enough for five experiments) was prepared according to the step 7. The first two immunocomplexes were made exactly according to the step 7. For the third sample, after one hour incubation of the capturing complex with the detection complex, the sample was placed on the magnet, the supernatant was removed and then 0.22 μ l (1 μ g) of SSB and 60 μ l 10 mM Tris acetate (TA) buffer were added to the beads and the sample was incubated for 15 minutes on the tube rotator. Next the beads were washed as regular prior to the pyrosequencing step. In the fourth sample, the capturing complex was washed for a total of three times with the HMNETBS buffer and resuspended in it for one hour. Next, the detection complex was added to the beads while the beads were resuspended in the HMNETBS buffer and the sample was incubated for one hour on the tube rotator. Finally, the beads were washed as regular prior to the pyrosequencing step. To make the detection complex for the fifth sample, 10 μ l 20 mM $MgCl_2$ was added along with the b-CTGC pyro-tag to the b-Ab and SA. Next, the prepared detection complex was added to the capturing complex and the sample was incubated for one hour on the tube rotator. After incubation, the sample was placed on the magnet, the supernatant was removed and then 0.22 μ l (1 μ g) of SSB and 60 μ l 10 mM TA buffer were added to the beads and the sample was incubated for 15 minutes on the tube rotator. Prior to the pyrosequencing step, all samples were placed on the magnet, and the beads were washed six times with 100 μ l DI water, and resuspended in 40 μ l DI water. The remainder of the procedure of transferring the sample to the pyrosequencing machine was identical to step 1 of this section. Figures A37 through A41 show the obtained results.

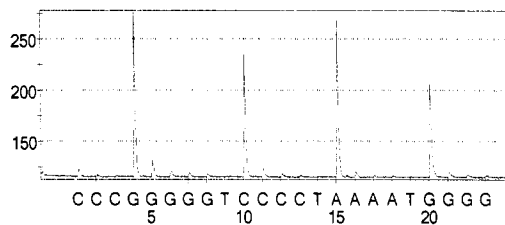


Figure A37. Whole immunocomplexes are captured on magnetic beads. Molar ratio of capturing complex to Ag to detection complex is 1:2:1, and molar ratio within the detection complex is 1:2:10.

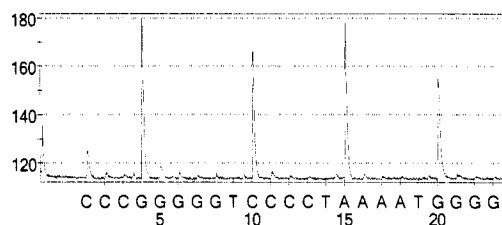


Figure A38. Capturing complex and detection complex are added together (control experiment). Molar ratio of capturing complex to Ag to detection complex is 1:0:1, and molar ratio within the detection complex is 1:2:10.

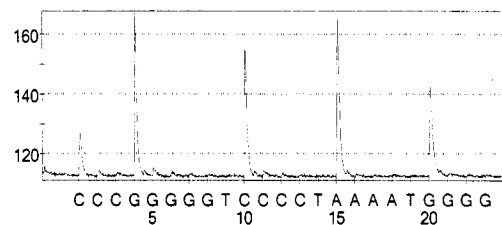


Figure A39. Capturing complex and detection complex are added together (control experiment). SSB is added to the whole sample. Molar ratio of capturing complex to Ag to detection complex is 1:0:1, and molar ratio within the detection complex is 1:2:10.

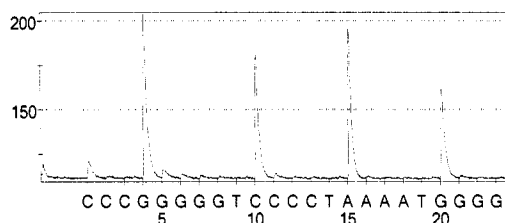


Figure A40. Capturing complex is washed and stored in the HMNETBS buffer. Capturing complex and detection complex are added together with the presence of the HMNETBS buffer (control experiment). Molar ratio of capturing complex to Ag to detection complex is 1:0:1, and molar ratio within the detection complex is 1:2:10.

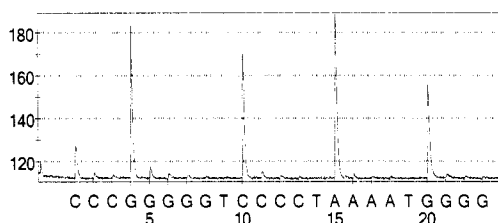


Figure A41. $MgCl_2$ is used in making the detection complex. Capturing complex and detection complex are added together (control experiment). SSB is added to the whole sample. Molar ratio of capturing complex to Ag to detection complex is 1:0:1, and molar ratio within the detection complex is 1:2:10.

Figure A37 demonstrates the obtained positive signals. On the other hand, Figure A38 illustrates the noise signals when no blocking agents were employed. The obtained S/N from these two samples is about 2.4, which is a poor result. The rest of the three control samples also show huge noise signals despite the fact that different blocking agents were present. Tween-20, which is a non-ionic detergent, usually disrupts protein-protein interaction, but seems to have had no effect in this experiment. BSA and fish gelatin are common protein blockers to reduce the non-specific bindings; however, they did not decrease the noise signals herein. SSB was used to disrupt any non-specific interactions between the single stranded DNA and proteins. $MgCl_2$ was added to test

whether an ion with multiple charges would eliminate any non-specific bindings. Neither one was able to remove the noise signals. Therefore, wherever this non-specific binding occurred, it could not be detected and eliminated.

12. In the twelfth step, the capturing complex was prepared without having the b-G pyro-tag. To make the whole immunocomplex for the positive experiments, antigen was added to the capturing complex, followed by the addition of the detection complex. In this experiment three different concentrations of antigen were examined. The molar ratio within the detection complex was kept at 1:2:10 in all samples. Pyrosequencing was performed on the whole complex. A simple representation of this experiment is shown in Figure A42.

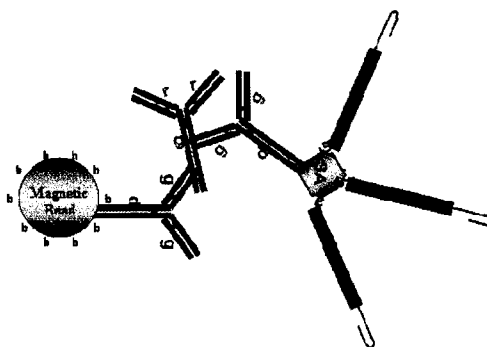


Figure A42. Whole immunocomplex is captured on magnetic bead.

The capturing complex was prepared according to step 7 except that the step of the addition of the b-G pyro-tag was skipped; no biotinylated pyro-tag was attached to the capturing complex. A big batch of the capturing complex (enough for four samples) was prepared. The detection complex was also prepared according to step 7. A big batch of the detection complex (enough for 4 samples) was also prepared. The molar ratios of

capturing complex to Ag to detection complex were 1:2:1, 1:1:1, and 1:0.5:1 in the three positive samples.

After the capturing complex was ready, the sample was placed on the magnet and the beads were washed twice with 100 μ l B&W buffer. Next, 30 μ l (gar)Ab (100 pmol) and 70 μ l PBS-1%BSA buffer were added to the first capturing complex sample, 15 μ l (gar)Ab (50 pmol) and 85 μ l PBS-1%BSA buffer were added to the second sample, 7.5 μ l (gar)Ab (25 pmol) and 92.5 μ l PBS-1%BSA buffer were added to the third sample, and 100 μ l PBS-1%BSA buffer was added to the fourth negative control sample. All four tubes were incubated for one hour on the tube rotator. After the incubation, the tubes were placed on the magnet and the beads were washed six times with 100 μ l DI water, and resuspended in 40 μ l DI water. The remainder of the procedure of transferring the samples to the pyrosequencing machine was identical to step 1 of this section. Figures A43 through A46 demonstrate the obtained results of this experiment.

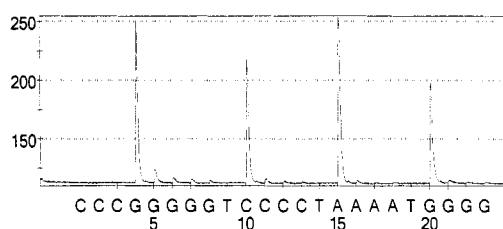


Figure A43. Whole immunocomplexes are captured on magnetic beads. Molar ratio of capturing complex to Ag to detection complex is 1:2:1, and molar ratio within the detection complex is 1:2:10.

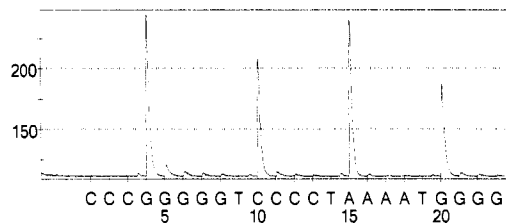


Figure A44. Whole immunocomplexes are captured on magnetic beads. Molar ratio of capturing complex to Ag to detection complex is 1:1:1, and molar ratio within the detection complex is 1:2:10.

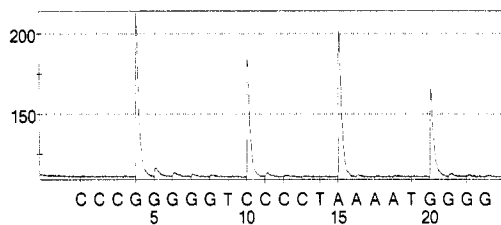


Figure A45. Whole immunocomplexes are captured on magnetic beads. Molar ratio of capturing complex to Ag to detection complex is 1:0.5:1, and molar ratio within the detection complex is 1:2:10.

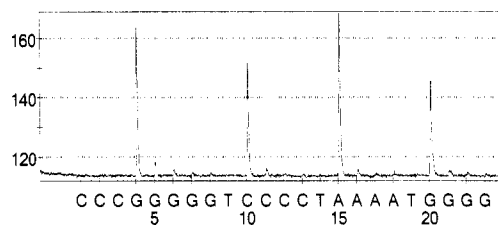


Figure A46. Capturing complex and detection complex are added together (control experiment). Molar ratio of capturing complex to Ag to detection complex is 1:0:1, and molar ratio within the detection complex is 1:2:10.

The objective of this experiment was to check if the system could generate quantitative results, which means that the intensity of signals generated during pyrosequencing would vary proportionally with the amount of Ag. As demonstrated in above figures, since no b-G was attached to the capturing complex, no C signals were released, and the source of signals was from the attached b-CTGC pyro-tag to the

detection complex. The intensity of GCAG signals slightly decreased from first sample to the second sample, although the amount of Ag was halved. The intensity of GCAG signals in the third sample also decreased when is compared to the previous experiment, yet not as much as anticipated. Therefore, at this stage no quantitative results were obtained. The non-specific binding between the capturing complex and the detection complex is still present in the fourth sample as illustrated in the last figure.

13. In the thirteenth step, the molar ratios of the detection complex to the capturing complex and the Ag were varied. To make the whole immunocomplex for the positive experiments, Ag was added to the capturing complex, followed by the addition of the detection complex. The ratio within the detection complex was kept at 1:2:10 in all samples. Pyrosequencing was performed on the whole complex. Figure A47 illustrates a basic structure of this immunocomplex.

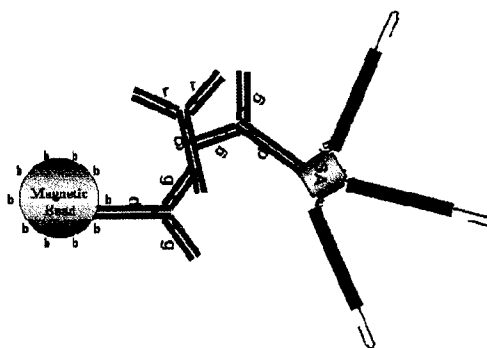


Figure A47. Whole immunocomplex is captured on magnetic bead.

Four positive samples and four control samples were made in this experiment. The molar ratios of capturing complex to Ag to detection complex in the positive samples were chosen to be 1:1:1, 1:1:0.5, 1:1:0.3, and 1:1:0.15. In the control samples the molar

ratios were chosen to be 1:0:1, 1:0:0.5, 1:0:0.3, and 1:0:0.15. A big batch of the capturing complex (enough for 8 samples) was prepared precisely according to step 12. To make enough detection complex for the two samples of 1:1:1 and 1:0:1, 60 μ l b-(α g)Ab (100 pmol) and 10 μ l SA (200 pmol) were added into a microcentrifuge tube and the tube was incubated for 30 minutes on the tube rotator. Next, 10 μ l b-CTGC (1000 pmol) was added to the mixture and the sample was incubated for one hour on the tube rotator. Thus, the remaining biotin binding sites of the SA were used to couple b-CTGC pyro-tags. Finally, the sample was incubated for another 30 minutes with free biotin to ensure that there was no biotin binding site available on the SA, making the detection complex ready for use. The detection complex for the samples of 1:1:0.5 and 1:0:0.5 were prepared likewise, except that all the volumes were halved. For 1:1:0.3 and 1:0:0.3 samples the volumes were divided by 3.3, and for the 1:1:0.15 and 1:0:0.15 samples all the volumes were divided by 6.67. Next, 15 μ l (g α r)Ab (50 pmol) and 85 μ l PBS-BSA buffer were added to the positive samples, and 100 μ l PBS-1%BSA buffer was added to the negative control samples. All eight tubes were incubated for one hour on the tube rotator. After the incubation, the tubes were placed on the magnet and the beads were washed six times with 100 μ l DI water, and resuspended in 40 μ l DI water. The remainder of the procedure of transferring the samples to the pyrosequencing machine was identical to step 1 of this section. Figures A48 through A55 demonstrate the obtained results of this experiment.

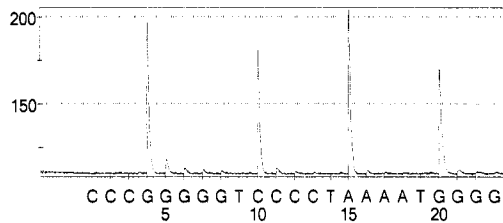


Figure A48. Whole immunocomplexes are captured on magnetic beads. Molar ratio of capturing complex to Ag to detection complex is 1:1:1, and molar ratio within the detection complex is 1:2:10.

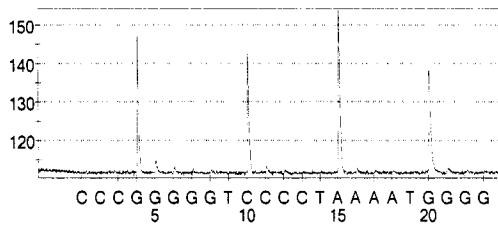


Figure A49. Capturing complex and detection complex are added together (control experiment). Molar ratio of capturing complex to Ag to detection complex is 1:0:1, and molar ratio within the detection complex is 1:2:10.

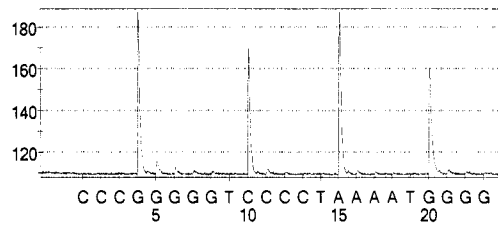


Figure A50. Whole immunocomplexes are captured on magnetic beads. Molar ratio of capturing complex to Ag to detection complex is 1:1:0.5, and molar ratio within the detection complex is 1:2:10.

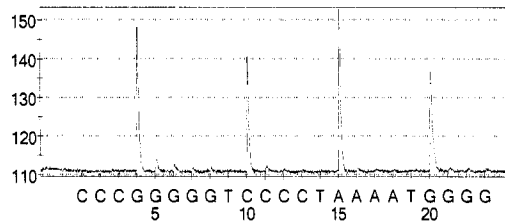


Figure A51. Capturing complex and detection complex are added together (control experiment). Molar ratio of capturing complex to Ag to detection complex is 1:0:0.5, and molar ratio within the detection complex is 1:2:10.

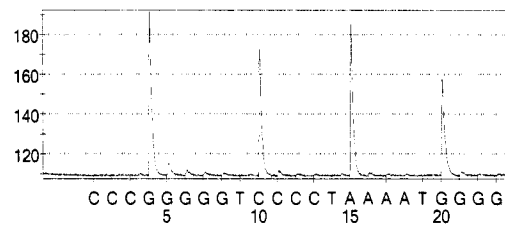


Figure A52. Whole immunocomplexes are captured on magnetic beads. Molar ratio of capturing complex to Ag to detection complex is 1:1:0.3, and molar ratio within the detection complex is 1:2:10.

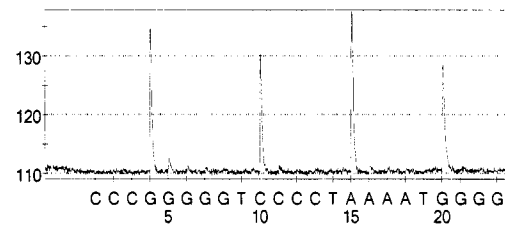


Figure A53. Capturing complex and detection complex are added together (control experiment). Molar ratio of capturing complex to Ag to detection complex is 1:0:0.3, and molar ratio within the detection complex is 1:2:10.

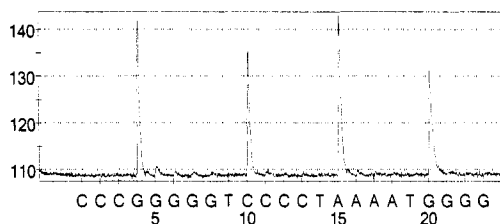


Figure A54. Whole immunocomplexes are captured on magnetic beads. Molar ratio of capturing complex to Ag to detection complex is 1:1:0.15, and molar ratio within the detection complex is 1:2:10.

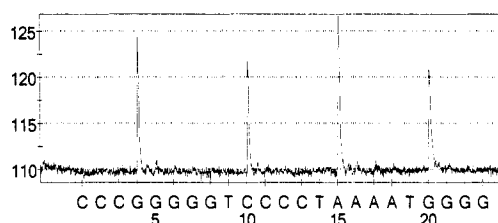


Figure A55. Capturing complex and detection complex are added together (control experiment). Molar ratio of capturing complex to Ag to detection complex is 1:0:0.15, and molar ratio within the detection complex is 1:2:10.

The objective of this experiment was to study the effects of concentration of the detection complex on the intensity of generated GCAG signals. In positive samples, the signal intensity did not significantly change from the first sample to the third sample. However, there is a sudden drop of signal intensity in the fourth sample. In the negative samples, effectively the same behavior was observed. The highest S/N was obtained by the third sample that was about 3.2, which is still very low. Therefore, decreasing the concentration of the detection complex did not have any beneficial effects on the results.

14. In the fourteenth step, trouble shooting was performed to discover the source of non-specific bindings. In the first sample, the capturing complex and the detection complex were added together without the presence of the Ag as shown in Figure A56.

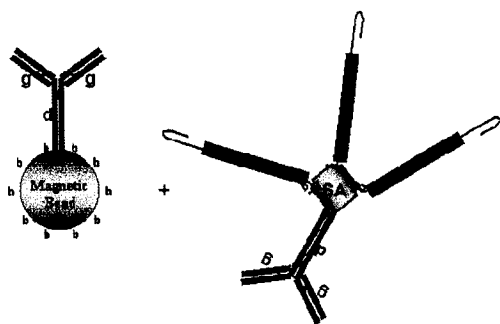


Figure A56. Capturing complex and detection complex are added together.

The capturing complex was prepared according to step 12 and the detection complex was made according to step 7. Next, they were added together and incubated for one hour on the tube rotator. Finally, the tube was placed on the magnet and the beads were washed six times with 100 μ l DI water, and resuspended in 40 μ l DI water. The remainder of the procedure of transferring the sample to the pyrosequencing machine was identical to step 1 of this section. Figure A57 demonstrates the obtained results.

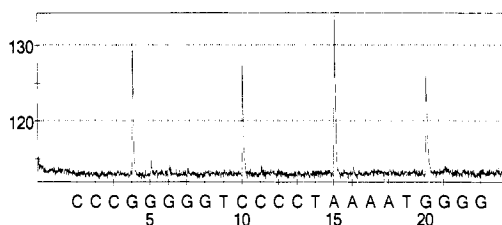


Figure A57. Capturing complex and detection complex are added together (control experiment). Molar ratio of capturing complex to Ag to detection complex is 1:0:1, and molar ratio within the detection complex is 1:2:10.

In the second sample, the detection complex was made without the presence of the detection Ab, and then the two complexes were added together without the presence of the Ag as shown in Figure A58.

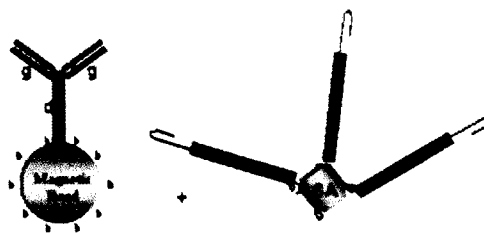


Figure A58. SA with the attached b-CTGC is added to the capturing complex.

The capturing complex was prepared according to step 12. To make the other complex, 5 μ l SA (100 pmol) and 5 μ l b-CTGC (500 pmol) were added into a tube and the sample was incubated for one hour on the tube rotator. Next, the sample was incubated for 30 minutes with free biotin to ensure that there was no biotin binding site available on the SA, making the complex ready for use. Finally, the SA with attached b-CTGC pyro-tag was added to the capturing complex and the sample was incubated for one hour on the tube rotator. After the incubation, the tube was placed on the magnet and the beads were washed six times with 100 μ l DI water, and resuspended in 40 μ l DI water. The remainder of the procedure of transferring the sample to the pyrosequencing machine was identical to step 1 of this section. Figure A59 demonstrates the obtained results of this experiment.

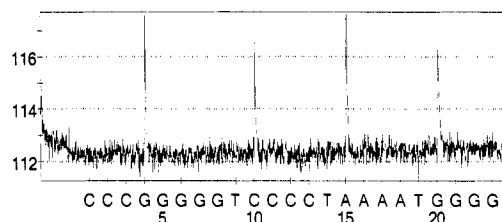


Figure A59. SA with attached b-CTGC is added to the capturing complex.

In the third sample, only the biotinylated pyro-tag was added to the capturing complex as shown in Figure A60.

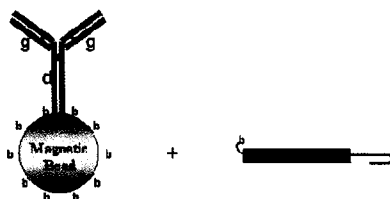


Figure A60. Biotinylated pyro-tag is added to the capturing complex.

The capturing complex was prepared according to step 12. Next, 5 μl b-CTGC (500 pmol) was added to the capturing complex and the sample was incubated for one hour on the tube rotator. Finally, the tube was placed on the magnet and the beads were washed six times with 100 μl DI water, and resuspended in 40 μl DI water. The remainder of the procedure of transferring the sample to the pyrosequencing machine was identical to step 1 of this section. Figure A61 demonstrates the obtained results of this experiment.

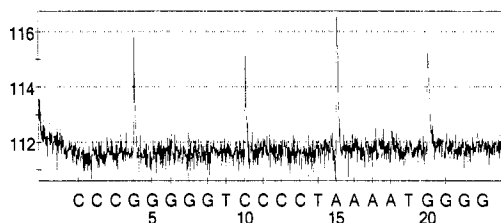


Figure A61. b-CTGC is added to the capturing complex.

In the fourth sample, no capturing Ab was coated on the beads. The beads were only coated with free biotin. Next, the detection complex was added to the beads as shown in Figure A62.

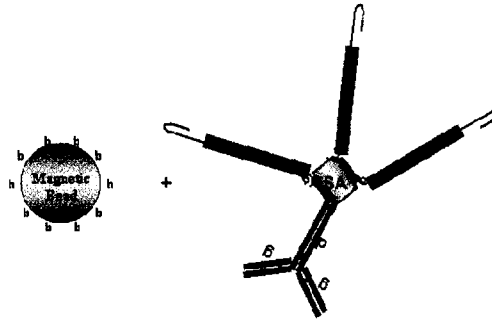


Figure A62. Detection complex is added to the biotin coated magnetic bead.

The detection complex was prepared according to step 7. To coat the beads with free biotin, 25 μl of beads was transferred into a microcentrifuge tube and the tube was placed on the magnet for two minutes. The supernatant was removed by a pipette while the tube remained on the magnet. Next, the beads were washed twice with 100 μl B&W buffer and the supernatant was removed. 35 μl free biotin solution and 65 μl B&W buffer were added to the beads, and the sample was incubated for 30 minutes on the tube rotator. Then the tube was placed on the magnet and the beads were washed twice with 100 μl B&W buffer. Finally, the detection complex was added to the beads and the sample was incubated for one hour on the tube rotator. After the incubation, the tube was placed on the magnet and the beads were washed six times with 100 μl DI water, and resuspended in 40 μl DI water. The remainder of the procedure of transferring the sample to the pyrosequencing machine was identical to step 1 of this section. Figure A63 demonstrates the obtained results.

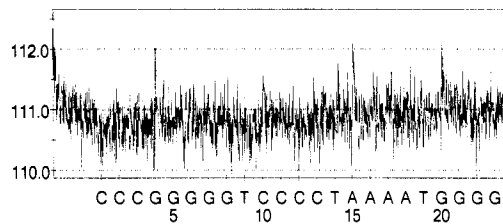


Figure A63. Detection complexes are added to the biotin coated magnetic beads.

Figure A57 indicates that the noise signals still exist when the capturing complex and the detection complex were added together without the presence of the Ag. Figure A59 shows that the intensity of the noise signals has decreased significantly when no detection Ab was present in the detection complex. Figure A61 demonstrated the same result with low intensity of noise signals when no detection Ab and SA were present in the sample. Figure A63 illustrates much lower noise signals when no capturing Ab was present in the capturing complex. These results infer that the non-specific binding mostly arises from the cross reactivity of the two antibodies present in the capturing and the detection complexes, and so the b-CTGC pyro-tag did not contribute to the non-specific bindings between the two complexes.

15. In the fifteenth step, trouble shooting was performed again to reconfirm the source of non-specific bindings. In the first sample, the capturing complex and the Ag were added together, followed by the addition of the detection complex. The molar ratio in which the capturing complex, Ag, and the detection complex were added was 1:1:1. Figure A64 illustrates a basic representation of this complex.

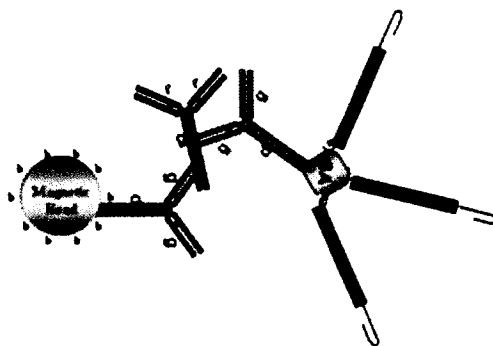


Figure A64. Whole immunocomplex is captured on magnetic bead.

The capturing complex was prepared according to step 12 and the detection complex was made according to step 7. Next, 15 μl (g α r)Ab (50 pmol) mixed with 85 μl PBS-1%BSA buffer was added to the capturing complex and the sample was incubated for one hour on the tube rotator. After the incubation, the tube was placed on the magnet and the beads were washed six times with 100 μl DI water, and resuspended in 40 μl DI water. The remainder of the procedure of transferring the sample to the pyrosequencing machine was identical to step 1 of this section. Figures A65 demonstrates the obtained results of this positive experiment.

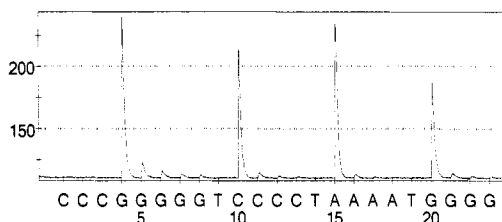


Figure A65. Whole immunocomplexes are captured on magnetic beads. Molar ratio of capturing complex to Ag to detection complex is 1:1:1, and molar ratio within the detection complex is 1:2:10.

In the second sample, the capturing complex and the detection complex were added together without the presence of the Ag as shown in Figure A66.

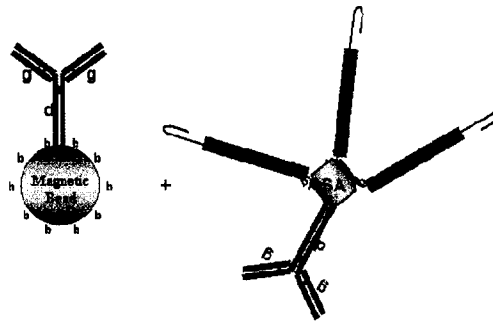


Figure A66. Capturing complex and detection complex are added together.

The capturing complex was prepared according to step 12 and the detection complex was made according to step 7. Next, they were added together and incubated for one hour on the tube rotator. Finally, the tube was placed on the magnet and the beads were washed six times with 100 μ l DI water, and resuspended in 40 μ l DI water. The remainder of the procedure of transferring the sample to the pyrosequencing machine was identical to step 1 of this section. Figure A67 demonstrates the obtained results.

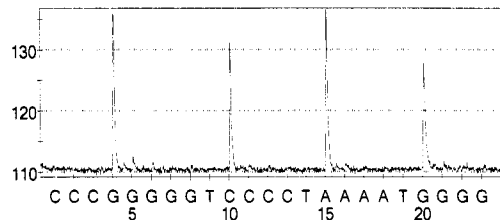


Figure A67. Capturing complex and detection complex are added together (control experiment). Molar ratio of capturing complex to Ag to detection complex is 1:0:1, and molar ratio within the detection complex is 1:2:10.

In the third sample, the detection complex was made without the presence of the detection Ab, and then the two complexes were added together without the presence of the Ag as illustrated in Figure A68.

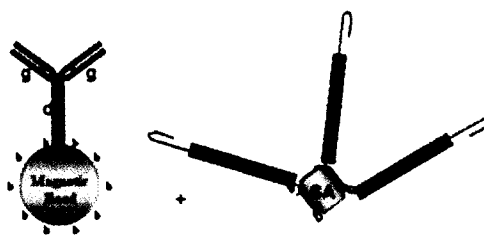


Figure A68. SA with the attached b-CTGC is added to the capturing complex.

The capturing complex was prepared according to step 12. To make the other complex, 5 μ l SA (100 pmol) and 5 μ l b-CTGC (500 pmol) were added into a tube and the sample was incubated for one hour on the tube rotator. Next, the sample was incubated for 30 minutes with free biotin to ensure that there was not any biotin binding site available on the SA, making the complex ready for use. Finally, the SA with attached b-CTGC pyro-tag was added to the capturing complex and the sample was incubated for one hour on the tube rotator. After the incubation, the tube was placed on the magnet and the beads were washed six times with 100 μ l DI water, and resuspended in 40 μ l DI water. The remainder of the procedure of transferring the sample to the pyrosequencing machine was identical to step 1 of this section. Figure A69 demonstrates the obtained results of this experiment.

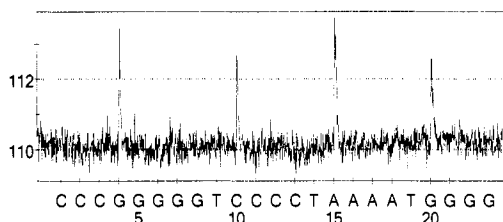
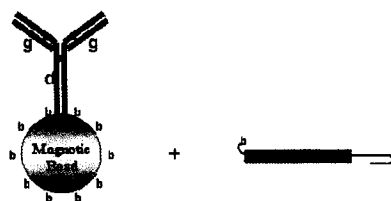


Figure A69. SA with attached b-CTGC is added to the capturing complex.

In the fourth sample, only the biotinylated pyro-tag was added to the capturing complex as demonstrated in Figure A70.



A70. Biotinylated pyro-tag is added to the capturing complex.

The capturing complex was prepared according to step 12. Next, 5 μ l b-CTGC (500 pmol) was added to the capturing complex and the sample was incubated for one hour on the tube rotator. Finally, the tube was placed on the magnet and the beads were washed six times with 100 μ l DI water, and resuspended in 40 μ l DI water. The remainder of the procedure of transferring the sample to the pyrosequencing machine was identical to step 1 of this section. Figure A71 demonstrates the obtained results of this experiment.

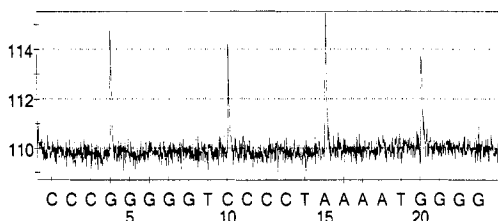


Figure A71. b-CTGC is added to the capturing complex.

In the fifth sample, no capturing Ab was coated on the beads. The beads were only coated with free biotin. Next, the detection complex was added to the beads as shown in Figure A72.

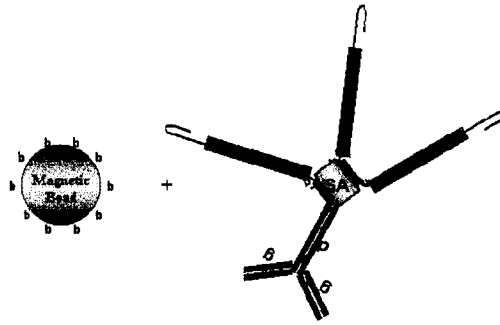


Figure A72. Detection complex is added to the biotin coated magnetic bead.

The detection complex was prepared according to step 7. To coat the beads with free biotin, 25 μl of beads was transferred into a microcentrifuge tube and the tube was placed on magnet for two minutes. The supernatant was removed by a pipette while the tube remained on the magnet. Next, the beads were washed twice with 100 μl B&W buffer and the supernatant was removed. 35 μl free biotin solution and 65 μl B&W buffer were added to the beads and the sample was incubated for 30 minutes on the tube rotator. Then the tube was placed on the magnet and the beads were washed twice with 100 μl B&W buffer. The detection complex was added to the beads and the sample was incubated for one hour on the tube rotator. After the incubation, the tube was placed on the magnet and the beads were washed six times with 100 μl DI water, and resuspended in 40 μl DI water. The remainder of the procedure of transferring the sample to the pyrosequencing machine is identical to step 1 of this section. Figure A73 demonstrates the obtained results.

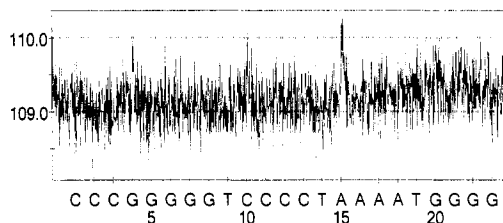


Figure A73. Detection complexes are added to the biotin coated magnetic beads.

The first sample, which was a positive experiment, generated high intensity of GCAG signals. The rest of the samples, which were the repeats in step 14, gave consistent results. These results confirm that the non-specific binding occurred from the cross reactivity of the two antibodies present in the capturing and the detection complexes, and the polyclonal b-(dag)Ab and (gar)Ab are not suitable antibodies to work with in this system.

The overall results in Appendix A had poor signal to noise ratios. A new assay was developed, as described in Chapter Four, which resulted in the highest signal response and the lowest background noise. Monoclonal matching antibodies were used instead of polyclonal antibodies in an attempt to eliminate cross reactivity between the complexes.

APPENDIX B CALCULATIONS

B.1. Calculating the theoretical ratio of antibody per bead in capturing complex

The manufacture's recommended ratio of antibody per bead was to have 20 µg of antibody per 1 mg of bead ($\frac{20 \mu\text{g (antibody)}}{1 \text{ mg (bead)}}$), which is a 0.02 mass ratio of antibody per bead. In order to theoretically determine the maximum amount of this mass ratio and ensure that the recommended mass ratio was more than the maximum mass ratio, the following calculations were performed.

The Data provided by Dynabeads manufacture's protocol and two references [19,20] for antibodies' surface area were:

- bead diameter = 2.8 µm
- 1 ml solution = 2×10^9 beads
- beads solution concentration = 30 mg/ml
- surface area of antibody = 10560 Å² [19], 4500 Å² [20]
- MW of antibody = 150 kD

The theoretical maximum mass ratio corresponds to the smallest antibody surface area.

- surface area per antibody = 4500 Å² = $4.5 \times 10^{-5} \mu\text{m}^2$
- surface area per bead = $4 \times \pi \times (1.4 \mu\text{m})^2 = 24.63 \mu\text{m}^2$
- maximum antibodies per bead = $\frac{24.63 \mu\text{m}^2}{4.5 \times 10^{-5} \mu\text{m}^2} = 5.47 \times 10^5$
- mass of antibodies =

$$5.47 \times 10^5 \times \frac{1 \text{ mol}}{6.02 \times 10^{23}} \times \frac{150 \times 10^3 \text{ g}}{\text{mol}} \times \frac{10^6 \mu\text{g}}{1 \text{ g}} = 1.36 \times 10^{-7} \mu\text{g}$$

- mass of bead = $\frac{30 \text{ mg}}{1 \text{ ml}} \times \frac{1 \text{ ml}}{2 \times 10^9} \times \frac{10^3 \mu\text{g}}{1 \text{ mg}} = 1.5 \times 10^{-5} \mu\text{g}$
- maximum mass ratio of antibody per bead = $\frac{1.36 \times 10^{-7} \mu\text{g}}{1.5 \times 10^{-5} \mu\text{g}} = 0.009$
- recommended mass ratio (0.02) > maximum theoretical mass ratio (0.009)

B.2. Calculating the volume of IL-8 capturing antibody for making 100 μl capturing complex

To determine the volume of IL-8 antibody for coating 100 μl of beads, considering the recommended ratio of antibody per bead, the following calculation was performed.

- beads solution concentration = 30 mg/ml
- antibody concentration = 0.996 mg/ml
- manufacture's recommended ratio of antibody per bead = $\frac{20 \mu\text{g (antibody)}}{1 \text{ mg (bead)}}$
- ratio of antibodies per 100 μl beads solution =

$$100 \mu\text{l} \times \frac{30 \text{ mg (bead)}}{1 \text{ ml}} \times \frac{20 \mu\text{g (antibody)}}{1 \text{ mg (bead)}} \times \frac{1 \text{ ml}}{10^3 \mu\text{l}} = 60 \mu\text{g (antibody)}$$
- volume of IL-8 antibody = $60 \mu\text{g} \times \frac{\text{ml}}{0.996 \text{ mg}} \times \frac{1 \text{ mg}}{10^3 \mu\text{g}} \times \frac{10^3 \mu\text{l}}{1 \text{ ml}} = 60.2 \mu\text{l}$